



LUDWIG-
MAXIMILIANS-
UNIVERSITÄT
MÜNCHEN

BIOZENTRUM DER LMU DEPARTMENT BIOLOGIE II

LMU Biozentrum • Großhaderner Str. 2

82152 Planegg-Martinsried • Germany



***pig-1* MELK and *ced-3* Caspase cooperate to control cell
polarity in the *C. elegans* NSM neuroblast**

Dissertation zur Erlangung des Doktorgrades der Naturwissenschaften
Doctor rerum naturalium (Dr. rer. nat.) an der Fakultät für Biologie der
Ludwig-Maximilians-Universität München

**Vorgelegt von Hai Wei
aus Shandong, China
31. 01. 2019**

1. Gutachter: Prof. Dr. Barbara Conradt
2. Gutachter: Prof. Dr. John Parsch
Tag der Abgabe: 31.01.2019
Tag der mündlichen Prüfung: 22.05.2019

Eidesstattliche Versicherung

Ich versichere hiermit an Eides statt, dass die vorgelegte Dissertation von mir selbständig und ohne unerlaubte Hilfe angefertigt ist.

Ort, datum 22.05.2019, Munich

Hai Wei

(Unterschrift)

Erklärung

Hiermit erkläre ich,

- dass die Dissertation nicht ganz oder in wesentlichen Teilen einer anderen Prüfungskommission vorgelegt worden ist.
- dass ich mich anderweitig einer Doktorprüfung ohne Erfolg nicht unterzogen habe.
- dass ich mich mit Erfolg der Doktorprüfung in keinem anderen Fach unterzogen habe.
- dass ich ohne Erfolg versucht habe, eine Dissertation einzureichen oder mich der Doktorprüfung zu unterziehen.

Ort, datum 22.05.2019, Munich

Hai Wei

(Unterschrift)

Table of contents

Abbreviations

Lists of Publication

List of Figures

Declaration of Contribution

Summary

Part I:

Abstract 1

Introduction

1. *C. elegans* is an ideal model for genetic and cell biological studies 3
2. Embryonic cell lineages in *C. elegans* 4
3. Central cell death pathway in *C. elegans* 6
4. *C. elegans* NSM neuroblast lineage 9
5. Asymmetric cell division and cell-fate determinants in the one-cell embryos 11
6. Asymmetric cell division and cell-fate determinants in other cell lineages 17
7. CES-1 Snail functions in *C. elegans* 19
8. *pig-1* MELK functions in *C. elegans* 23

Part II (Results):

Chapter I

Caenorhabditis elegans ces-1 Snail represses *pig-1* MELK expression to control asymmetric cell division. 25

GENETICS 206: 2069–2084. <https://doi.org/10.1534/genetics.117.202754>

Supplemental materials 41

Chapter II

Caenorhabditis elegans ced-3 Caspase Is Required for Asymmetric Divisions That Generate Cells Programmed To Die. 54

GENETICS 210: 3 983-998. <https://doi.org/10.1534/genetics.118.301500>

Supplemental materials 70

Part III:

Discussion 73

1. CES-1 Snail acts as a transcriptional repressor of *pig-1* MELK in the NSM neuroblasts 74
2. Other regulators of *pig-1* MELK have similar functions in the NSM neuroblast 76
3. *ces-1* Snail is involved in various developmental processes 77

| | |
|--|-----|
| 4. <i>pig-1</i> MELK is involved in various developmental processes | 79 |
| 5. <i>pig-1</i> MELK may play a role in cell cycle progression in the NSMnb lineage | 81 |
| 6. The correct asymmetric positioning of the NSMnb cleavage plane depends on CED-3 caspase activity | 82 |
| 7. <i>pig-1</i> MELK affects the kinetics of the NSMsc death by indirectly influencing the activity of CED-3 Caspase | 84 |
| 8. <i>pig-1</i> MELK and <i>ced-3</i> Caspase cooperate to regulate asymmetric cell division in the NSMnb | 84 |
| References | 86 |
| Acknowledgments | 99 |
| Curriculum Vitae | 100 |

Abbreviations

bHLH: basic region Helix-Loop-Helix

ChIP-seq: chromatin immunoprecipitation sequencing

ces: cell death specification

EMT: Epithelial-Mesenchymal Transition

GEFs: Guanine-nucleotide-exchange factors

GAPs: GTPase-activating proteins

gf: gain-of-function

lf: loss-of-function

MELK: Maternal Embryonic Leucine-zipper kinase

NSMnb: NSM neuroblast

NSMsc: NSM sister cell

pig: *par-1*-like gene

TFs: Transcription Factors

TSS: transcriptional start sites

List of Publications

H. Wei*, B. Yan*, J. Gagneur, and B. Conradt, 2017 *Caenorhabditis elegans ces-1* Snail represses *pig-1* MELK expression to control asymmetric cell division. *GENETICS* 206: 2069–2084.

Mishra N., **H. Wei**, and B. Conradt, 2018 *Caenorhabditis elegans ced-3* Caspase Is Required for Asymmetric Divisions That Generate Cells Programmed To Die. *GENETICS* 210: 3 983-998.

Qingliang Li* **H. Wei*** Lijing Liu Xiaoyuan Yang Xiansheng Zhang Qi Xie, 2017 Unfolded protein response activation compensates endoplasmic reticulum - associated degradation deficiency in *Arabidopsis*. *Journal of Integrative Plant Biology* 59: 7 506-52.

* These authors contributed equally to this work.

List of Figures

| | |
|--|----|
| Figure 1: Life cycle of <i>C. elegans</i> at 20 °C | 5 |
| Figure 2: Central cell death pathway in <i>C. elegans</i> | 8 |
| Figure 3: Schematic of the asymmetric division of the NSMnb during embryogenesis | 10 |
| Figure 4: Schematic of cell divisions in early <i>C. elegans</i> embryogenesis | 12 |
| Figure 5: Schematic of symmetry breaking in one-cell stage embryo | 14 |
| Figure 6: AP cell polarity established during first round of asymmetric cell division | 16 |
| Figure 7: A gradient of apoptotic potential formed in an engulfment pathway-dependent manner prior the NSMnb division | 18 |
| Figure 8: CES-1 Snail acts as a transcriptional repressor to control downstream targets | 22 |
| Figure 9: Schematic of PIG-1 protein and % identity and (conserved) residues of <i>C. elegans</i> PIG-1 protein compared to MELK from other organisms | 24 |
| Figure 10: Percent embryonic lethality in <i>pig-1</i> and <i>ced-3</i> lf mutants | 80 |
| Figure 11: Expression of CED-3::GFP in the NSMnb lineage | 83 |

Declaration of contribution

In this thesis, I present my doctoral research, which was conducted in the last 4 years. The results section comprises of two chapters, chapter I and chapter II. Both chapters represent cooperation with other scientists and have been published in the journal *GENETICS* in 2017 and 2018.

Chapter I:

H. Wei*, B. Yan*, J. Gagneur, and B. Conradt, 2017 *Caenorhabditis elegans ces-1* Snail represses *pig-1* MELK expression to control asymmetric cell division. *GENETICS* 206: 2069–2084. <https://doi.org/10.1534/genetics.117.202754>

In this chapter, Bo Yan and Julien Gagneur analyzed CES-1 ChIP-seq data that was acquired from the modENCODE Project (<http://www.modencode.org>). I determined the phenotype of the NSMnb in *pig-1(lf)* animals and conducted all genetic experiments. Barbara Conradt, Bo Yan and I prepared the manuscript. I also helped with the manuscript revision. In this paper, I presented in Figure 5, 6, 7, 8, 9, S1, S2, S3, S4 and wrote the respective figure legends.

Chapter II:

Mishra N., **H. Wei**, and B. Conradt, 2018 *Caenorhabditis elegans ced-3* Caspase Is Required for Asymmetric Divisions That Generate Cells Programmed To Die. *GENETICS* 210: 3 983-998. <https://doi.org/10.1534/genetics.118.301500>

In this chapter, Nikhil Mishra performed all experiments related to the QL/R.p lineages and I conducted all genetic experiments related to the NSMnb lineage. Barbara Conradt, Nikhil Mishra and I wrote the manuscript and I helped with the manuscript revision. In this paper, I generated the data presented in Figure 8 and wrote the respective figure legend.

Signature: Hai Wei

Bo Yan

Nikhil Mishra

Barbara Conradt

Summary

In Chapter I of Part II (Results), I address the question of how *ces-1* Snail controls the establishment of cell polarity in the NSM neuroblast. Based on my studies, I identified *pig-1* MELK as a downstream target of *ces-1* Snail, which plays essential roles in establishing and/or maintaining cell polarity in the NSM neuroblast.

In chapter II of Part II (Results), I attempt to answer the question of why CED-3 protein, which is the *C. elegans* Caspase and which acts as the executor of cell death, is present at a high level in the mother (NSM neuroblast) of the NSM and NSM sister cell, which normally doesn't die. One possible reason may be that *ced-3* Caspase plays a non-killing role in the NSM neuroblast. My studies indicate that *ced-3* Caspase and *pig-1* MELK acts in parallel to control the correct positioning of the cleavage plane of the NSM neuroblast.

Taken together, these two studies demonstrate that *pig-1* MELK and *ced-3* Caspase are two important factors that control cell polarity in the NSM neuroblast.

Part I

Abstract

Snail-like genes encode zinc-finger transcription factors that play essential roles in development, and one of their well-known functions is the epithelial-mesenchymal transition (EMT) induction. Many studies performed in organisms ranging from *Drosophila melanogaster* to mammals have reported that Snail transcription factors regulate various aspects of stem cell development, such as cell polarity and cell cycle progression. However, the mechanisms through which Snail-like genes regulate these developmental processes are not completely understood. To uncover these mechanisms, I studied the neurosecretory motor neuron neuroblast (NSMnb) lineage during *C. elegans* embryogenesis. In the NSMnb lineage, we have previously found that CES-1 Snail controls cell cycle progression by regulating expression of the gene *cdc-25.2* CDC25. However, the mechanism by which *ces-1* controls the asymmetric division of the NSMnb is unknown. By analyzing CES-1 ChIP-seq data acquired from the modENCODE Project, we identified more than 3,000 potential targets of CES-1 Snail. From the potential candidates that are involved in regulating asymmetric cell division, *pig-1* was found to play an essential role in asymmetric NSMnb division. *pig-1* encodes the sole *C. elegans* ortholog of Maternal Embryonic Leucine-zipper kinase (MELK) kinase. Through genetic studies, I confirmed that *pig-1* acts downstream of *ces-1* to control the asymmetric positioning of the NSMnb cleavage plane. Furthermore, by using a single-copy transcriptional reporter of *pig-1*, I observed that loss of *ces-1* increases the transcriptional level of *pig-1*, while gain of *ces-1* activity decreases the level of *pig-1*. Therefore, I conclude that CES-1 Snail regulates asymmetric positioning of the NSMnb cleavage plane by repressing expression of the gene *pig-1*. In the NSMnb, CES-1 Snail coordinates the cell cycle through *cdc-25.2* and asymmetric positioning of the cleavage plane through *pig-1* to ensure asymmetric cell division and the generation of two daughter cells of different sizes and fates: the larger NSM, which survives, and the smaller NSM sister cell (NSMsc), which dies. Apart from influencing the positioning of the cleavage plane, *ces-1* and *pig-1* also play roles in controlling the orientation of the NSMnb cleavage plane and in specifying the fate of the daughter cell, NSMsc.

On the other hand, I show that *ced-3*, which encodes a Caspase and which usually executes cell death in *C. elegans*, also plays a role in regulating the asymmetric

positioning of the NSMnb cleavage plane. Loss of *ced-3* alone did not affect the asymmetric positioning of the NSMnb cleavage plane at lateral-dorsal side, but loss of both *ced-3* and *pig-1* reversed the cleavage plane to the medial-ventral side and generated a small NSM and a large NSMsc. This indicates that in the NSMnb lineage, *ced-3* may have other functions in addition to executing cell death in the smaller daughter (NSMsc). Furthermore, I confirmed that this function is dependent on the Caspase activity of CED-3 protein.

Taken together, *ces-1* Snail and *pig-1* MELK are two key factors that coordinate cell polarity and cell fate in the NSMnb lineage during *C. elegans* embryogenesis. In addition, *ced-3* Caspase acts in parallel to *pig-1* and *ces-1* to promote the correct positioning of the cleavage plane in the NSMnb.

Introduction

1. *C. elegans* is an ideal model for genetic and cell biological studies

C. elegans is an excellent genetic model to study developmental biology and neurobiology because of its small body size, short life cycle, transparency, well annotated genome and invariant cell lineage. Due to these advantages, forward and reverse genetics can be used at the level of the whole organism or in specific cell lineages to address various biological problems. The invariant cell lineage of *C. elegans* makes it possible to study asymmetric cell division and cell death at the single-cell level *in vivo*, which is difficult in other organisms.

In addition, several other features make *C. elegans* a very powerful model organism in the lab. For example, *C. elegans* is a self-fertilizing hermaphrodite, capable of producing hundreds of offspring per animal. Larvae of *C. elegans* can be frozen at -80°C and kept for many years. In addition, growth conditions of *C. elegans* vary from 12°C to 25°C , which means that the rate of development can be controlled and temperature-sensitive mutants can be isolated. Incubated at higher temperatures for a short time, *C. elegans* are able to generate males for genetic crosses or perform heat-shock experiments (Sulston and Hodgkin 1988). Furthermore, it is easy to collect enough materials for biochemical and cell-biology experiments, and it is cheap to maintain *C. elegans* in the lab. Overall, *C. elegans* is an excellent model organism for studying fundamental genetic and molecular mechanisms. Moreover, since $\sim 40\%$ of genes that are related to human diseases have orthologs in the *C. elegans* genome (Culetto 2000; Shaye and Greenwald 2011), studying *C. elegans* is very helpful in order to advance the knowledge of processes associated with human health and diseases.

2. Embryonic cell lineages in *C. elegans*

The life of *C. elegans* begins as a zygote, which then develops through four different larval stages (L1, L2, L3 and L4) before maturing into an adult. At the end of each larval stage, it proceeds through a transition state in which a new cuticle is formed and the old cuticle is molted (Byerly *et al.* 1976). It needs only 2-3 days (depending on the incubation temperature) from a one-cell stage embryo to an adult (Figure 1) (Byerly *et al.* 1976). Using Differential Interference Contrast (DIC) microscopy, J. E. Sulston and H. R. Horvitz determined the post-embryonic cell lineages in 1977 (Sulston and Horvitz 1977). Subsequently, J. E. Sulston, E. Schierenberg, J. G. White and J.N.Thomson identified all embryonic cell lineages in 1983 (Sulston *et al.* 1983). Based on their work, it is known that all the lineages in *C. elegans* are essentially invariant and reproducible between different individual animals. Therefore, through continuous observation of a live embryo, it is possible to track multiple cell lineages during embryogenesis and to identify the mother cell and the fates of their daughter cells.

In *C. elegans*, the nomenclature of embryonic cell lineages includes a blast cell name (e.g. AB) followed by letters indicating either an anterior/posterior (a/p) or left/right (l/r) divisions without a period between them. The post-embryonic lineages are written as a blast cell name followed by a/p or l/r divisions separated by a period. For example, the embryonic NSMnb left (NSMnbL) cell is named as ABaraapapaa without a period. The post-embryonic PVM cell is named as QL.paa and SDQL cell is named as QL.pap with a period inside.

As the NSMnbL and the NSMnbR divide along a ventral-lateral/dorsal-medial axis at ~ 410 min after the first zygotic cell division (Albertson and Thomson 1976; Ellis and Horvitz 1986), the NSML and NSMR are named ABaraapapaav and ABaraappaav respectively. In my thesis, I studied these two lineages, NSMnbL or NSMnbR, and tried to determine interrelationships between asymmetric cell division and apoptotic cell death.

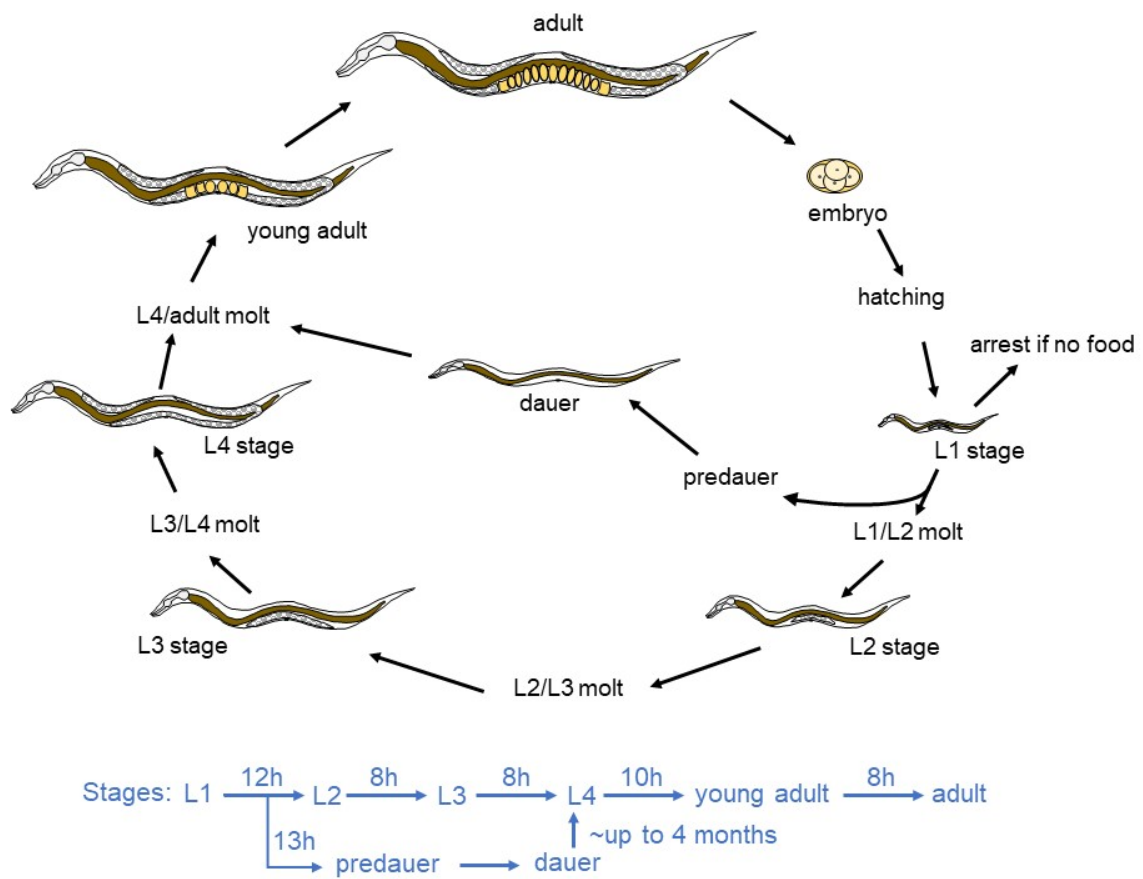


Figure 1. Life cycle of *C. elegans* at 20 °C. The life cycle of a *C. elegans* starts from a zygote. Once the impermeable eggshell is formed after fertilization, the embryo can develop independently from the mother. At 20 °C, the embryo takes around 16 h to develop to the L1 stage and 2.5 days to reach the adult stage (developmental time is shown at the bottom in blue color). When an animal in the L1 stage cannot find food, it develops into a dauer, which can survive up to ~4 months at 15 °C. Upon restoration of food supply, dauers can resume development and reach the L4 stage and develop to an adult (Byerly *et al.* 1976; Kenyon 1988).

3. Central cell death pathway in *C. elegans*

C. elegans is a transparent organism, which makes it possible to distinguish cell corpses from living cells based on the morphology and refractivity in vivo using DIC microscopy (Alison M. G. Robertson 1982). With this advantage, cell death lineages can be identified during embryogenesis and post-embryogenesis. In other words, we can make recordings of the animal's development, identify dying cells and subsequently study their mother or founder cell (Sulston and Horvitz 1977; Sulston *et al.* 1983).

Programmed cell death can be classified into different types based on the developmental stage during which it occurs, namely during embryogenesis or post-embryogenesis, and based on the tissue in which it occurs, namely in the soma or germline (Sulston and Horvitz 1977; Sulston *et al.* 1983; Gumienny *et al.* 1999). I focus on the NSMnb lineage which occurs during embryogenesis and is part of the soma (Ellis and Horvitz 1986). In a wild-type hermaphrodite, out of the 1090 somatic cells generated, 131 cells undergo programmed cell death and 113 of these 131 cells die during embryogenesis (Sulston and Horvitz 1977; Sulston *et al.* 1983). Through morphological and genetic studies of *C. elegans*, the progression of cell death is separated into three sequential phases: specification phase, activation phase and execution phase (Horvitz 1999). In the specification phase, cells will be determined to undergo programmed cell death or to survive. Once the fate is decided, the cell activates the process of cell death in the following activation phase. Finally, during the execution phase, the cell undergoing cell death is engulfed and degraded by a neighboring cell. If any phase before engulfment and degradation is disrupted, it will lead to inappropriately surviving cells in some cell death lineages (Ellis and Horvitz 1986; Conradt and Horvitz 1998).

The core machinery of the cell death pathway in *C. elegans* consists of four factors: *egl-1*, *ced-9*, *ced-4* and *ced-3*. These genes act in a linear pathway to trigger the cell death fate (Hengartner *et al.* 1992; Shaham and Horvitz 1996; Conradt and Horvitz 1998). *egl-1* encodes a pro-apoptotic protein, which contains a BH3 domain (Conradt and Horvitz 1998; Bouillet and Strasser 2002). This domain is important for binding to the anti-apoptotic CED-9 protein. *ced-9* encodes a homolog of the human proto-oncoprotein B-Cell Lymphoma 2 (Bcl-2), which acts as an anti-apoptotic factor (Hengartner and Horvitz 1994). *ced-4* encodes an ortholog of human apoptotic protease activating factor 1 (Apaf-1), which forms the apoptosome and recruits and activates the

downstream Caspase (Yuan *et al.* 1992; Zou *et al.* 1997). *C. elegans ced-3* encodes an aspartate specific cysteine protease and homolog of human Caspase-3 (and Caspase-7) (Yuan *et al.* 1993), which executes cell death in dying cells. CED-3 Caspase is synthesized as an inactive zymogen that is named pro-CED-3, which forms a homodimer and is activated by the CED-4 apoptosome to generate the active CED-3 Caspase composed of two cleaved CED-3 proteins (Yang *et al.* 1998; Huang *et al.* 2013). Through genetic studies, Conradt and Horvitz found that *egl-1* acts upstream of *ced-9* to promote the activation of CED-4 and CED-3 (Conradt and Horvitz 1998). While *ced-9* acts upstream of *ced-4* to inhibit the cell death process (Hengartner *et al.* 1992), *ced-4* acts upstream of *ced-3* to facilitate the activation of *ced-3* Caspase (Figure 2B) (Shaham and Horvitz 1996). The activation of CED-3 Caspase and, hence, the activation of cell death, occurs in three sequential steps. In the first step, *egl-1* is transcribed and EGL-1 protein is synthesized, which binds to CED-9. Second, binding of EGL-1 to CED-9 disrupts the interaction between CED-9 and CED-4 and releases CED-4 from the preexisting CED-9-CED-4 complex (Conradt and Horvitz 1998; Del Peso *et al.* 1998; Yan *et al.* 2004). Finally, four released CED-4 asymmetric dimers form an octameric apoptosome to facilitate the activation of CED-3 Caspase (Figure 2A) (Xue *et al.* 1996; Chen *et al.* 2000; Huang *et al.* 2013). Once CED-3 is activated, it cleaves several downstream substrates to degrade and kill the cell. In addition, several other genes have been reported to be involved in regulating cell death in *C. elegans*. These include *csp-1* (Caspase homolog-1) (Shaham 1998; Denning *et al.* 2013), *csp-2* (Caspase homolog-2) (Shaham 1998; Geng *et al.* 2009), *dad-1* (*dad*, defender against apoptotic death) (Sugimoto *et al.* 1995) and *ces-1* (*ces*, cell death specification) (Ellis and Horvitz 1991; Metzstein and Horvitz 1999). All these factors affect the apoptotic fate in different lineages by influencing the core killing machinery.

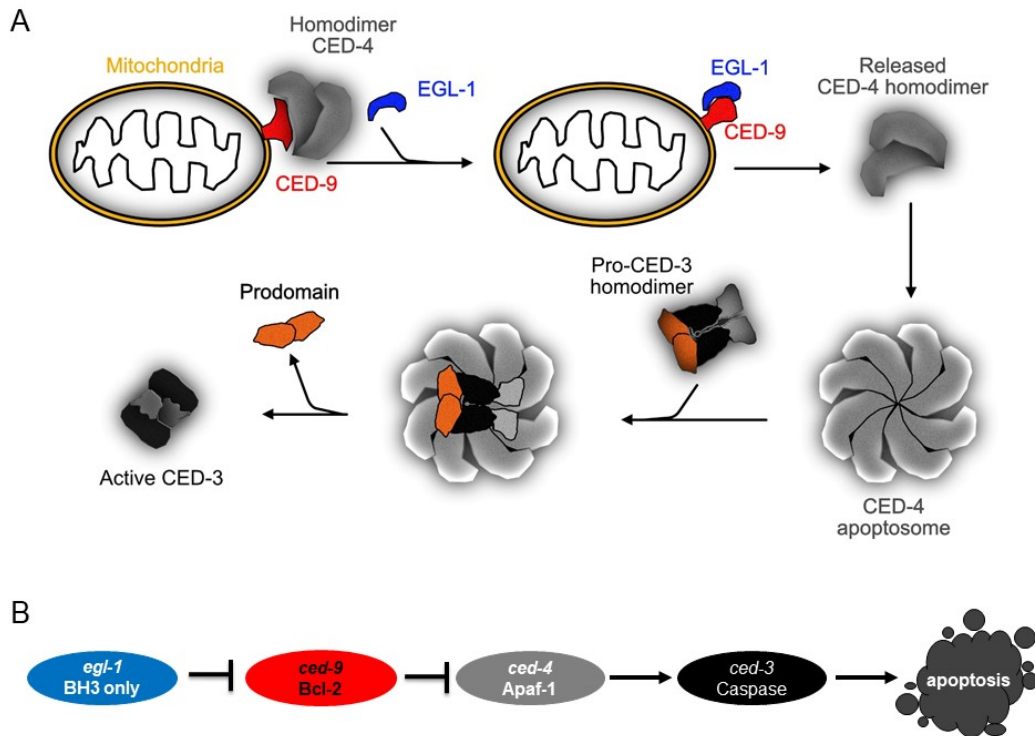


Figure 2. Central cell death pathway in *C. elegans*. (A) The activation of cell death executor CED-3 Caspase occurs in three sequential steps. First, in response to cell death stimuli, pro-apoptotic factor EGL-1 is activated and binds to the mitochondria-localized anti-apoptotic factor CED-9. Second, physical interaction between EGL-1 and CED-9 disrupts the interaction between CED-9 and CED-4, which releases CED-4 from the CED-9/CED-4 complex. Finally, released CED-4 homodimers polymerize to form an octameric apoptosome to facilitate the activation of pro-CED-3 zymogen. (B) Factors of central cell death machinery in *C. elegans* act in a linear genetic pathway to initiate cell death.

4. NSM neuroblast lineage in *C. elegans*

In wild-type *C. elegans*, two bilaterally symmetric NSM neuroblast cells exist (NSMnbL and NSMnbR), which originate from the AB blastomere cell and are generated around 230 min post fertilization. At ~ 410 min post fertilization, each of these two NSM neuroblasts divide asymmetrically to give rise to two daughter cells of different sizes and fates (Sulston *et al.* 1983; Hatzold and Conradt 2008). During the NSMnb division in wild-type embryos, the cleavage plane is oriented in a ventral-lateral to dorsal-medial direction to give rise to two daughter cells. The larger daughter cell (NSM) localizes to the ventral-medial side, and the smaller daughter cell (NSMsc) localizes to the dorsal-lateral side (Figure 3). The larger daughter cell (NSM) survives and differentiates into a serotonergic motor neuron, whereas the smaller daughter cell (NSMsc) dies ~ 22 min post its birth at 20°C (Sulston *et al.* 1983; Hatzold and Conradt 2008).

As mentioned above, in wild-type embryos, each NSMnb divides asymmetrically to give rise to a smaller NSMsc, which undergoes cell death. In this process, active CED-3 Caspase acts as a critical factor in executing the apoptotic fate of the smaller daughter cell (NSMsc). Loss of *ced-3* causes 100% inappropriate NSMsc survival (Ellis and Horvitz 1986; Shaham *et al.* 1999). Therefore, the kinetics of cell death or execution of the apoptotic fate of the NSMsc depends on the central cell death pathway. In addition, using a NSM-specific *tph-1* reporter, it has been reported that disruption of the asymmetric cell division of the NSMnb results in the formation of extra NSMs (Hatzold and Conradt 2008; Yan *et al.* 2013; Wei *et al.* 2017), which indicates that the apoptotic fate of the NSMsc is affected. Moreover, the Garriga lab found that loss of QL.p cell polarity also influences the fate of its daughter cells. Therefore, they proposed that cell polarity regulates the fate of daughter cells by controlling the asymmetric segregation of neural fate determinants to daughter cells (Guenther and Garriga 1996; Frank *et al.* 2005; Cordes *et al.* 2006). However, the mechanisms of how these cell-fate determinants are asymmetrically distributed and which cell-fate determinants are involved in this process are poorly understood. Out of all cell death lineages during embryogenesis, the NSMnb lineage was chosen to study this question. Using a cell boundary marker (*ltIs44, P_{pie-1mCherry::ph^{PLCδ}}*) (Kachur *et al.* 2008), I can distinguish the two NSM neuroblasts and follow their developmental progression easily during embryogenesis, allowing for studies to be performed at a single-cell level *in vivo*. By studying the NSMnb lineage, I can detect the expression or distribution of cell-fate

determinants during the asymmetric cell division or track these factors in the two daughter cells that have different fates. Based on the above mentioned advantages, the embryonic NSMnb lineage is a very useful tool to study asymmetric cell division and cell death.

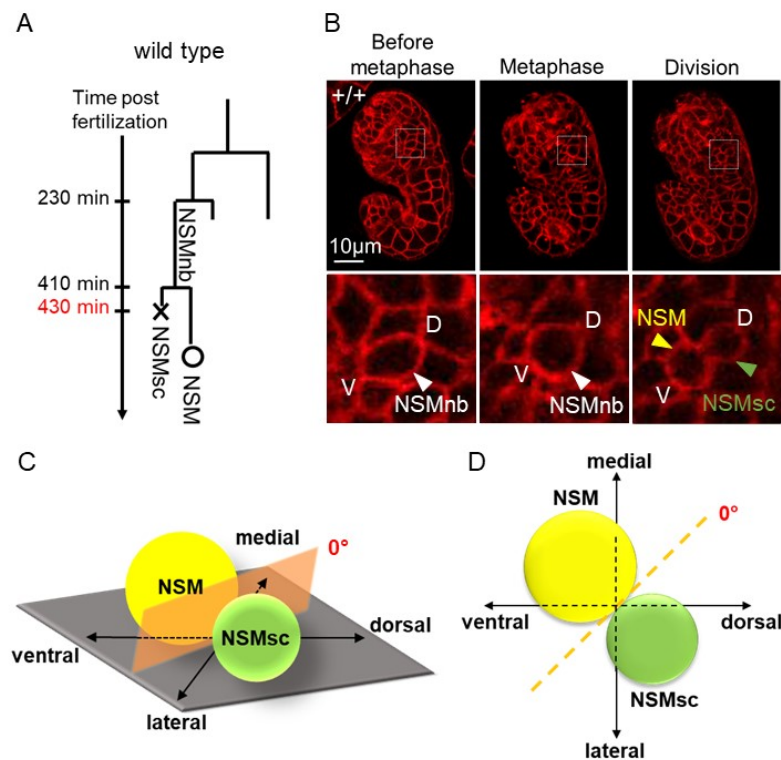


Figure 3. Schematic of the asymmetric division of the NSMnb during embryogenesis. (A) The NSMnb lineage in wild type. The smaller daughter NSMsc dies around 22 min post its birth while the larger daughter survives. (B) Confocal images of the NSMnb before metaphase, at metaphase and during cell division. “V” means the ventral side and “D” means the dorsal side; the NSM and the NSMsc are marked in different colors. The cell boundary marker is an integrated transgene (*ItIs44, P_{pie-1mCherry::ph^{PLCδ}}*) on chromosome V. (C) Schematic showing the location of the NSM and NSMsc post asymmetric division in a lateral view. The orange transparent rectangle indicates the orientation of the NSMnb cleavage plane. (D) Schematic showing the location of the NSM and the NSMsc post asymmetric division in an anterior view. The orange dotted line indicates the orientation of the NSMnb cleavage plane.

5. Asymmetric cell division and cell-fate determinants in one-cell embryos

In all multicellular animals, asymmetric cell division is an essential and fundamental process that plays important roles during development. Live imaging of this process in specifically interested lineages is very challenging (or essentially impossible) in developing animals. Compared to other organisms, *C. elegans* is a good model to study progression of asymmetric cell division in developing embryos.

The life cycle of *C. elegans* starts from a zygote and goes through many rounds of cell division and differentiation. It then finally develops into a multicellular organism with 959 somatic cells (and 1031 somatic cells in an adult male) (Sulston and Horvitz 1977; Kimble and Hirsh 1979; Sulston *et al.* 1983). During this process, cells acquire different fates to form various organs or tissues. One of the prominent mechanisms in *C. elegans* to achieve this is through asymmetric cell division, which generates two daughter cells of different fates in which the smaller cell usually dies or differentiates into a specific type of cell while the larger cell usually survives or differentiates into another specific type of cell. At the beginning of embryogenesis, the first asymmetric division cleaves the zygote P0 into a larger anterior blastomere AB and a smaller posterior blastomere P1. Subsequently, P1 divides asymmetrically to generate the two daughter cells, EMS and P2, which have different sizes and fates. Soon after, two additional asymmetric divisions divide EMS into MS and E, and divide P2 into C and P3. Thereafter, P3 undergoes another asymmetric cell division to give rise to D and P4. In this manner, six founder cells, AB, MS, E, C, D and P4, are produced via 5 asymmetric divisions (Figure 4) (Sulston *et al.* 1983). During these asymmetric cell divisions, cell-fate determinants are distributed asymmetrically into different daughter cells. For this reason, the descendants of each founder cell will finally develop into a specific kind of cell type. For instance, most of the hypodermis and pharyngeal neurons are generated from the AB blastomere, while intestine and germline originate from the E cell and P4 cell, respectively (Sulston *et al.* 1983).

During the formation of cell polarity in early embryogenesis, four sequential steps namely symmetry breaking, polarity establishment, polarity maintenance and asymmetric division occur in an ordered way to ensure normal development. Based on decades of studies, many mechanisms of how cell polarity in early embryogenesis is established have been discovered. After fertilization, the entire actomyosin network localized under the cell membrane undergoes contractions, which depends on non-

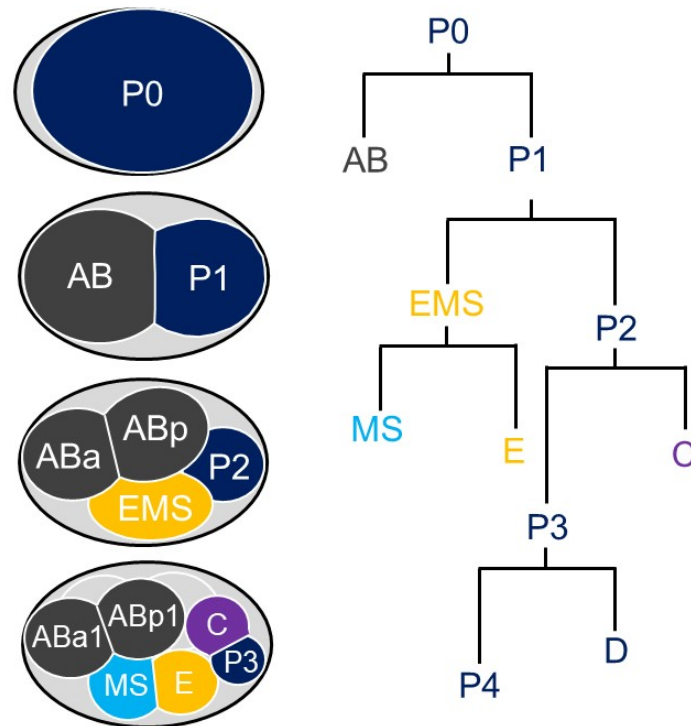


Figure 4. Schematic of cell divisions in early embryogenesis of *C. elegans*. Left side is anterior and right side is posterior, top is dorsal and bottom is ventral. During early embryogenesis, six founder cells that are marked in different colors are generated through five asymmetric divisions. Various colors indicate that each founder cell has its own characteristic cell cycle and lineage in the further developmental process. For instance, hypodermis, some neurons and anterior pharynx are generated from AB cell. Muscle cells, somatic gonad, majority of the pharynx and gland cells are generated from MS cell. On the other hand, E and D cells give rise to intestine and muscle tissues, C cell differentiates into muscle, hypodermis and neurons, and P4 engenders germline precursor cells.

muscle myosin II heavy chain NMY-2 and the associated light chain 4 MLC-4 (Shelton *et al.* 1999). Studies on the cortical contractions in early embryogenesis revealed that RHO-1 (a Rho family GTPase) and LET-502 (a Rho-binding kinase) work together to promote the activity of NMY-2 (Motegi and Sugimoto 2006; Schonegg 2006), thereby controlling the surface contractions of the whole cortical actomyosin network. Fertilization induces sequential events to break the symmetry of the oocyte. Before symmetry breaking, centrioles brought by the sperm recruit the pericentriolar material to assemble centrosomes and nucleate microtubules. Relying on short cortical microtubules, centrosomes walk randomly in the zygote. In the beginning of symmetry breaking, the random walking centrosomes juxtapose to the cell cortex which results in the formation of a small smooth cortical domain (Cuenca 2003; Cowan and Cowan 2004; Bienkowska and Cowan 2012). This domain ceases surface contractions of the cortical actomyosin network and breaks the symmetry of the zygote. In this process,

microtubules play a minor role (Sonneville 2004; Tsai and Ahringer 2007). Following symmetry breaking, the local cessation of cortical contractions depends on RHO-1 activity around centrosomes. Guanine-nucleotide-exchange factors (GEFs) promote the generation of active RHO-1-GTP, while GTPase-activating proteins (GAPs) promote the formation of inactive RHO-1-GDP. In *C. elegans*, ECT-2 and RGA-3/4 are GEF and GAPs of RHO-1 (Schmutz *et al.* 2007; Schonegg *et al.* 2007; Tse *et al.* 2012), respectively. In the symmetry breaking process, it has been proposed that the absence of ECT-2 in the vicinity of centrosomes is important for the inactivation of RHO-1, which leads to the local cessation of cortical contractions (Figure 5) (Motegi and Sugimoto 2006; Schonegg 2006). RGA-3, ECT-2 and RHO-1 present a similar localization under the cell cortex in one-cell embryos. It has been hypothesized that a balance exists between RGA-3/4 and ECT-2 on regulating RHO-1 activity, but it is yet unknown how this balance is established during polarization to promote generating anterior and posterior cortical contractions (Schonegg *et al.* 2007). In addition, CYK-4 has also been reported to play a similar role like GAP to inhibit the function of RHO-1 (Jenkins *et al.* 2006). However, detailed functions of CYK-4 seem to be unclear, because most of the CYK-4 is inactive at this stage (Jenkins *et al.* 2006; Tse *et al.* 2012). In addition, PAR-2 protein is also reported to act in a partial redundant pathway to break this symmetry.

During polarity establishment in early embryogenesis, PAR proteins play a central role to set up an anterior-posterior (A-P) polarity with two mutually exclusive domains, PAR-3/PAR-6/PKC-3 localized to the anterior side and PAR-1/PAR-2 localized to the posterior side (Cuenca 2003; Munro *et al.* 2004; Goldstein and Macara 2007). This is important for the asymmetric distribution of cell-fate determinants (Figure 6). In addition, during this anteriorly-directed flow of cortical materials, contraction of the actomyosin network establishes different cortical tensions along the anterior-posterior axis. These different cortical tensions in anterior and posterior are important for the movements of surface materials (Hird and White 1993; Mayer *et al.* 2010). In other words, asymmetric distribution of PAR proteins and flow of actomyosin network act together to set up the polarity during early embryogenesis (Zonies *et al.* 2010; Motegi *et al.* 2011). After the polarity establishment phase, the cell polarity maintenance phase occurs and the mutual inhibition of anterior and posterior cortical localized PAR domains is important to maintain the established polarity. In this process, PAR-2 plays a critical role to maintain this mutual inhibition (Cuenca 2003). Centrosomes or the

cortical actomyosin network does not act or has a minor role during this maintenance (Cowan and Cowan 2004; Ai *et al.* 2011). Once cell polarity is established by these three subsequent steps, it results in the asymmetric distribution of cell-fate determinants in the anterior and posterior cytoplasm, which then give rise to two daughter cells that carry different fate determinants (Thorpe *et al.* 1997; Tabara *et al.* 1999; Takeshita and Sawa 2005; Zonies *et al.* 2010). In my study, I use the NSM neuroblast lineage to study the genetic mechanisms that are required for the asymmetric positioning and orientation of the cleavage plane and the asymmetric distribution of cell-fate determinants.

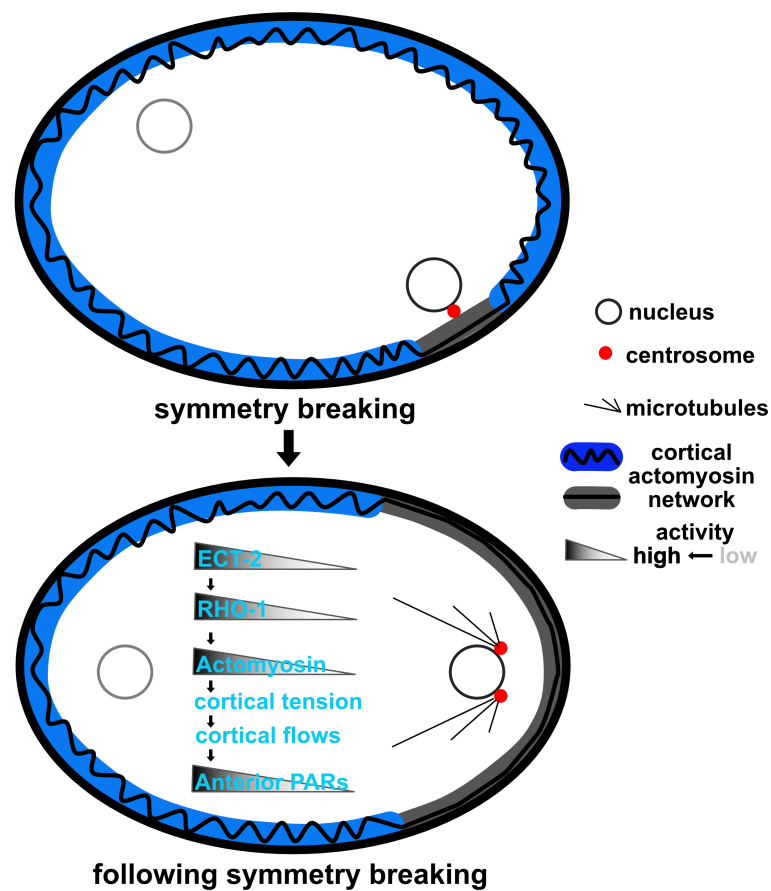


Figure 5. Schematic of symmetry breaking in one-cell stage embryo. In the beginning of symmetry breaking, cortical contractions of the actomyosin network (blue marked wiggled line) are ceased when the centrosome becomes juxtaposed to the cell cortex, which results in the formation of a smooth domain along the cell cortex (grey marked smooth line). Following symmetry breaking, due to the inactivation of RHO-1 near centrosomes, the local cessation of cortical contractions extend to the whole posterior. Cortical contractions along the anterior-posterior generate cortical tensions, which induce cortical flows to distribute cortical materials.

Mechanisms of asymmetric distribution of cell-fate determinants are well studied in early embryogenesis. PAR proteins establish and maintain cell polarity before asymmetric division. Subsequently, other components that act downstream of PAR proteins promote the generation of cytoplasmic asymmetries to determine different fates in the daughter cells. In early embryogenesis, many factors have been shown to be asymmetrically distributed. MEX-5 and MEX-6 are considered to be the two primary asymmetry mediators, because the asymmetric localization of many factors depends on them in early embryos (Schubert *et al.* 2000). MEX-5/6 are enriched in the anterior part of the one-cell embryo since their cytoplasmic motility in the anterior and the posterior side is different (Tenlen *et al.* 2008; Daniels *et al.* 2010). PAR-1, which encodes a serine/threonine kinase, might act with PAR-4 to phosphorylate MEX-5/6 to increase their motility in the posterior, and hence, regulating MEX-5/6 asymmetric cytoplasmic localization (Tenlen *et al.* 2008; Griffin *et al.* 2011). Once the gradient of MEX-5/6 is formed in an anterior-posterior way, it then promotes the asymmetric localization of various cell-fate determinants (Figure 6). For instance, MEX-5/6 restrict the polarity mediators MEX-1, POS-1 and the cell-fate regulator PIE-1 to the posterior side of the one-cell embryo prior to division (Reese *et al.* 2000). Asymmetric localization of these three factors is dependent on MEX-5/6 induced degradation events. It has been reported that PIE-1, MEX-1 and POS-1 have tandem CCCH domains in their protein sequences. The first zinc finger (ZF1) domain is important for the degradation, because it binds to ZIF-1, which encodes a SOCS box protein and is an essential partner of the CUL-2 E3 Ubiquitin ligase complex to recruit substrates (DeRenzo *et al.* 2003). By checking a transgene reporter of *zif-1* 3' UTR in early embryogenesis, MEX-5/6 was reported to play a key role in promoting the expression of ZIF-1 by binding to its 3'UTR (Oldenbroek *et al.* 2012). The synthesized ZIF-1 is necessary for the degradation of PIE-1, MEX-1 and POS-1 in the AB cell as well as in the daughter cell of subsequent P cell divisions. Such asymmetric localizations are established through translational regulation by MEX-5/6 (Guvén-Ozkan *et al.* 2010). However, MEX-5/6 can also influence asymmetric localization through physical interactions. For example, the Polo-like kinases PLK-1 and PLK-2 are enriched in the anterior side of the one-cell embryo by directly binding to MEX-5/6 (Budirahardja and Gonczy 2008; Nishi *et al.* 2008). Moreover, MEX-3, a cell polarity mediator, also interacts with MEX-5/6 at the protein level (Huang *et al.* 2002).

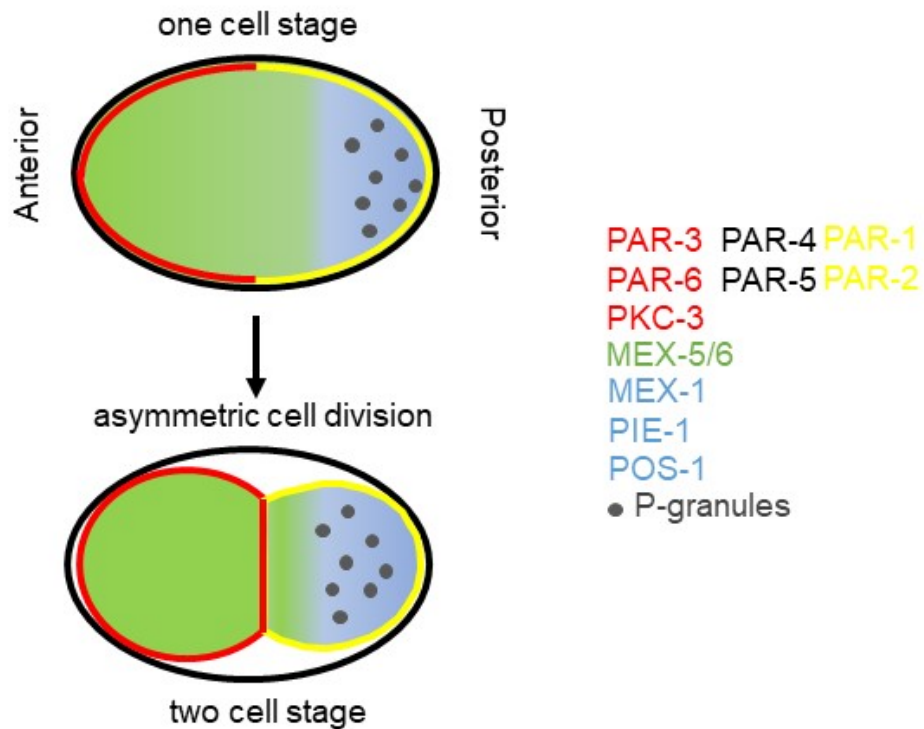


Figure 6. AP cell polarity established during first round of asymmetric cell division. Interaction between centrosome and cell cortex in *C. elegans* zygote breaks the symmetric status to build an AP (anterior-posterior) polarity where PAR-3/PAR-6/PKC-3 localize to the anterior domain and PAR-1/PAR-2 localize to the posterior domain. PAR-1 inhibits the accumulation of MEX-5/6 at the posterior side, which results in the enrichment of MEX-5/6 at the anterior. Thereafter, MEX-5/6 prevents the accumulation of PIE-1, MEX-1, POS-1 and P granules in the anterior domain, as well as enhances the asymmetric distribution of PAR-3/PAR-6/PKC-3. As a result of these asymmetric distributions in the one-cell embryo, P0 then divides asymmetrically to give rise to two daughter cells, AB and P1, with different fates.

6. Asymmetric cell division and distribution of cell-fate determinants in other cell lineages

In addition to the one-cell stage, asymmetric distribution of cell-fate determinants is also observed in other embryonic lineages. Recently, our lab found that mRNA messages of *egl-1*, which encodes a pro-apoptotic BH3-only member of the Bcl-2 family, are asymmetrically localized in the two daughter cells of the RID lineage (Sherrard *et al.* 2017). This asymmetric distribution of *egl-1* mRNA could be enabled by the polarity of the mother cell. In addition, other studies from our lab have demonstrated that unequal amounts of TAC-1 are assembled on the two centrosomes during asymmetric division of the mother cell in two different cell lineages, the NSMnb and the QL.p lineages. Using fluorescently tagged TAC-1 (TAC-1::GFP and TAC-1::mKate2) as reporter, more TAC-1 fluorescent signals were found to be associated with the ventral and anterior centrosomes in the NSMnb and the QL.p, respectively (Chakraborty *et al.* 2015; Mishra *et al.* 2018). TAC-1 is a substrate of CED-3 Caspase, which could be dissociated from the centrosomes upon being cleaved by CED-3. Therefore, the asymmetry in the amounts of centrosomal TAC-1 suggests that a gradient of active CED-3 Caspase may exist along the ventral-dorsal axis in the NSMnb and along the anterior-posterior axis in the QL.p (Figure 7).

In addition, it has been reported that *ces-1*, which encodes a C2H2 zinc-finger transcription factor and functions as an anti-apoptotic factor to repress the central cell death pathway, has a much higher concentration in the large daughter (NSM) compared to the small daughter (NSMsc) (Hatzold and Conradt 2008). *ces-1* was classified as an anti-apoptotic factor and was identified as a Snail family zinc-finger protein by the Horvitz lab (Ellis and Horvitz 1991; Metzstein and Horvitz 1999b). A subsequent study from our lab revealed that CES-1 blocks the cell death pathway by antagonizing HLH2/HLH3 in order to inhibit the expression of the proapoptotic gene *egl-1* (Thellmann 2003). This mechanism could explain why the large daughter cell (NSM), with higher CES-1 level, survives, whereas the small daughter cell (NSMsc), with lower CES-1 level, dies. Furthermore, studies with the embryonic HSN/PHB and NSMnb lineages and with the postembryonic QL and QR lineages suggest that the apoptotic fate of the small daughter cell is controlled by asymmetric division of the mother cell (Frank *et al.* 2005; Cordes *et al.* 2006; Wei *et al.* 2017).

Taken together, these findings suggest that pro- or anti-apoptotic factors are segregated asymmetrically in the RID, NSMnb, QL, QR and potentially other cell death lineages

in a very organized manner, which indicates that the mother cell may determine the fates of the two daughter cells prior to their generation. In this study, I attempt to understand how asymmetric cell division is regulated in cell death lineages. To that end, I use the NSM neuroblast lineage as model.

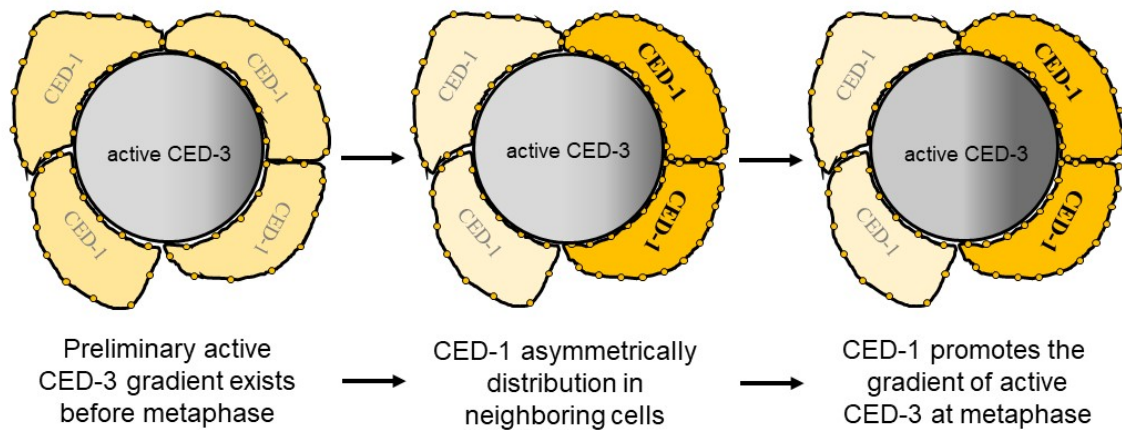


Figure 7. A gradient of apoptotic potential formed in an engulfment pathway-dependent manner prior to NSMnb division. ~5 min before the NSMnb metaphase, a basal level of the active CED-3 Caspase promotes clustering of the engulfment factor CED-1 on the dorsal neighbor cells. In turn, this asymmetric enrichment of CED-1 reinforces the gradient of active CED-3 in the NSMnb, which divides to generate two daughter cells with unequal apoptotic potential.

7. CES-1 Snail functions in *C. elegans*

Snail family members are transcription factors (TFs) that often function as transcriptional repressors. Snail TFs have been identified in various organisms, including the nematode *C. elegans*, and have been reported to be involved in many developmental processes, like epithelial-mesenchymal transition (EMT) (Nieto *et al.* 1994; Batlle *et al.* 2000; Cano *et al.* 2000), neuronal differentiation (Blanco *et al.* 2002), cell death (Ellis and Horvitz 1991), tumorigenesis and carcinoma (Hemavathy *et al.* 2000; Barrallo-Gimeno 2005). In 1984, the first member of the Snail family TFs was discovered in *Drosophila* (Grau *et al.* 1984; Nusslein-Volhard *et al.* 1984; Boulay *et al.* 1987). Subsequently, more members were found in *Drosophila*, vertebrates and non-vertebrate chordates (Corbo *et al.* 1997; Langeland *et al.* 1998; Sefton *et al.* 1998; Knight and Shimeld 2001; Manzanares *et al.* 2001). Snail family TFs can be classified into three major subclasses: Snail, Slug and Scratch (Nieto 2002). Analysis of their protein sequences have shown that most of them have a conserved C-terminus, which contains several zinc-finger domains. While their N-terminus are quite divergent, apart from the Snail and Gfi-1 (SNAG) domain (Thisse *et al.* 1995; Katoh and Katoh 2005), Slug family members also contain a distinct Slug domain and Scratch family members contain a unique Scratch domain at their N-terminus (Manzanares *et al.* 2001). Most of the Snail type proteins resemble to Snail (Barrallo-gimeno and Nieto; Manzanares *et al.* 2001). Snail-type TFs usually contain three to five C2H2 zinc finger domains, which are important for the DNA binding affinity (Evans and Hollenbergt 1988). From *in vitro* and *in vivo* studies, Snail-type TFs have high binding ability to CAGGTG ('E-box') (Reece-Hoyes *et al.* 2009) and ACAGGTG ('Snail-box') motifs (Thellmann 2003) and function as either repressors or activators to regulate transcription of their target genes. In vertebrates, the SNAG domain, which is responsible for recruiting histone deacetylases, is important for the repressor activity of Snail TFs (Peinado *et al.* 2004). However, Snail-type TFs in *C. elegans* and *Drosophila* do not have this domain. In addition to the one mediated by the SNAG repressor domain, other inhibitory mechanisms were also reported. For instance, Snail-type TFs can physically interact with dCtBP and Ebi to mediate the repression of their targets (Nibu *et al.* 1998; Qi *et al.* 2008). In addition, Snail-type TFs were also found to compete with the basic region helix-loop-helix (bHLH) members of TFs to bind to the same conserved motifs. Because of this competition, high level of Snail-type TFs prevent the binding of the

bHLH TFs to targets and thereby inhibit these transcription activators (Kataoka *et al.* 2000; Thellmann 2003).

In 1991, the Horvitz lab identified *ces-1* as a suppressor of the apoptotic fate of the NSMsc and showed that this is accomplished through the regulation of an apoptotic gene that acts upstream of *ced-4* and *ced-3* (Ellis and Horvitz 1991). In 1998, the Horvitz lab found that *ces-1* acts upstream of *egl-1* to affect cell fate of the NSMsc (Conradt and Horvitz 1998). In 1999, the Horvitz lab reported that *ces-1* encodes a zinc-finger TF that is similar to the *Drosophila* neuronal differentiation protein Scratch and belongs to the Snail family (Metzstein and Horvitz 1999b). In *Drosophila*, three Snail members (*snail*, *escargot* and *worniu*) and three Scratch members (*scratch*, *scratch-like1* and *scratch-like2*) have been reported, while in *C. elegans*, only three Snail type C2H2 TFs (*ces-1*, K02D7.2 and *scrt-1*) have been identified according to the amino acid sequence similarity (Nieto 2002; Reece-Hoyes *et al.* 2009). The lack of neither K02D7.2 nor *scrt-1* function has been found to cause any developmental defects, whereas a strong gain-of-function (gf) of *ces-1* has been observed to result in a defective asymmetric cell division or perturbed cell fate in some neuroblasts (Thellmann 2003; Hatzold and Conradt 2008; Yan *et al.* 2013).

The protein sequence of CES-1 is most homologous to the Snail type superfamily member Scratch. CES-1 has been found to act as a transcriptional repressor in the NSMnb lineage, which is similar to most Snail-type members that function as negative regulators of transcription in other organisms. Based on the study in the NSMnb lineage, CES-1 specifically inhibits *egl-1* transcription by competing with HLH-2/HLH-3 heterodimers to bind to the E-box or Snail-box motif in the *egl-1* transcriptional regulatory region (Thellmann 2003). This binding represses the transcription of *egl-1* and is crucial for the fate determination of the NSMsc. In addition, CES-1 is also involved in controlling cell cycle by negatively regulating the transcription of *cdc-25.2* in the NSMnb (Yan *et al.* 2013). *cdc-25.2* encodes a CDC25-like phosphatase, which is a regulator of cell cycle progression (Figure 8). Moreover, in animals carrying the *ces-1(n703gf)* mutation, the position and orientation of the NSMnb cleavage plane are abnormal (Hatzold and Conradt 2008). This suggests that *ces-1*, as a TF repressor, has a role in controlling cell polarity in the NSMnb and other cell lineages. However, the underlying mechanisms of how *ces-1* controls cell polarity of the NSMnb are not yet clear. The Garriga lab found that *pig-1*, which is homologous to mammalian MELK, regulates cell polarity in the QL/R and the HSN/PHB lineages (Cordes *et al.* 2006). A

few years ago, the lab of Ou conducted a ChIP-seq analysis of HAM-1 (acquired from the modENCODE Project), which contains a winged helix DNA binding domain. They found that HAM-1 acts as an upstream transcriptional activator of *pig-1* and controls the establishment and/or maintenance of cell polarity in the HSN/PHB and the Q.p lineages (Feng *et al.* 2013a). Based on the way that they identified *pig-1* as a direct target of *ham-1* in the Q.p, I attempt to determine some downstream targets of *ces-1*, which can regulate the establishment and/or maintenance of cell polarity in the NSMnb using a similar method. Therefore, we analyzed the CES-1 ChIP-seq data in order to identify new potential downstream targets that are involved in regulating cell polarity. Interestingly, *pig-1* was also identified as a potential CES-1-target. To further understand this interaction, I investigated the role of *pig-1* in the NSMnb lineage.

Taken together, *C. elegans* CES-1, as a Snail-type transcriptional regulator, is not only involved in the determination of cell fate, but it is also involved in the regulation of cell cycle progression and cell polarity.

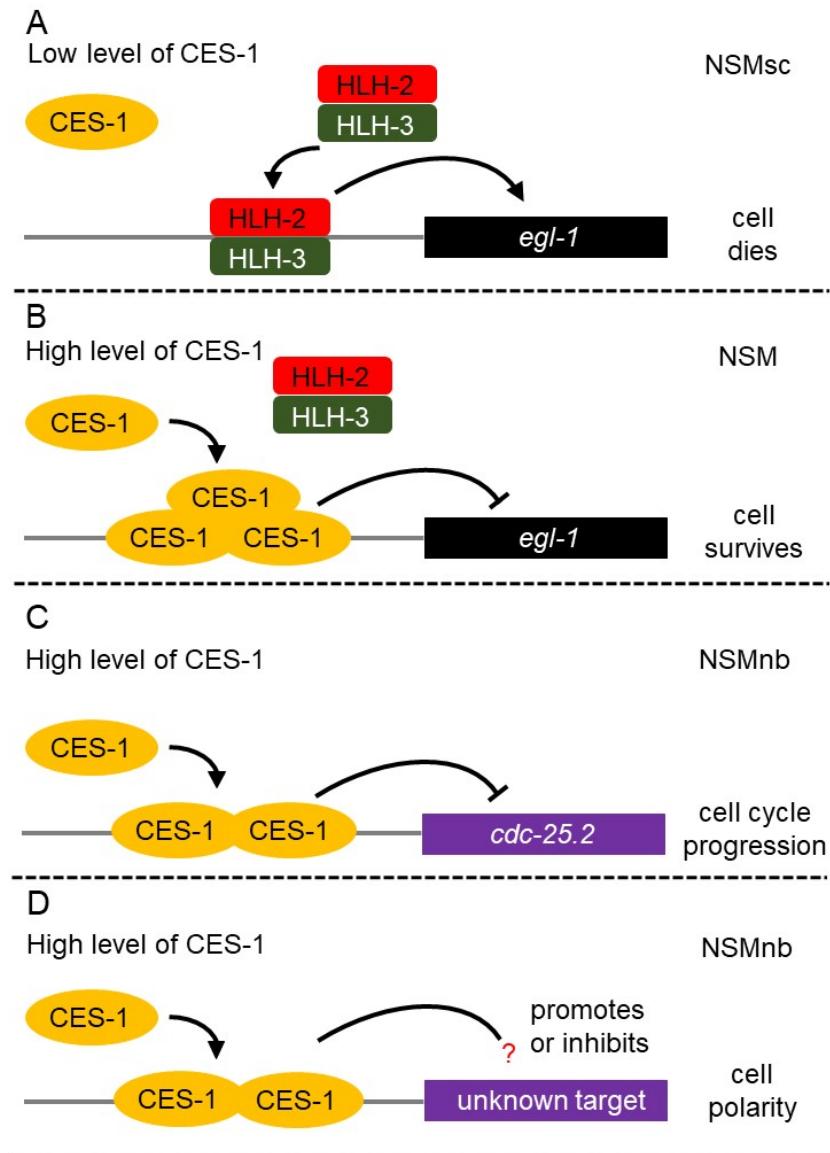


Figure 8. CES-1 Snail acts as a transcriptional repressor to control downstream targets. (A-B) CES-1 Snail competes with HLH-2/HLH-3 homodimer to bind to the *egl-1* regulatory element (Region B domain). Due to the low levels of CES-1, HLH-2/HLH-3 binds to the Region B domain to promote transcription of *egl-1* and to initiate the apoptotic process in the NSMsc. Conversely, excessive CES-1 binds to the Region B domain to prevent HLH-2/HLH-3 from binding to the Region B domain and this inhibits the transcription of *egl-1* in the NSM. (C) CES-1 Snail binds to the regulatory element of *cdc-25.2* to inhibit transcription in the NSMnb. (D) CES-1 Snail positively or negatively regulates an unknown target to control the establishment of cell polarity in the NSMnb.

8. *pig-1* MELK functions in *C. elegans*

Maternal embryonic leucine zipper kinase (MELK) encodes a serine/threonine kinase, which was first identified from cDNA libraries generated from mice using unfertilized oocytes and preimplantation embryos (Heyer *et al.* 1997). The determination of the protein structure of human MELK enabled us to study the functions of MELK orthologs in different organisms. Because of the serine/threonine kinase domain at the N-terminus, MELK is classified as a member of the AMPK/Snf1 superfamily (Heyer *et al.* 1999). The protein structure of MELK is highly conserved across a variety of mammalian and non-mammalian organisms (Figure 9) (Cordes *et al.* 2006; Ganguly *et al.* 2015), but the biological function appears to be distinct in different organisms. In mammals, MELK has been shown to be involved in cell cycle progression, stem cell proliferation, spliceosome assembly and carcinogenesis (Vulsteke *et al.* 2004; Nakano *et al.* 2005; Badouel *et al.* 2010; Du *et al.* 2014). In non-mammals, such as *Zebra fish* and *Xenopus* (Blot *et al.* 2002; Saito *et al.* 2005; Le Page *et al.* 2011), MELK has been reported to affect the progression of cell division, propagation and homeostasis of some organ-specific stem cells. However, recent studies in *C. elegans* revealed that MELK plays a role in controlling cell polarity and cell fate in certain neuroblasts (Cordes *et al.* 2006; Wei *et al.* 2017), which has not been described in other organisms.

pig-1 is a *par-1*-like gene, which encodes the sole *C. elegans* ortholog of MELK. As mentioned above, PAR-1 belongs to the serine/threonine kinase superfamily and is important for the establishment of cell polarity in the one-cell stage embryo (Guo and Kemphues 1995). Similar to other members of the AMPK/Snf1 family, *pig-1* MELK also encodes a serine/threonine kinase that has a kinase domain at its N-terminus and a kinase-associated (KA) domain at its C-terminus. According to studies in mammals, the activity of AMPK/Snf1 family members depends on their phosphorylation status, and they are substrates of LKB1 kinase (Lizcano *et al.* 2004). LKB1 encodes a serine/threonine kinase that is highly conserved across various organisms and plays critical roles in the progression of tumorigenesis. Through further study, LKB1 was discovered to act together with a pseudokinase, STRAD, and an adaptor protein, MO25, in a complex (Baas *et al.* 2003; Boudeau *et al.* 2003). With combination of these two factors, LKB1 activates diverse downstream kinases through phosphorylating some conserved threonine residues in their activation loop (Hawley *et al.* 2003). After studying the orthologs of mammalian LKB1 (PAR-4), STRAD (STRD-1) and MO25 (MOP-25.1 and MOP-25.2) in *C. elegans*, the Garriga lab discovered that the *par-*

4/strd-1/mop-25.2 complex regulates the kinase activity of *pig-1* MELK by phosphorylating a conserved threonine (T169) residue (Chien *et al.* 2013). This phosphorylation is important for the activity of *pig-1* MELK to control the asymmetric positioning of the cleavage plane as well as the fate of the daughter cells in the HSN/PHB, the QL and the QR neuroblast lineages. However, loss of *mop-25.1* did not result in any defects in these lineages. In addition, HAM-1, which has a winged helix DNA binding domain, has been reported to act upstream of *pig-1* MELK to control the asymmetric cell division by positively regulating the transcription of the *pig-1* gene in the HSN/PHB and the Q.p lineages (Frank *et al.* 2005; Feng *et al.* 2013b). The factors mentioned above are positive regulators of *pig-1* MELK in *C. elegans*, while the negative regulators of *pig-1* MELK *in vivo* are unclear so far.

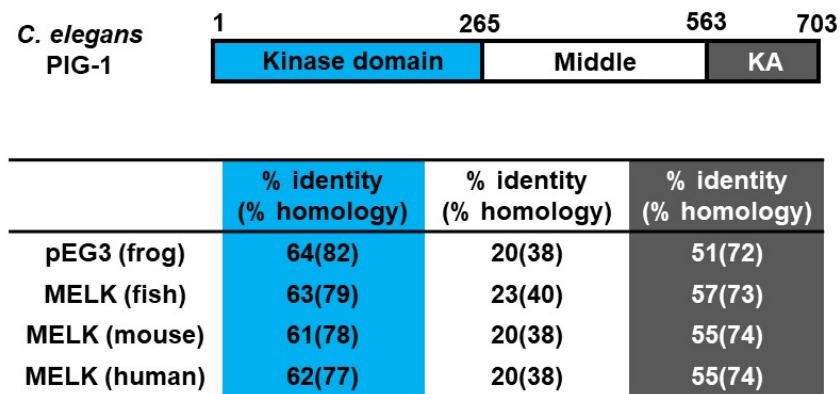


Figure 9. Schematic of PIG-1 protein and % identity and (conserved) residues of *C. elegans* PIG-1 protein compared to MELK from other organisms. Schematic diagram of domain architecture of the PIG-1 protein, depicting the N-terminal kinase domain (blue color) and the C-terminal kinase-associated (KA) domain (grey color). The sizes of each domain are shown above the diagram. Below the diagram is a table comparing each domain of PIG-1 to orthologs in frog, fish, mouse and human.

Caenorhabditis elegans CES-1 Snail Represses *pig-1* MELK Expression To Control Asymmetric Cell Division

Hai Wei,^{*1} Bo Yan,^{*1,2} Julien Gagneur,^{†,3,4} and Barbara Conradt^{*4}

^{*}Center for Integrated Protein Science Munich – CIPSM, Department Biology II, Ludwig-Maximilians-University Munich, 82152 Planegg-Martinsried, Germany and [†]Gene Center Munich, Ludwig-Maximilians-University Munich, 81377 Munich, Germany

ABSTRACT Snail-like transcription factors affect stem cell function through mechanisms that are incompletely understood. In the *Caenorhabditis elegans* neurosecretory motor neuron (NSM) neuroblast lineage, CES-1 Snail coordinates cell cycle progression and cell polarity to ensure the asymmetric division of the NSM neuroblast and the generation of two daughter cells of different sizes and fates. We have previously shown that CES-1 Snail controls cell cycle progression by repressing the expression of *cdc-25.2* CDC25. However, the mechanism through which CES-1 Snail affects cell polarity has been elusive. Here, we systematically searched for direct targets of CES-1 Snail by genome-wide profiling of CES-1 Snail binding sites and identified >3000 potential CES-1 Snail target genes, including *pig-1*, the ortholog of the oncogene maternal embryonic leucine zipper kinase (MELK). Furthermore, we show that CES-1 Snail represses *pig-1* MELK transcription in the NSM neuroblast lineage and that *pig-1* MELK acts downstream of *ces-1* Snail to cause the NSM neuroblast to divide asymmetrically by size and along the correct cell division axis. Based on our results we propose that by regulating the expression of the MELK gene, Snail-like transcription factors affect the ability of stem cells to divide asymmetrically and, hence, to self-renew. Furthermore, we speculate that the deregulation of MELK contributes to tumorigenesis by causing cells that normally divide asymmetrically to divide symmetrically instead.

KEYWORDS Snail-like transcription factor; ChIP-seq; maternal embryonic leucine zipper kinase (MELK); asymmetric cell division; *Caenorhabditis elegans*

SNAIL-LIKE zinc-finger transcription factors are critical for animal development and their deregulation has been implicated in tumorigenesis and metastasis (Barrallo-Gimeno and Nieto 2009; Puisieux *et al.* 2014; Nieto *et al.* 2016). The best-known function of Snail-like transcription factors is their role in orchestrating epithelial-mesenchymal transitions (EMTs), which are essential for development. Through EMTs, epithelial cells are converted into mesenchymal cells, which lack apico-basal polarity but have migratory properties, and thus contribute to the formation of various tissues and organs. In this context, Snail-like transcription factors directly repress the transcription of genes required for

apico-basal polarity and cell adhesion and thereby promote the induction of EMT. Snail-like transcription factors have also been shown to regulate fundamental processes such as cell proliferation and cell survival in animals as diverse as nematodes and mammals (Metzstein and Horvitz 1999; Yan *et al.* 2013; Puisieux *et al.* 2014). Recently, Snail-like transcription factors have also been implicated in various aspects of stem cell function (Guo *et al.* 2012; Desgrosellier *et al.* 2014; Hwang *et al.* 2014; Lin *et al.* 2014; Horvay *et al.* 2015; Ye *et al.* 2015; Tang *et al.* 2016). There is mounting evidence that in stem cell lineages, Snail-like transcription factors can promote not only self-renewal and, hence, the maintenance of an undifferentiated state, but also cell fate specification and, hence, the acquisition of a differentiated state. How the functions of Snail-like transcription factors in stem cell lineages are controlled, and through what mechanisms Snail-like transcription factors affect various aspects of stem cell function, remains largely unknown.

In *Caenorhabditis elegans*, the function of the Snail-like transcription factor CES-1 has been studied in the neurosecretory motor neuron (NSM) neuroblast lineage. About 410 min after the first cleavage of the *C. elegans* zygote, the NSM neuroblast

Copyright © 2017 by the Genetics Society of America

doi: <https://doi.org/10.1534/genetics.117.202754>

Manuscript received April 10, 2017; accepted for publication June 16, 2017; published Early Online June 26, 2017.

Available freely online through the author-supported open access option.

Supplemental material is available online at www.genetics.org/lookup/suppl/10.1534/genetics.117.202754/-/DC1.

¹These authors contributed equally to this work.

²New England Biolabs, Ipswich, MA 01938.

³Present address: Department of Informatics, Technical University Munich, 85748 Garching, Germany.

⁴Corresponding authors: E-mail: conradt@bio.lmu.de; and gagneur@in.tum.de

(NSMnb) divides asymmetrically by size and fate and gives rise to a larger daughter, the NSM, which differentiates into a serotonergic motor neuron, and a smaller daughter, the NSM sister cell (NSMsc), which dies within ~20 min (Sulston *et al.* 1983). The gene *ces-2* encodes a bZIP transcription factor similar to the mammalian Hepatic Leukemia Factor (HLF) and acts as a negative regulator of *ces-1* Snail expression in the NSM neuroblast lineage (Metzstein *et al.* 1996; Metzstein and Horvitz 1999; Hatzold and Conradt 2008). Loss-of-function (lf) mutations of *ces-2* HLF or a gain-of-function (gf) mutation of *ces-1* Snail (*n703gf*) cause the NSMnb to divide symmetrically to give rise to two daughter cells of similar sizes (Ellis and Horvitz 1991; Hatzold and Conradt 2008). [The *n703gf* mutation is located in a *cis*-regulatory region of the *ces-1* gene and, as shown for *ces-2*(lf) mutations, presumably causes the mis- or overexpression of the *ces-1* gene in the NSM neuroblast lineage (Metzstein and Horvitz 1999; Hatzold and Conradt 2008).] In addition, presumably as a result of redundantly acting factors, the loss of *ces-1* does not appear to cause defects in the NSM neuroblast lineage; however, the loss of *ces-1* does suppress defects in the NSM neuroblast lineage caused by the loss of *ces-2* HLF (Ellis and Horvitz 1991). Moreover, rather than dividing along the ventral-lateral to dorsal-medial axis, in *ces-2* lf or *ces-1* gf animals, the NSMnb divides along different axes (Hatzold and Conradt 2008). Furthermore, a weak lf mutation of the gene *cya-1*, which encodes *C. elegans* Cyclin A, prevents the division of some NSMnbs, and this effect is greatly enhanced by the loss of *ces-2* or by *ces-1*(*n703gf*) (Yan *et al.* 2013). Therefore, it has been proposed that in the NSMnb, *ces-1* Snail coordinates cell polarity and cell cycle progression to allow the NSMnb to divide asymmetrically along the appropriate axis. Finally, *ces-1* Snail affects cell cycle progression in the NSMnb by directly repressing the transcription of the *cdc-25.2* gene, which encodes a *C. elegans* CDC25 phosphatase protein (Kim *et al.* 2010; Yan *et al.* 2013). The mechanism through which *ces-1* Snail affects cell polarity in this lineage is currently unknown.

In this study, we report results from our analysis of CES-1 Snail ChIP-seq data, which were acquired as part of the modENCODE project (Gerstein *et al.* 2010). Genome-wide profiling of CES-1 Snail binding sites identifies >3000 potential target genes in mixed-stage *C. elegans* embryos. In addition, gene ontology analysis of potential CES-1 Snail target genes confirms known and predicts novel functions of CES-1 Snail. Furthermore, we investigate the function of one potential CES-1 Snail target gene, the gene *pig-1*, which encodes an AMP-activated protein kinase (AMPK)-related protein kinase most similar to maternal embryonic leucine zipper kinase (MELK). We find that *pig-1* MELK acts downstream of *ces-1* Snail to cause the NSMnb to divide asymmetrically by size and along the correct axis.

Materials and Methods

ChIP-Seq data processing and analysis

The raw sequencing files of the CES-1 ChIP-seq experiments were obtained from the modENCODE website (DCCid;

modENCODE 3857). The alignment and all analyses were based on *C. elegans* genome WS220. Raw sequencing data from CES-1 ChIP-seq experiments were mapped to the *C. elegans* genome using bowtie2 (Langmead and Salzberg 2012). For each sample, the numbers of total and mapped reads are shown in Supplemental Material, Table S1. After mapping reads to the genome, peak calling algorithm MACS2 (Zhang *et al.* 2008) was used to identify regions of ChIP enrichment. Each biological repeat and corresponding control was used as treatment and control, respectively. The following parameters were used to predict CES-1 binding sites: *q*value (minimum FDR) cutoff 0.01 and *mfold* “5,50.” MACS2 reported the summit, localization, and fold change of each binding site (peak). To measure the consistency from replicated experiments and identified reproducible binding sites, the IDR (irreproducible discovery rate) was calculated between the two repeats as described (Li *et al.* 2011). Only the reproducible binding sites (IDR cut-offs 0.1) were used for subsequent analysis. To show the concordance of the two repeats, correlation analysis was performed for the fold change of each pair of reproducible peaks (Figure 2A). The reproducible peaks from the two repeats were merged for downstream analysis.

The potential target genes of CES-1 were identified using the following criteria: if a merged peak is located in the transcription unit or within the 5' promoter region (2 kb upstream of transcription start site) of a gene, this gene was defined as a potential target. The potential target genes were used for gene ontology (GO) analysis using DAVID6.8 (Huang *et al.* 2009) at biological level 4. The overrepresented GO terms of CES-1 were compared with the overrepresented GO terms of 10 additional transcription factors (embryonic stage) (PHA-4, NHR-2, BLMP-1, ELT-3, LIN-13, CEH-39, GEI-11, MED-1, CES-1, MEP-1, LSY-2) (Table S3). The potential targets of these transcription factors were predicted using the same criteria based on the peaks reported by the modENCODE pipeline. The interpreted data files (gff3) containing the binding sites for each transcription factor were downloaded from modENCODE database (<http://www.modencode.org>).

Strains and genetics

All *C. elegans* strains were maintained at 20° as described in Brenner (1974). Bristol N2 was used as the wild-type strain. The following mutations and transgenes were used: LGI: *ces-1* (*n703gf*) *ces-1*(*n703 n1434*) (Ellis and Horvitz 1991), *ces-1*(*tm1036*) (Yan *et al.* 2013), *ces-2*(*bc213*) (Hatzold and Conradt 2008); LGII: *bcSi50* (*P_{ces-1}ces-1::yfp*) (this study), *bcSi43* (*P_{pig-1}gfp*) (this study), *ltIs202* (*P_{spd-2}gfp::spd-5*) (Woodruff *et al.* 2015); LGIII: *bcls66* (*P_{tph-1}his-24::gfp*) (Yan *et al.* 2013); LGIV: *pig-1*(*gm344*) (Cordes *et al.* 2006), *pig-1*(*tm1510*) (National BioResource Project; <https://shigen.nig.ac.jp/c.elegans/>); and LGV: *ltIs44* (*P_{pie-1}mCherry::ph^{PLCδ}*) (Audhya *et al.* 2005).

Molecular biology

Plasmid pBC1531 (*P_{pig-1}gfp*) was generated using Gibson cloning. Briefly, using the primer pairs Ppig-1 vec F and Ppig-1

gfp R, Ppig-1 gfp F and gfptbb2gb R, and gfp tbb-2utr F and 4BP-SpeI-tbb-2 r' UTR, three DNA fragments (*pig-1* promoter/5' upstream region, *gfp* and *tbb-2* 3'UTR) were generated and combined using the primers Ppig-1 vec F and 4BP-SpeI-tbb-2 r' UTR. The resulting full-length fragment was then cloned into MosSCI vector pCFJ350 (Frokjaer-Jensen *et al.* 2012) sites AvrII and SpeI using T4 ligase to generate plasmid pBC1531 ($P_{pig-1}gfp$). Plasmid pBC1448 ($P_{ces-1}ces-1::yfp$) was generated by digesting the full-length *ces-1* rescuing fragment from pBC510 (Hatzold and Conradt 2008) using *ApaI* and *SmaI* enzymes, and inserting this fragment into MosSCI vector pCFJ350.

Transgenic animals

Germline transformations were performed as described in Mello and Fire (1995). For the generation of the $P_{pig-1}gfp$ MosSCI lines, plasmid pBC1531 was injected at a concentration of 10 ng/ μ l with the co-injection markers pCFJ601 at 50 ng/ μ l, pGH8 at 10 ng/ μ l, pCFJ90 at 2.5 ng/ μ l, and pCFJ104 at 5 ng/ μ l into the Universal MosSCI strain EG8079 (Frokjaer-Jensen *et al.* 2014) and integrated (single copy) on chromosome II to generate *bcSi43*. For the generation of the $P_{ces-1}ces-1::yfp$ MosSCI line, plasmid pBC1448 was injected at a concentration of 10 ng/ μ l with the co-injection markers pCFJ601 at 50 ng/ μ l, pGH8 at 10 ng/ μ l, pCFJ90 at 2.5 ng/ μ l, and pCFJ104 at 5 ng/ μ l into the MosSCI strain EG6699 (Frokjaer-Jensen *et al.* 2012) and integrated (single copy) on chromosome II to generate *bcSi50*.

Phenotypic analyses and microscopy

The number of surviving NSMsc was determined in L4 larvae using the *bciS66* ($P_{tph-1}his-24::gfp$) transgene as described in Yan *et al.* (2013). NSM and NSMsc volume and the position and orientation of the NSMnb division were analyzed using the *ltIs44* ($P_{pie-1}mCherry::ph^{PLC\delta}$) transgene essentially as described (Chakraborty *et al.* 2015). The orientation of the NSMnb cleavage plane was additionally analyzed using *ltIs44* in combination with the *ltSi202* ($P_{spd-2}gfp::spd-5$) transgene, with which the position of the two centrosomes prior to cell division can be observed. Imaging was performed as follows. Embryos were imaged using a Leica TCS SP5 II confocal microscope. For all confocal imaging, the laser power setting was kept constant. Before confocal recording, all strains were incubated at 20° overnight. Six to ten adults were dissected to obtain mixed-stage embryos and embryos were mounted on 2% agar pads. Slides were sealed with petroleum jelly to avoid drying out and incubated at 25° until the embryos reached the comma stage of development. For all reporters, a Z-stack of 8–8.5 μ m with a step size of 0.5 μ m was used to record the NSMnb and its two daughter cells. Recording was started before NSMnb division and continued postcytokinesis. For determining “Dorsal-lateral/2nd cell volume ratio” and the orientation of the NSMnb cleavage plane, a noise reduction function was applied using the Leica Application Suite (LAS) software to remove background. To determine the cell volume of the NSM and the NSMsc, the ventral-medially located NSM and the dorsal-laterally located NSMsc

were identified by following the division of the NSMnb. After completion of cytokinesis, for every Z-slice, a region of interest (ROI) was drawn around the cell boundary of either the NSM or the NSMsc, the area of the ROI was determined for every Z-slice, and all areas of a certain cell summed up to obtain an estimate of the cell volume. The “Dorsal-lateral/2nd cell volume ratio” was determined by dividing the volume of the daughter located dorsal-laterally (the NSMsc and its derivatives) by the volume of the 2nd daughter (the NSM and its derivatives). The expression of the *bcSi43* ($P_{pig-1}gfp$) transgene was quantified in the NSMnb before division using the *ltIs44* ($P_{pie-1}mCherry::ph^{PLC\delta}$) transgene to mark the boundary of the NSMnb cell membrane. Quantification of *bcSi43* expression was performed on raw confocal images. Following confocal acquisition, for every Z-slice in which a distinct cell boundary of the NSMnb could be seen, the intensity of GFP fluorescence within the cell boundary was determined by drawing a ROI. The intensities of GFP fluorescence obtained for all Z-slices of a certain cell (six Z-slices) were summed up to obtain the total GFP fluorescence intensity of that particular cell. Total GFP fluorescence intensity was then divided by the total area of the ROI in the six Z-slices of that cell to obtain GFP concentration (fluorescence intensity/ μ m²). The same procedure was used to determine GFP concentration in animals carrying the *bcSi43* ($P_{pig-1}gfp$) transgene in Z3 (p4a). The mean “GFP concentration” of background signal obtained from a control strain only carrying the *ltIs44* ($P_{pie-1}mCherry::ph^{PLC\delta}$) transgene (1.7 fluorescence intensity/ μ m²) was too low to influence the GFP concentration of +/+, *ces-1(n703gf)*, +/+¹, *ces-1(tm1036)*, and +/+² during recordings. The same confocal laser power setting was used for the control and all experimental strains (+/+, *ces-1(n703gf)*, +/+¹, *ces-1(tm1036)*, and +/+²).

Data availability

The raw sequencing files of the CES-1 ChIP-seq experiments are available on the modENCODE website (DCCid; modENCODE 3857). The worm strains and reagents used in this study are available on request.

Results

To systematically identify CES-1 Snail binding sites in the *C. elegans* genome, we analyzed ChIP-seq (chromatin immuno-precipitation combined with massively parallel DNA sequencing) data that had been generated as part of the modENCODE Project (Gerstein *et al.* 2010). As previously described, for ChIP-seq experiments, the modENCODE Project used stable transgenic *C. elegans* lines, each of which carries a transgene (for example, $P_{ces-1}ces-1::gfp$ referred to as “*wgIs174*”) that mediates the synthesis of a specific, GFP-tagged *C. elegans* transcription factor (*i.e.*, CES-1::GFP) under the control of its endogenous promoter and *cis*-regulatory regions (Sarov *et al.* 2006, 2012). Chromatin bound by GFP-tagged protein was precipitated using an anti-GFP antibody and subjected to Illumina-based sequencing following the

modENCODE pipeline (Zhong *et al.* 2010). The nonprecipitated chromatin, which represents the total genomic DNA (input), was used as control. As starting material for CES-1::GFP ChIP-seq experiments, the modENCODE project used mixed-stage embryos. Finally, we obtained the *wgls174* transgene and confirmed that it is expressed in appropriate cells during embryogenesis, such as cells of the developing pharynx (Figure S1).

Identification and characterization of CES-1 Snail binding sites

The modENCODE project performed CES-1::GFP ChIP-seq experiments in two independent biological replicates (Repeat1 and Repeat2). This led to a data set of ~7 million total reads in each replicate (Table S1), which provides sufficient coverage for ChIP-seq experiments of *C. elegans* transcription factors (Landt *et al.* 2012). Here, we analyzed this data set following the ENCODE and modENCODE guidelines (Landt *et al.* 2012). The reads of the two biological replicates and the corresponding controls were aligned with the *C. elegans* genome (WS220) and subjected to peak calling using MACS2 (Zhang *et al.* 2008). The CES-1 binding sites (peaks) were visualized using Integrative Genomics Viewer (IGV) (Robinson *et al.* 2011). As shown for chromosome IV in Figure 1A, the two biological replicates generated highly similar binding profiles. The reproducibility of the data was assessed by estimating the IDR between the replicates (Landt *et al.* 2012). Applying FDR (false discovery rate; calculated and reported by MACS2) and IDR cut-offs of ≤ 0.01 and ≤ 0.1 , respectively, we identified 3417 reproducible CES-1 binding sites. Furthermore, for reproducible peaks, we found that the fold change of CES-1 binding is highly correlative (Pearson correlation 0.83) (Figure 2A). In addition, for the majority of reproducible peaks, the peak summits obtained from the two replicates are located within 100 bp of each other (Figure 2B), which indicates good concordance between the replicates. For subsequent analyses, we used the “merged peak” of reproducible peaks, which is generated by combining each pair of reproducible peaks.

The majority of merged peaks have lengths in the range of 200–500 bp (Figure 2C). Using MEME-chip (Bailey *et al.* 2009), we determined motifs enriched in these merged peaks. One motif identified [CAGC(T/A)GC] is similar to the classical Snail binding site (CAGGTG) (Figure 3), which has previously been shown to function as a CES-1 binding site (Metzstein and Horvitz 1999; Thellmann *et al.* 2003; Reece-Hoyes *et al.* 2009). In addition, we identified two *de novo* motifs [AAT(T/G/C)(A/C/G)AAT and AGACG(C/G)AG], which are significantly enriched (Figure 3) and which have previously not been shown to act as CES-1 binding sites. Finally, we evaluated the locations of the CES-1 peaks relative to protein-coding transcripts and observed a small yet significant enrichment of CES-1 peaks within 2 kb of transcriptional start sites (TSS) (67 vs. 62% for spatially randomized peak positions, P -value ≤ 0.0001 ; Figure 2D).

Identification of potential CES-1 Snail target genes

The proximity of a binding site to the promoter is currently the best indicator for functional relevance. According to WS220, the genome size of *C. elegans* is 100 megabases (Mb) and contains 20,389 protein-coding genes. Genes are often located <2 kb from each other, either on the same or opposite strands. Furthermore, in most cases, the *cis*-regulatory regions sufficient for proper gene expression lie within 2 kb upstream of the TSS (Reinke *et al.* 2013). Therefore, if a CES-1 peak is located within the transcription unit or within 2 kb upstream of the TSS of a gene, this gene can be considered a potential CES-1 target gene. Using these criteria, >80% of the CES-1 peaks have at least one potential target gene, and a total of 3199 genes are identified as potential CES-1 target genes (Table S2). Among these target genes are classical Snail targets such as the gene *hmr-1*, which encodes *C. elegans* E-cadherin, and *sax-7*, which encodes the *C. elegans* ortholog of the human cell adhesion transmembrane-receptor L1 CAM (Puisieux *et al.* 2014; Nieto *et al.* 2016).

Gene ontology analysis of potential CES-1 Snail target genes

We performed GO analysis using the NIH Database for Annotation, Visualization, and Integrated Discovery (DAVID) (Huang *et al.* 2009) to identify the “biological processes” (at Level 4) that are enriched among potential CES-1 target genes. This identified “cell cycle process” and “programmed cell death” among the most highly enriched processes (Table S3) confirming results from previous studies of *ces-1* function (Ellis and Horvitz 1991; Thellmann *et al.* 2003; Yan *et al.* 2013) (see below). GO analysis also predicts novel functions of *ces-1* Snail. For example, CES-1 target genes are overrepresented in biological processes related to sexual differentiation, aging, nervous system development, and cell signaling. Furthermore, we selected 50 of the most highly enriched “biological processes” and assessed their enrichment among the potential target genes of 10 other *C. elegans* transcription factors for which embryonic ChIP-seq data sets are available from modENCODE (BLMP-1, CEH-39, ELT-3, GEI-11, LIN-13, LYS-2, NHR-2, MED-1, MEP-1, and PHA-4) (Figure 4 and Table S3). Broad GO terms that are related to animal development (such as “larval development,” “embryo development,” “system development,” or “animal organ development”) are enriched among the target genes of most of these transcription factors as expected due to the known importance of transcription factors during development. Compared to the other transcription factors, CES-1 shares more similarities with the FoxA transcription factor PHA-4, the homeodomain transcription factor CEH-39, and the zinc-finger transcription factor LIN-13, which act as organ identity factor (PHA-4), X chromosome-signal element (CEH-39), and cell fate regulator (LIN-13), respectively (Figure 4) (Horner *et al.* 1998; Melendez and Greenwald 2000; Gladden and Meyer 2007).

CES-1 Snail affects the ability of the NSMnb to divide asymmetrically; however, the target gene or genes of CES-1 Snail in

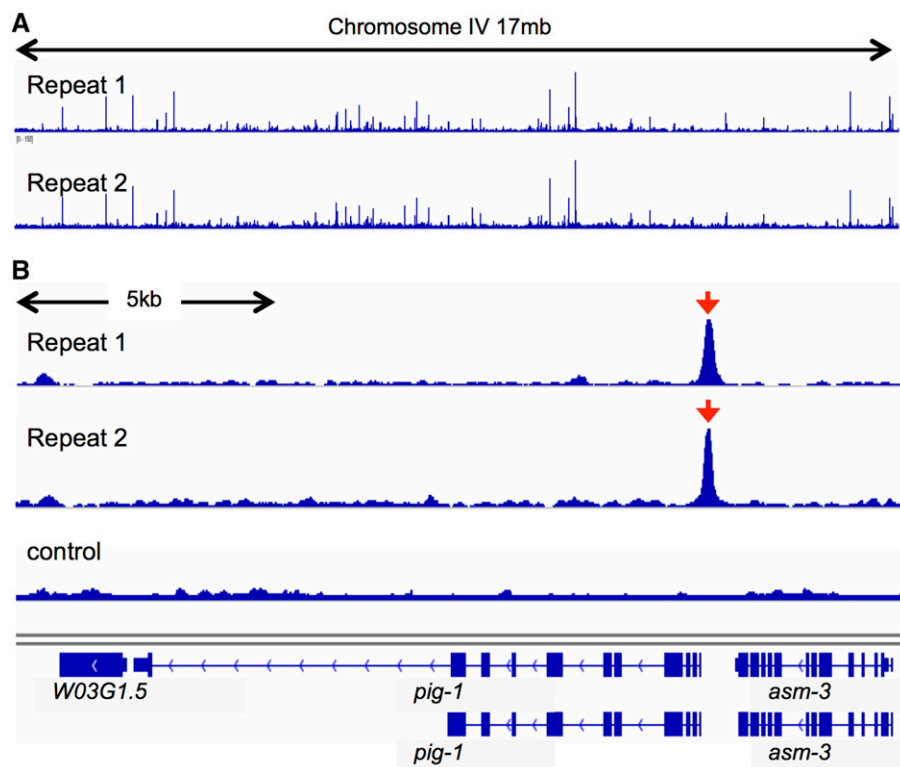


Figure 1 Visualization of CES-1 binding sites. CES-1 peaks from two biological replicates were predicted using MACS2 and visualized using IGV. (A) Overview of all CES-1 binding sites on chromosome IV. (B) Representative CES-1 binding sites in 20-kb region on chromosome IV that spans the *pig-1* locus. Red arrows point to the CES-1 binding sites.

this context are unknown. For this reason, we screened biological processes enriched among CES-1 Snail target genes for processes related to asymmetry and cell polarity and identified “asymmetric cell division” as highly enriched (enrichment of P -value $9.70E-04$) (Table S3). Furthermore, among the target genes associated with “asymmetric cell division” (Table S5), we identified the gene *pig-1*, which is also associated with “programmed cell death” (enrichment of P -value $2.25E-18$) (Table S4). *pig-1* encodes an AMP-activated protein kinase (AMPK)-related protein kinase most similar to MELK (Cordes *et al.* 2006; Ganguly *et al.* 2015). Interestingly, the *pig-1* MELK gene has previously been implicated in the asymmetric division of a number of *C. elegans* neuroblasts that divide to generate a smaller daughter that dies (Cordes *et al.* 2006) and in the programmed elimination of cells during *C. elegans* embryogenesis (Denning *et al.* 2012; Hirose and Horvitz 2013). Finally, the CES-1 Snail binding site profile revealed that there is a strong binding site just upstream of the TSS of the *pig-1* MELK gene (Figure 1B).

***ces-1* Snail represses *pig-1* MELK expression in the NSM neuroblast lineage**

To test whether CES-1 Snail controls *pig-1* MELK expression in the NSM neuroblast lineage, we generated a transcriptional reporter in which the expression of the *gfp* gene is driven by an 850-bp fragment that spans bp -1 to bp -850 of the region immediately upstream of the *pig-1* TSS ($P_{pig-1gfp}$) (Figure 1B). (This 850-bp fragment covers the CES-1 binding site identified through ChIP-seq.) We generated a stable transgenic *C. elegans* line carrying a single copy of this reporter (MossSCI allele) and analyzed *gfp* expression in the

NSMnb. We found that in wild-type animals, *gfp* is expressed at a low level in the NSMnb (Figure 5, A and B; $+/+$). This level was reduced by $\sim 20\%$ in animals homozygous for the *ces-1* *gf* mutation *n703gf*. To confirm that this decrease was specific to the presence of the *ces-1* *gf* mutation, we outcrossed this strain to remove *n703gf* ($+/+$), and this brought the level of *gfp* expression back to that observed in the wild type. Furthermore, the level of *gfp* expression was increased by $\sim 25\%$ in animals homozygous for the *ces-1* *lf* mutation *tm1036*, and outcrossing to remove *tm1036* ($+/+$) confirmed that this increase is specific to the loss of *ces-1* (Figure 5, A and B). Finally, we analyzed *gfp* expression of the $P_{pig-1gfp}$ transgene in a second cell, Z3 (p4a). As shown in Figure S2, *gfp* expression in Z3 was not affected by the *ces-1* mutations. Based on these results, we conclude that *ces-1* Snail represses *pig-1* MELK transcription and, hence, *pig-1* MELK expression in the NSMnb.

***pig-1* MELK is required for the correct position of the NSMnb cleavage plane**

To determine whether *ces-1* Snail affects the asymmetric division of the NSMnb by acting through *pig-1* MELK, we analyzed the NSM neuroblast lineage in animals homozygous for strong *lf* mutations, *pig-1(gm344)* and *pig-1(tm1510)* (Cordes *et al.* 2006). [Both alleles are deletions that remove 524 bp (*gm344*; bp -381 to bp $+143$) or 1487 bp (*tm1510*; bp $+178$ to bp $+1664$) of the *pig-1* locus, respectively (Figure S3).] First, we analyzed the position of the cleavage plane during NSMnb division. In wild-type animals, the cleavage plane is shifted toward the dorsal-lateral side of the NSMnb (Sulston *et al.* 1983). Consequently, the NSMnb divides

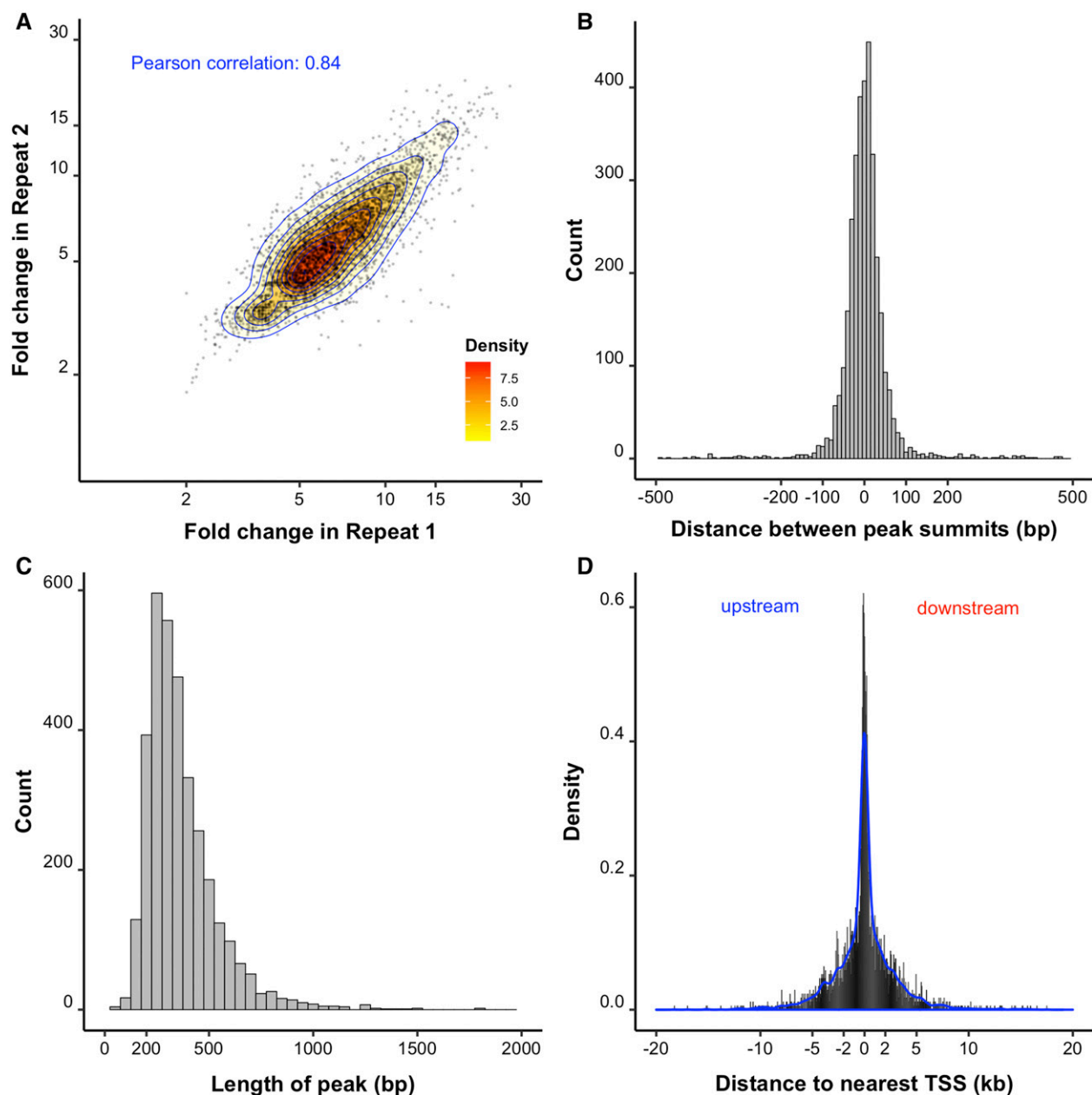


Figure 2 Characterization of CES-1 binding sites. CES-1 peaks were predicted using MACS2. (A) Density plot comparison between the fold change (fold enrichment for the peak summit against random Poisson distribution with local lambda, calculated by MACS2) of reproducible peaks from Repeat 1 and Repeat 2. Reproducible peaks from two biological replicates were identified using IDR cut-offs ≤ 0.1 . Each dot represents a reproducible peak. Log 10 scale is used for x and y axis. (B) Distribution of the distances (in base pairs) between the summits of pairs of reproducible peaks. Reproducible peaks from two biological replicates were identified using IDR cutoff ≤ 0.1 . (C) Distribution of the lengths (in base pairs) of the merged peaks. (D) Distribution of the distances (in kilobases) between CES-1 binding sites (peak summits of the merged peaks) and the TSS of the nearest protein-coding transcripts.

asymmetrically by size to give rise to a smaller daughter located dorsal-laterally, the NSMsc, and a larger daughter located ventral-medially, the NSM, with an average ratio of NSMsc to NSM volume of 0.69 (Figure 6). As shown below, mutations in *ces-2*, *ces-1*, and *pig-1* not only affect the position of the NSM cleavage plane, but also its orientation (Figure 7). However, regardless of the orientation of the cleavage plane, one cell (presumably the NSMsc) immediately moves into the dorsal-lateral position. For this reason, we determined the volume ratio of the two daughter cells by dividing the volume

of the daughter located dorsal-laterally by the volume of the other or “2nd” daughter (presumably the NSM) and refer to this ratio as “dorsal-lateral/2nd cell volume ratio” (Figure 6).

As shown previously, in animals homozygous for a 1f mutation of *ces-2* (*bc213*) or the *ces-1* gf mutation *n703gf*, the NSMnb divides symmetrically with an average dorsal-lateral/2nd cell volume ratio of 1.05 and 1.08, respectively (Figure 6) (Hatzold and Conradt 2008). We found that in *pig-1*(*gm344*) or *pig-1*(*tm1510*) animals, the NSMnb also divides symmetrically with an average ratio of 1.04 and 1.03,

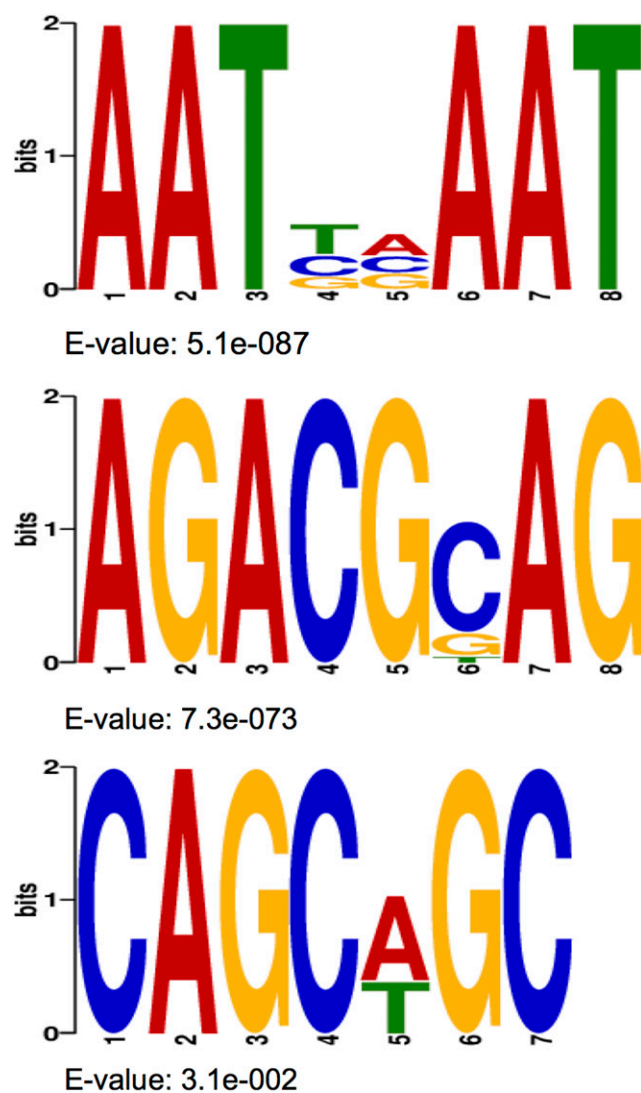


Figure 3 Motifs enriched in CES-1 peaks. Motifs enriched in CES-1 peaks (merged peaks from two biological repeats) were identified using MEME-chip. *E*-value represents fold enrichment. The last motif [CAGCA(T/A)G] is similar to the classic Snail binding site (CAGGTG).

respectively. Therefore, *pig-1* MELK is required for the ability of the NSMnb to divide asymmetrically by size. Furthermore, *ces-1* acts downstream of *ces-2* to affect NSMsc survival, and the loss of *ces-1* completely suppresses the defect in asymmetric NSMnb division observed in *ces-2(bc213)* animals (Figure 6) (Hatzold and Conradt 2008). In contrast, the loss of *ces-1* fails to suppress this defect in *pig-1(gm344)* animals, which indicates that in the NSMnb, *ces-1* Snail does not act downstream of *pig-1* MELK.

***pig-1* MELK is required for the correct orientation of the NSMnb cleavage plane**

Next, we analyzed the orientation of the cleavage plane during NSMnb division. In wild-type animals, the NSMnb divides along the ventral-lateral to dorsal-medial axis so that its daughter cells are positioned dorsal-laterally (NSMsc) and ventral-medially (NSM) (Figure 7). However, as previously

shown, in the majority of *ces-2(bc213)* or *ces-1(n703gf)* animals, different cleavage planes are observed (Figure 7) (Hatzold and Conradt 2008). We observed the same defect in the majority of *pig-1(gm344)* or *pig-1(tm1510)* animals, which demonstrates that *pig-1* MELK is also required for the polarization of the NSMnb and its ability to divide along the ventral-lateral to dorsal-medial axis. Interestingly, we also observed a defect in cleavage plane orientation in animals homozygous for the *ces-1* lf mutation *tm1036*. Specifically, in 44% of *ces-1(tm1036)* animals, the cleavage plane of the NSMnb was shifted by +90° (Type II cleavage) (Figure 7). [This specific shift was also observed in 27% of animals homozygous for another *ces-1* lf mutation, *n703 n1434* (Figure 7B).] Furthermore, the same +90° shift was observed in about half of *ces-1(tm1036); ces-2(bc213)* animals, confirming that *ces-1* is epistatic to *ces-2*. However, in both *pig-1(gm344)* animals and *ces-1(tm1036); pig-1(gm344)* animals, various cleavage planes other than the specific +90° shift were observed in the majority of animals (Figure 7B). Therefore, *pig-1* MELK is epistatic to *ces-1* Snail, which indicates that *pig-1* MELK acts downstream of *ces-1* Snail to affect the orientation and most likely also position of the NSMnb cleavage plane.

***pig-1* MELK function in the NSM neuroblast is haploinsufficient**

As described above, we found that *ces-1(n703gf)* reduces *gfp* expression of the $P_{pig-1gfp}$ transgene by ~20% in the NSMnb whereas the *ces-1* lf mutation *tm1036* increases it by ~25%. This suggests that relatively small differences in the level of *pig-1* expression affect *pig-1* function in the NSMnb and cause a detectable phenotype. To test whether *pig-1* function in the NSMnb is haploinsufficient, we analyzed the position and orientation of the NSMnb cleavage plane in animals heterozygous for *pig-1(gm344)* [*pig-1(gm344)/+*]. As shown in Figure 6B and Figure 7B, we found that *pig-1(gm344)/+* animals exhibit defects similar to the defects observed in homozygous *pig-1(gm344)* animals. Therefore, *pig-1* MELK function in the NSMnb is haploinsufficient.

The loss of *pig-1* MELK has a modest effect on the cell death fate of the NSMsc

Apart from its roles in the NSMnb, *ces-1* Snail also plays a role in the daughters of the NSMnb. Immediately after NSMnb division, CES-1 Snail protein is detectable in the larger NSM, but not in the smaller NSMsc (Hatzold and Conradt 2008). The absence of CES-1 Snail in the NSMsc allows a heterodimer of HLH-2 and HLH-3 (HLH-2/HLH-3) (similar to the *Drosophila melanogaster* bHLH proteins, Daughterless and Achaete-scute, respectively) to activate transcription of the proapoptotic gene *egl-1* BH3-only and thereby trigger NSMsc death (Conradt and Horvitz 1998; Thellmann *et al.* 2003). In contrast, the presence of CES-1 Snail in the NSM blocks the ability of HLH-2/HLH-3 to activate *egl-1* BH3-only transcription and thereby causes NSM survival (Thellmann *et al.* 2003). In *ces-2* lf animals [and most probably in *ces-1(n703gf)* animals], CES-1 Snail protein is present in both

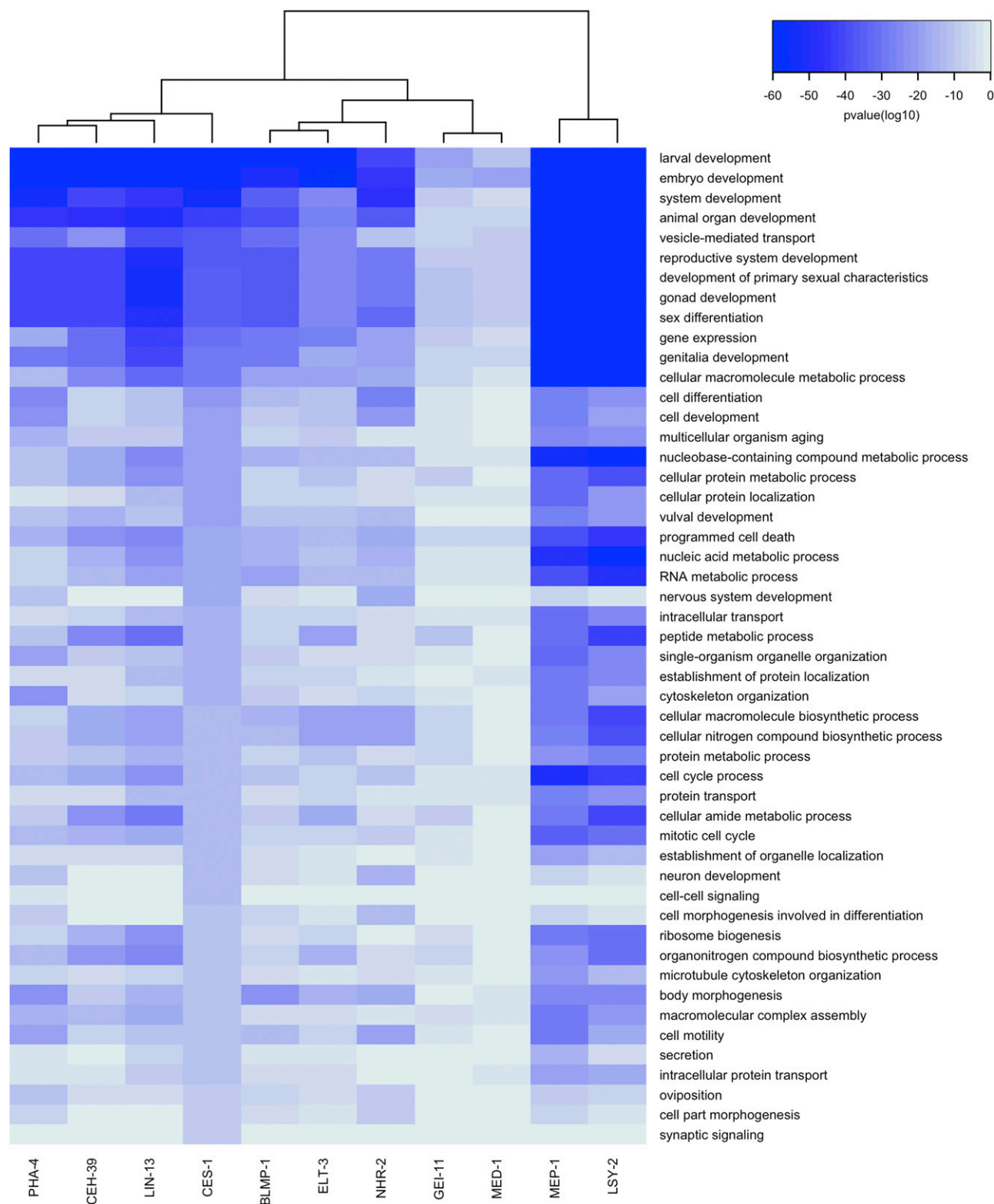


Figure 4 Gene ontology analysis. The potential target genes of PHA-4, NHR-2, BLMP-1, ELT-3, LIN-13, CEH-39, GEI-11, MED-1, CES-1, MEP-1, and LSY-2 were identified based on ChIP-seq experiments using *C. elegans* embryos as starting material that had been performed as part of the modENCODE project. GO analysis was performed at biological process Level 4 using DAVID. The overrepresented GO terms of CES-1 were ranked by *P*-value, and redundant GO categories were removed manually. The top 50 most highly enriched CES-1 GO terms were chosen for comparative GO study. The heat map shows the *P*-values (log 10) of these GO terms for the different transcription factors. The hierarchical clustering (performed based on the average agglomeration method) indicates the correlation between these transcription factors in embryos.

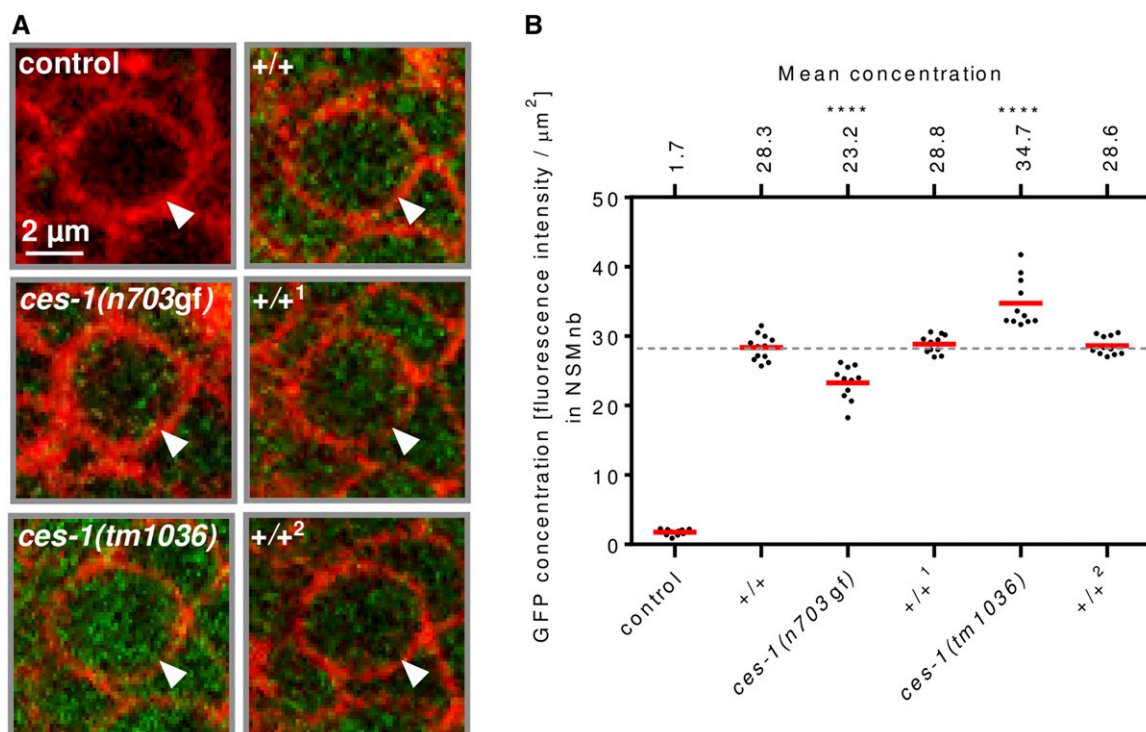


Figure 5 *ces-1* Snail represses *pig-1* MELK expression in the NSMnb. (A) Confocal images of representative NSMnbs at metaphase in control, wild-type (+/+, +/+¹, +/+²), *ces-1(n703gf)*, and *ces-1(tm1036)* animals. Control animals were transgenic for *ItIs44* (P_{pie-1} *mCherry::ph^{PLC β}*) transgene. Wild-type (+/+, +/+¹, +/+²), *ces-1(n703gf)*, and *ces-1(tm1036)* animals were transgenic for *bcSi43* (P_{pig-1} *gfp*) and *ItIs44* (P_{pie-1} *mCherry::ph^{PLC β}*) transgenes. +/+¹ indicates a strain from which *ces-1(n703gf)* was outcrossed. +/+² indicates a strain from which *ces-1(tm1036)* was outcrossed. White arrow heads indicate NSMnb. Bar, 2 μ m. (B) GFP concentration [fluorescence intensity/ μ m²] in NSMnb in control animals (control) and in animals carrying the transgene P_{pig-1} *gfp* (*bcSi43*) in various genetic backgrounds [+/+, *ces-1(n703gf)*, +/+¹, *ces-1(tm1036)*, +/+²] ($n = 11-13$). Each dot represents the GFP concentration in one NSMnb. Red horizontal lines indicate mean concentrations, which are stated on top. Gray dotted line indicates the mean concentration in wild type (+/+). Statistical significance was determined using the Student's *t*-test (**** $P \leq 0.0001$). All statistical analyses were done in comparison to wild type (+/+).

daughters after NSMnb division (Hatzold and Conrardt 2008). Consequently, *egl-1* BH3-only transcription is repressed in both daughters and both daughters survive and differentiate into motor neurons (Ellis and Horvitz 1991; Thellmann *et al.* 2003). Therefore, in the NSMnb daughters, *ces-1* Snail is critically involved in the coordination of cell survival and cell fate specification.

To determine whether *pig-1* MELK also plays a role in cell survival and cell fate specification in the NSMnb daughters, we analyzed the effect of the loss of *pig-1* MELK on the fate of the NSMsc. In wild-type animals, the NSMsc dies (0% NSMsc survival); however, as previously shown (Ellis and Horvitz 1991; Hatzold and Conrardt 2008), in *ces-2(bc213)* or *ces-1(n703gf)* animals, 80.6 or 97.4% of the NSMsc inappropriately survive, respectively (Figure 8A). We found that in *pig-1(gm344)* or *pig-1(tm1510)* animals, 2.1 or 1.2% of the NSMsc survived, respectively. Furthermore, while the loss of *ces-1* completely suppresses NSMsc survival in *ces-2(bc213)* animals (Ellis and Horvitz 1991; Hatzold and Conrardt 2008), it had no effect on the modest NSMsc survival rate in *pig-1(gm344)* animals (Figure 8A), demonstrating that in the NSM neuroblast lineage, *pig-1* MELK acts downstream of *ces-1* Snail in the coordination of cell survival and cell fate specification as well.

Finally, we tested whether the loss of *pig-1* affects the kinetics of the NSMsc death. We found that in the wild type, from the time it is born, it takes the NSMsc an average of 21.9 min to become refractile and, hence, die (Figure 8, B and C). In contrast, in *pig-1(gm344)* or *pig-1(tm1510)* animals, it takes the NSMsc an average of 30.0 or 28.9 min, respectively, to become refractile and die. Therefore, while the loss of *pig-1* MELK only modestly affects the cell death fate of the NSMsc, it decreases the speed with which this fate is executed.

Discussion

Genome-wide profiling of DNA binding sites identifies novel functions of *CES-1* Snail

The binding sites of the *D. melanogaster* Snail transcription factor have previously been identified using chromatin immuno-precipitation combined with microarray analysis (ChIP-on-chip) (Zeitlinger *et al.* 2007; Rembold *et al.* 2014). We analyzed data generated by the modENCODE Project for *C. elegans* *CES-1* Snail using chromatin immuno-precipitation combined with massively parallel DNA sequencing (ChIP-seq) (Gerstein *et al.* 2010). Our analyses indicate that during embryonic development, *C. elegans* *CES-1* Snail may contribute to the transcriptional regulation of >3000 genes. Among these genes

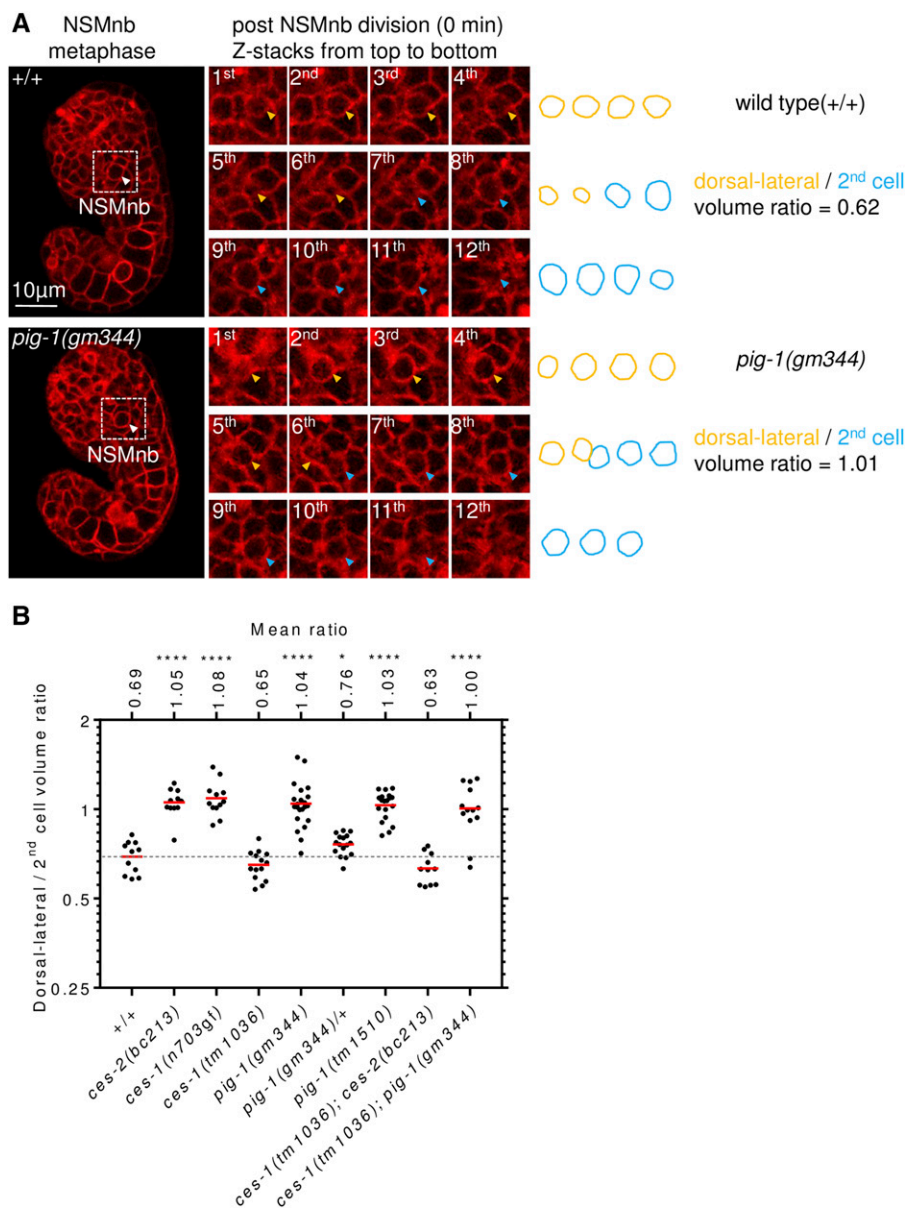


Figure 6 *pig-1* MELK is required for the correct position of the NSMnb cleavage plane. (A) (Left) Fluorescence images of representative wild-type (+/+) and *pig-1(gm344)* embryo carrying the transgene *Itls44* ($P_{pie-1}mCherry::ph^{PLC\beta}$). The white arrows point to the NSMnb, which is at metaphase. Bar, 10 μ m. (Center) Representative series of eight consecutive confocal fluorescence images (Z-stacks, from top to bottom, 0.5- μ m step size) of dorsal-lateral cell and 2nd cell immediately after the NSMnb divided in wild type (+/+) or *pig-1(gm344)*. The orange and blue arrows point to the dorsal-lateral cell or the 2nd cell, respectively. (Right) Schematic representations of the areas of the dorsal-lateral (orange) or 2nd cell (blue) in the consecutive images of the Z-stacks shown in the center and volume ratio of these two representative animals. (B) Volume ratio of dorsal-lateral daughter cell to 2nd daughter cell postcytokinesis in different genotypes [wild type (+/+), *ces-2(bc213)*, *ces-1(n703gf)*, *ces-1(tm1036)*, *pig-1(gm344)*, *pig-1(gm344)/+*, *pig-1(tm1510)*, *ces-1(tm1036); ces-2(bc213)* and *ces-1(tm1036); pig-1(gm344)*] ($n = 12-23$). All strains were homozygous for the *Itls44* ($P_{pie-1}mCherry::ph^{PLC\beta}$) transgene. Each dot represents the ratio of one pair of daughter cells. Red horizontal lines represent the mean ratio obtained for a given genotype, which is stated on top. Gray dotted line indicates the +/+ mean ratio. Statistical significance was determined using the Student's *t*-test (* $P \leq 0.05$, **** $P \leq 0.0001$). All statistical analyses were done in comparison to wild type (+/+).

are genes whose orthologs in *D. melanogaster* and/or mammals are known targets of Snail-like transcription factors, confirming conservation among Snail-like transcription factors of fundamental functions, such as in the control of cell adhesion (Puisieux *et al.* 2014; Nieto *et al.* 2016). Gene ontology analysis of potential *CES-1* target genes also reveals novel functions of *CES-1* Snail; however, the actual contribution of *ces-1* Snail to these biological processes is currently unknown.

Two *CES-1* Snail target genes have previously been described, the BH3-only gene *egl-1* and the CDC25 gene *cdc-25.2* (Thellmann *et al.* 2003; Yan *et al.* 2013). Interestingly, neither *egl-1* nor *cdc-25.2* are among the 3199 genes identified using the criteria that the *CES-1* Snail binding site lies within the transcription unit or within 2 kb upstream of the TSS. In the case of *egl-1* BH3-only, *CES-1* Snail binds to and acts through a conserved *cis*-regulatory element, which lies

~3 kb downstream of the *egl-1* transcription unit (Thellmann *et al.* 2003). (There is a *CES-1* Snail peak ~2.5–4.0 kb downstream of *egl-1*, which may represent *CES-1* Snail binding to region B.) In the case of *cdc-25.2*, a *CES-1* Snail binding site is found ~4.8–6.5 kb upstream of the TSS of *cdc-25.2* (Yan *et al.* 2013). Therefore, the *CES-1* Snail binding sites in the *egl-1* and *cdc-25.2* loci are among the ~20% of the 3417 binding sites that could not be assigned to a target gene using our criteria.

Our analysis of the sequences covered by *CES-1* Snail peaks identified three motifs that are significantly enriched, among them a motif that is similar to the Snail binding site, which has been shown to function as a *CES-1* binding site *in vitro*, in *C. elegans* and in the yeast one-hybrid system (Metzstein and Horvitz 1999; Thellmann *et al.* 2003; Reece-Hoyes *et al.* 2009). The two other motifs are more highly enriched and potentially represent novel *CES-1* binding sites. Interestingly,

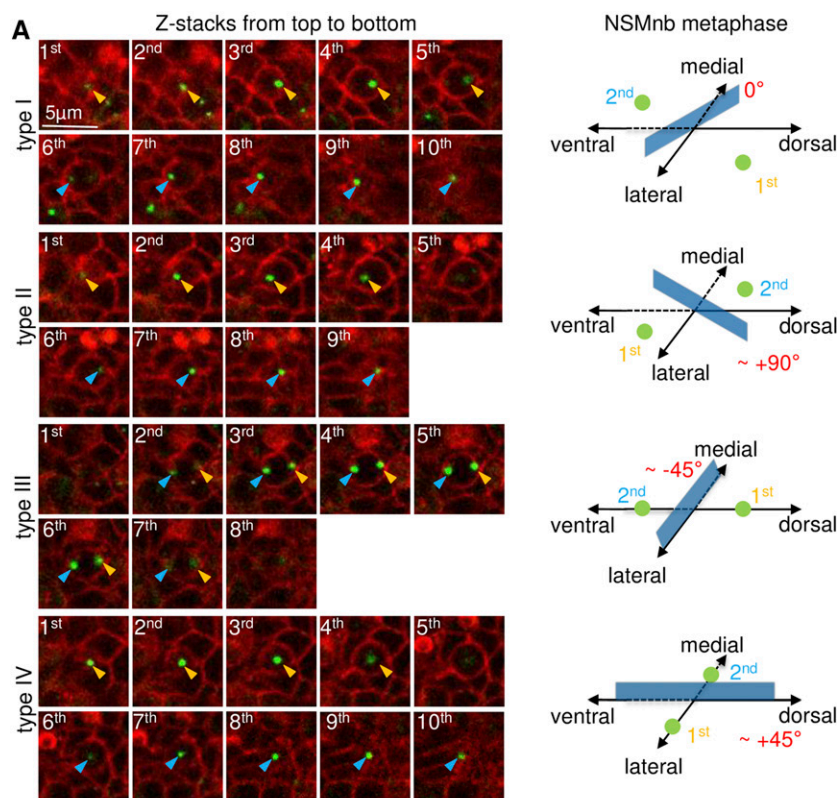
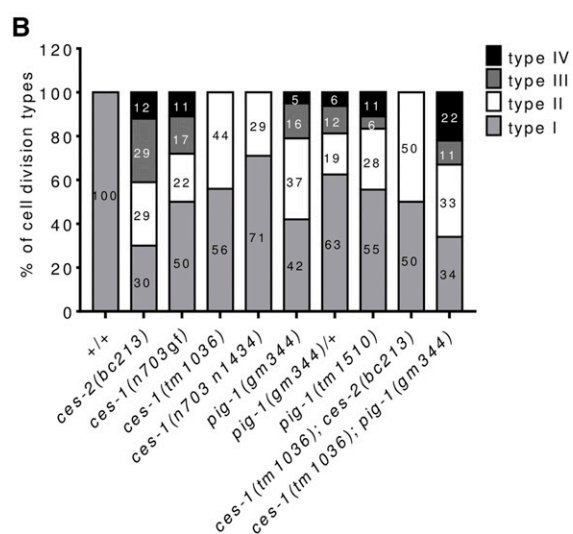


Figure 7 *pig-1* MELK is required for the correct orientation of the NSMnb cleavage plane. (A) (Left) Series of 8–10 consecutive confocal fluorescence images (0.5- μ m step size) from top to bottom of Z-stacks of representative wild-type (type I) or *pig-1(gm344)* (type II–IV) animals exhibiting different orientations of the NSMnb cleavage plane and, hence, different types of cell divisions (type I–V). The orientation of the cleavage plane was determined based on the position of the centrosomes and the position of the daughter cells immediately after the completion of the NSMnb division. Orange arrows point to the centrosomes that segregate into the dorsal-lateral cell and blue arrows point to the centrosomes that segregate into the 2nd cell. All embryos analyzed were homozygous for the transgene *lts1202* ($P_{spd-2}::gfp::spd-5$), which visualizes centrosomes, and for the transgene *lts44* ($P_{pie-1}::mCherry::ph^{PLC\delta}$), which labels the plasma membrane. Bar, 5 μ m. (Right) Schematic representations of different cell division types (type I–IV) observed for the NSMnb in the animals shown left. Blue translucent rectangles represent cleavage planes of the NSMnb. Red numbers indicate the shifts (+ indicates clockwise shift, – indicates counterclockwise shift) relative to wild type (type I) (0°). (B) Percentage cell division types observed in different genotypes [wild type (+/+), *ces-2(bc213)*, *ces-1(n703gf)*, *ces-1(tm1036)*, *ces-1(n70301434)*, *pig-1(gm344)*, *pig-1(gm344)+*, *pig-1(tm1510)*, *ces-1(tm1036)*; *ces-2(bc213)* and *ces-1(tm1036)*; *pig-1(gm344)*] ($n = 14$ –19). All strains were homozygous for the *lts44* ($P_{pie-1}::mCherry::ph^{PLC\delta}$) transgene.



these two motifs differ from a motif that was recently identified for *CES-1* Snail using protein-binding microarrays (CCTGTTG) (Narasimhan *et al.* 2015). For protein-binding microarrays, purified GST-tagged fusions of the DNA-binding domain of the transcription factor of interest plus 50 flanking amino acids are tested for “hybridization” to an array containing DNA probes each 35 bp in length. In contrast, for ChIP-seq, GFP-tagged, full-length *CES-1* Snail protein is tested for binding to chromatin in *C. elegans* embryos (Gerstein *et al.* 2010). Hence, the different *CES-1* Snail binding motifs identified might be a result of different experimental conditions.

ces-1 Snail affects the polarity of the NSMnb and its ability to divide asymmetrically by size by repressing *pig-1* MELK expression

Among the potential *CES-1* Snail target genes, we identified the gene *pig-1* MELK, which has previously been implicated in asymmetric cell division and the programmed elimination of cells during embryogenesis (Cordes *et al.* 2006; Denning *et al.* 2012; Hirose and Horvitz 2013). We demonstrate that *pig-1* MELK is required (in a haploinsufficient manner) for the correct position and orientation of the cleavage plane during the division of the NSMnb. Furthermore, we provide evidence that *pig-1* MELK acts downstream of *CES-1* Snail and

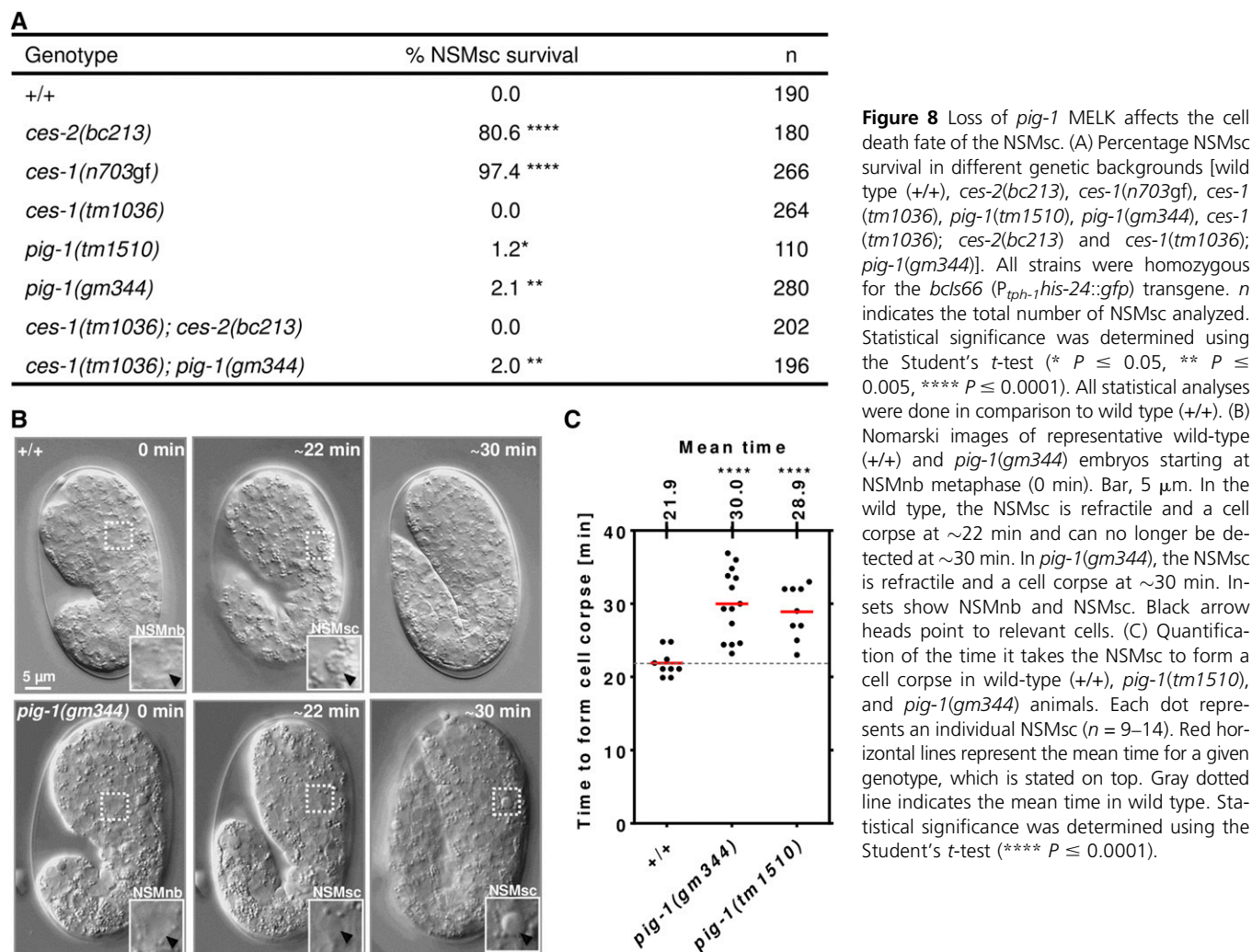


Figure 8 Loss of *pig-1* MELK affects the cell death fate of the NSMsc. (A) Percentage NSMsc survival in different genetic backgrounds [wild type (+/+), *ces-2(bc213)*, *ces-1(n703gf)*, *ces-1(tm1036)*, *pig-1(tm1510)*, *pig-1(gm344)*, *ces-1(tm1036); ces-2(bc213)* and *ces-1(tm1036); pig-1(gm344)*]. All strains were homozygous for the *bcls66* ($P_{tph-1}his-24::gfp$) transgene. *n* indicates the total number of NSMsc analyzed. Statistical significance was determined using the Student's *t*-test (* $P \leq 0.05$, ** $P \leq 0.005$, **** $P \leq 0.0001$). All statistical analyses were done in comparison to wild type (+/+). (B) Nomarski images of representative wild-type (+/+) and *pig-1(gm344)* embryos starting at NSMnb metaphase (0 min). Bar, 5 μ m. In the wild type, the NSMsc is refractile and a cell corpse at ~30 min and can no longer be detected at ~22 min. In *pig-1(gm344)*, the NSMsc is refractile and a cell corpse at ~30 min. Insets show NSMnb and NSMsc. Black arrow heads point to relevant cells. (C) Quantification of the time it takes the NSMsc to form a cell corpse in wild-type (+/+), *pig-1(tm1510)*, and *pig-1(gm344)* animals. Each dot represents an individual NSMsc ($n = 9-14$). Red horizontal lines represent the mean time for a given genotype, which is stated on top. Gray dotted line indicates the mean time in wild type. Statistical significance was determined using the Student's *t*-test (**** $P \leq 0.0001$).

that *CES-1* represses *pig-1* MELK transcription. Therefore, we propose that *CES-1* Snail affects the polarization of the NSMnb and its ability to divide asymmetrically by repressing *pig-1* MELK expression (Figure 9A). Apart from blocking the death of the NSMsc, *ces-1(n703gf)* blocks the death of the IL2 sister cell (Ellis and Horvitz 1991). Interestingly, the loss of *pig-1* has been shown to affect the survival of the IL2 sister cell as well (Cordes *et al.* 2006). Therefore, *ces-1* Snail may also act through *pig-1* MELK to control the asymmetric division of the IL2 neuroblast.

The loss of *ces-2* or *ces-1(n703gf)* affect the position and orientation of the NSMnb cleavage plane as well as the fate of the NSMsc (Ellis and Horvitz 1991; Hatzold and Conrard 2008) (Figure 9B). The loss of *pig-1* MELK affects the position and orientation of the NSMnb cleavage plane, but has only a modest effect on NSMsc fate. [The fact that the loss of *pig-1* MELK has only a modest effect on NSMsc fate explains why *pig-1* was previously thought to not play a role in the NSM neuroblast lineage (Cordes *et al.* 2006).] The loss of *ces-2* and presumably also *ces-1(n703gf)* increases *ces-1* Snail expression, which, after NSMnb division, results in detectable levels of *CES-1* Snail protein and repression of *egl-1* BH3-only transcription in

both daughter cells (Hatzold and Conrard 2008). In contrast, the loss of *pig-1* MELK does not increase *ces-1* Snail expression in the NSM neuroblast lineage (Figure S4). Therefore, we propose that NSMsc survival in *ces-2(bc213)* and *ces-1(n703gf)* animals is a result of the inappropriate presence and amount of *CES-1* Snail in the NSMsc rather than the symmetric division along different cell division axes of the NSMnb *per se*. *CES-1* Snail could also potentially have additional target genes that are required for the segregation of cell fate determinants, such as “apoptotic potential,” during NSMnb division (Chakraborty *et al.* 2015) (Figure 9A).

Regulation of *PIG-1* MELK activity through control of gene expression

The activity of AMPK-related protein kinases (of which MELK kinases form a subgroup) can be regulated by upstream kinases such as mammalian liver kinase B1 (LKB1) (Lizcano *et al.* 2004), which forms a complex with the proteins STRAD and MO25 (Alessi *et al.* 2006). Indeed, there is evidence that in asymmetric cell division and in the programmed elimination of cells, *pig-1* acts in a pathway that is also dependent on *par-4* and/or *strd-1* and *mop-25.2*, which encode *C. elegans*

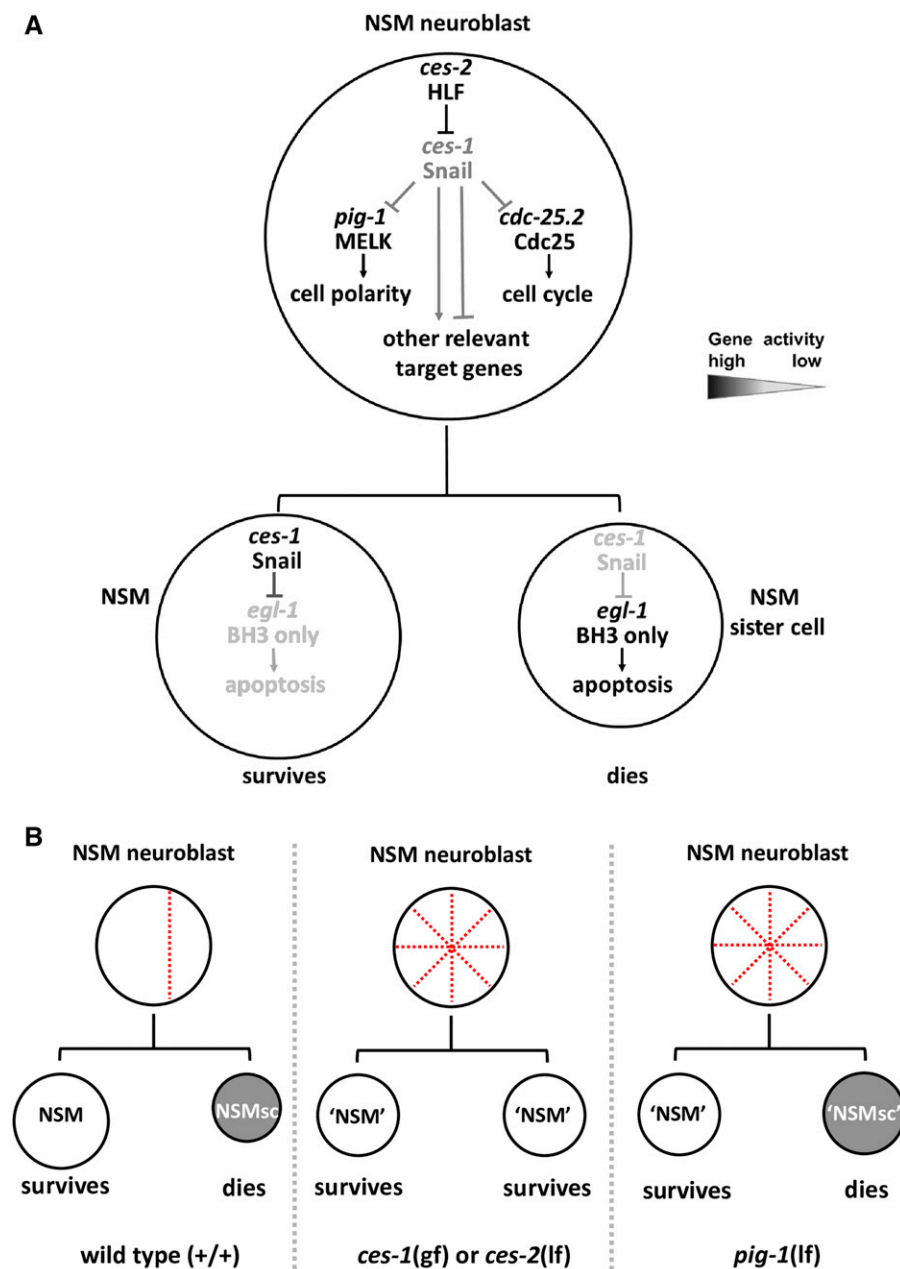


Figure 9 *ces-1* Snail controls the position and orientation of the NSMnb cleavage plane by repressing the expression of *pig-1* MELK. (A) Genetic model of the functions of *ces-1* Snail in the NSM lineage in wild type. See text for details. (B) Schematics of NSMnb division and fate of the NSM and NSMsc in wild type (+/+), *ces-1* gain of function or *ces-2* loss of function, and *pig-1* loss of function. The red dotted lines in the NSMnb indicate the position and orientation of the cleavage plane. See text for details.

homologs of mammalian LKB1, STRAD, and MO25 (Denning *et al.* 2012; Chien *et al.* 2013; Hirose and Horvitz 2013; Pacquelet *et al.* 2015). Our results indicate that *CES-1* Snail-dependent control of *pig-1* MELK expression contributes to the regulation of *PIG-1* MELK activity in the NSMnb and that small changes in expression level (~20% more or less) have phenotypic consequences. In support of the notion that control of expression is a mechanism through which the activities of MELK-like kinases are regulated, in the Q.a/p neuroblast, *pig-1* MELK expression is under the control of the Storkhead-box protein 1-like transcription factor *HAM-1*, whose loss also affects asymmetric cell division in this lineage (Guenther and Garriga 1996; Feng *et al.* 2013). Therefore, we speculate that transcriptional control of MELK genes may be relevant in vertebrates as well and that Snail-

and Storkhead-box protein 1-like transcription factors might contribute to this process.

How does *pig-1* MELK affect the position and orientation of the NSMnb cleavage plane?

In the *C. elegans* one-cell embryo, the loss of *pig-1* MELK synergizes with the loss of *ani-1* [which encodes one of two *C. elegans* anillins (Maddox *et al.* 2005)] to cause a defect in the position of the cleavage plane (Pacquelet *et al.* 2015). In this context, *PIG-1* and *ANI-1* may affect cleavage plane position by regulating the accumulation of myosin at the cell cortex (Pacquelet *et al.* 2015). Indeed, in early embryos, *PIG-1* MELK protein has been shown to localize to the cell cortex between adjacent cells. However, in the dividing Q.a/p neuroblasts, which like the NSM neuroblasts divide asymmetrically

to give rise to a daughter that is programmed to die, PIG-1 seems to localize to the two centrosomes (Chien *et al.* 2013). This suggests that in neuroblasts, PIG-1 MELK most likely acts through a mechanism that differs from that in the early embryo. Furthermore, we have recently shown that certain aspects of the polarization of the NSMnb, such as the generation at metaphase of a gradient of apoptotic potential (*i.e.*, active CED-3 caspase), depend on the activity of the central *C. elegans* cell death pathway as well as the two parallel partially redundant *C. elegans* engulfment pathways (Chakraborty *et al.* 2015; Conradt *et al.* 2016; Lambie and Conradt 2016). How a *pig-1* MELK-dependent pathway may intersect with these pathways to cause the asymmetric division of the NSMnb is currently unknown.

Relevance for stem cells and tumorigenesis

Snail-like transcription factors affect various aspects of stem cell function such as self-renewal (Guo *et al.* 2012; Desgrosellier *et al.* 2014; Hwang *et al.* 2014; Lin *et al.* 2014; Horvay *et al.* 2015; Ye *et al.* 2015; Tang *et al.* 2016). In order to self-renew, stem cells need to divide asymmetrically and give rise to two daughters of different fates. Interestingly, at least in mouse and in the zebrafish, the MELK gene is expressed in stem cells, such as neural and hematopoietic stem cells (Nakano *et al.* 2005; Saito *et al.* 2005, 2012). Furthermore, there is increasing evidence (including the evidence presented here) that MELK proteins play a critical role in asymmetric cell division and that their loss or overexpression causes cells that normally divide asymmetrically to divide symmetrically instead (Cordes *et al.* 2006; Tassan 2011; Pacquelet *et al.* 2015). Therefore, we speculate that Snail-like transcription factors are critical for self-renewal because they control MELK expression in stem cell lineages and, hence, the function of MELK in asymmetric cell division.

In some stem cell lineages, Snail-like transcription factors, however, have also been shown to promote the acquisition of a differentiated state (Lin *et al.* 2014; Horvay *et al.* 2015; Tang *et al.* 2016). Studies of CES-1 Snail in the NSM neuroblast lineage may provide a framework for how this could be accomplished mechanistically. In the NSM neuroblast lineage, CES-1 Snail coordinates cell cycle progression and cell polarity in the NSMnb and thereby enables this neuroblast to divide asymmetrically (Hatzold and Conradt 2008; Yan *et al.* 2013). Immediately after NSMnb division, in contrast, CES-1 Snail is critical for cell fate specification and the acquisition of a differentiated state: its absence in the NSMsc causes the NSMsc to acquire the cell death fate and its presence in the NSM allows the NSM to acquire a neuronal fate (Ellis and Horvitz 1991; Thellmann *et al.* 2003; Hatzold and Conradt 2008). The different functions of CES-1 Snail in the NSMnb and its daughter cells can be explained by differences in CES-1 Snail abundance: CES-1 Snail protein is present at a low, undetectable level in the NSMnb and this low level may be necessary and sufficient to control the transcription of *pig-1* MELK and *cdc-25.2* CDC25. Immediately after NSMnb division, this level is increased to a detectable level in the NSM and probably decreased to an even lower level in the NSMsc

(Hatzold and Conradt 2008). Therefore, a level sufficient for transcriptional repression of *egl-1* BH3-only is reached in the NSM but not the NSMsc. [Indeed, the *cis*-acting element of the *egl-1* BH3-only locus necessary for CES-1 Snail-dependent repression contains four Snail binding sites to which CES-1 protein binds in a cooperative manner, at least *in vitro* (Thellmann *et al.* 2003).] By analogy to the *C. elegans* NSM neuroblast lineage, we speculate that the concentrations and, hence, target genes of Snail-like transcription factors in stem cell lineages may change during asymmetric stem cell divisions to promote self-renewal in stem cells, and cell fate specification and terminal differentiation in the nonstem cell daughter.

Finally, the deregulation of both Snail-like transcription factors and MELK has been implicated in tumorigenesis in numerous types of cancers and may even play a central role in cancer stem cells (Puisieux *et al.* 2014; Ganguly *et al.* 2015). Based on our findings in *C. elegans*, we speculate that the deregulation of Snail-like transcription factors or MELK results in the inability of stem cells to divide asymmetrically, and that this loss of self-renewal is a crucial step in tumorigenesis.

Acknowledgments

The authors thank E. Lambie, N. Mishra, and E. Zanin for comments on the manuscript and members of the Conradt laboratory for discussion; L. Jocham, N. Lebedeva, and M. Schwarz for excellent technical support; N. Mishra for generating plasmid pBC1531; K. Oegema for providing strain OD847 (*tsi202*); the National Human Genome Research Institute “model organism encyclopedia of DNA elements” project (modENCODE; <http://www.modencode.org/>) for providing ChIP-seq data. Some strains used in this study were provided by the Caenorhabditis Genetics Center (CGC; <https://cbs.umn.edu/cgc/home>) and the National BioResource Project (NBRP; <https://shigen.nig.ac.jp/c.elegans/>). H.W. was supported by a predoctoral fellowship from the China Scholarship Council (<https://www.csc.edu.cn/>).

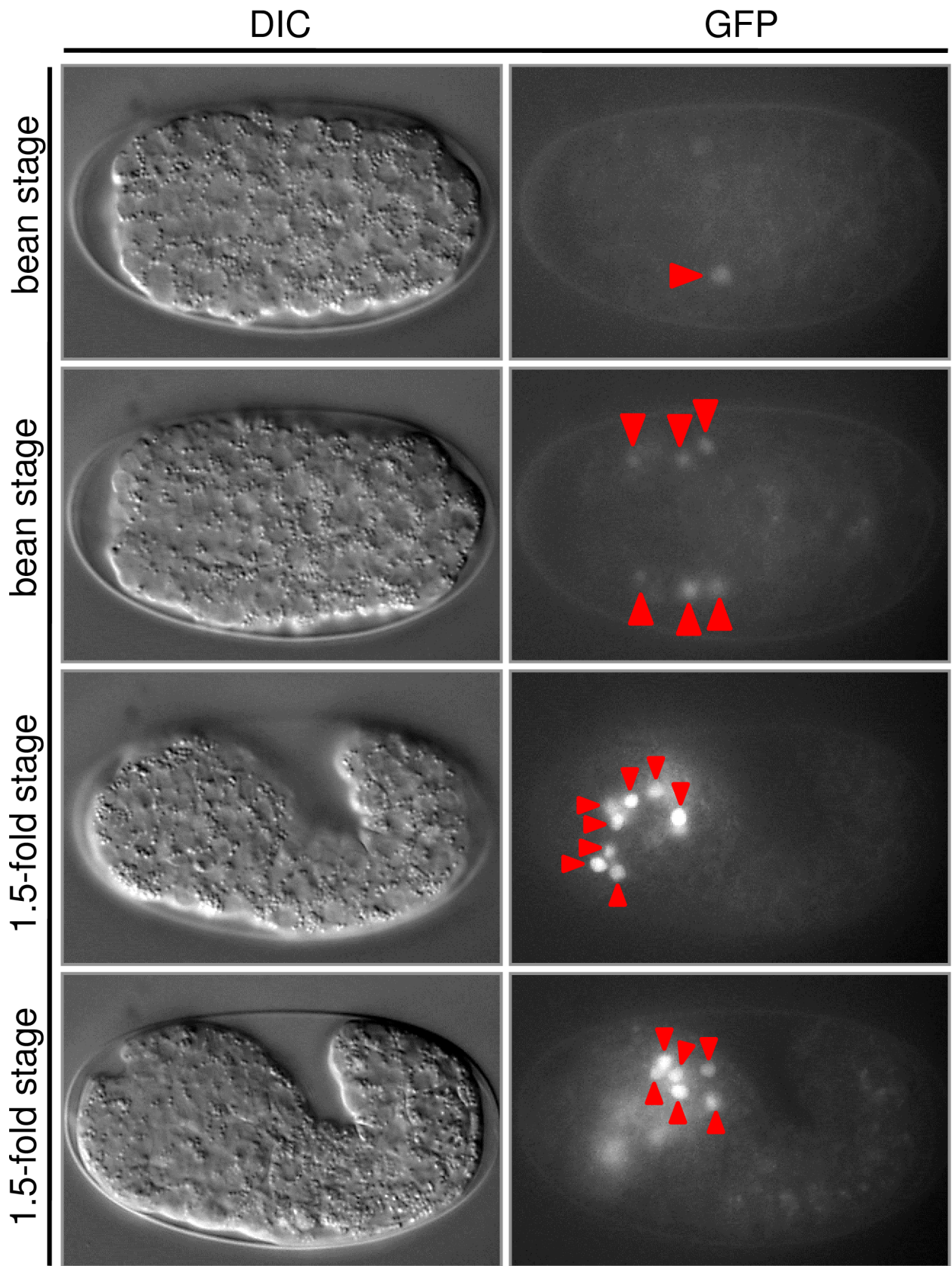
Literature Cited

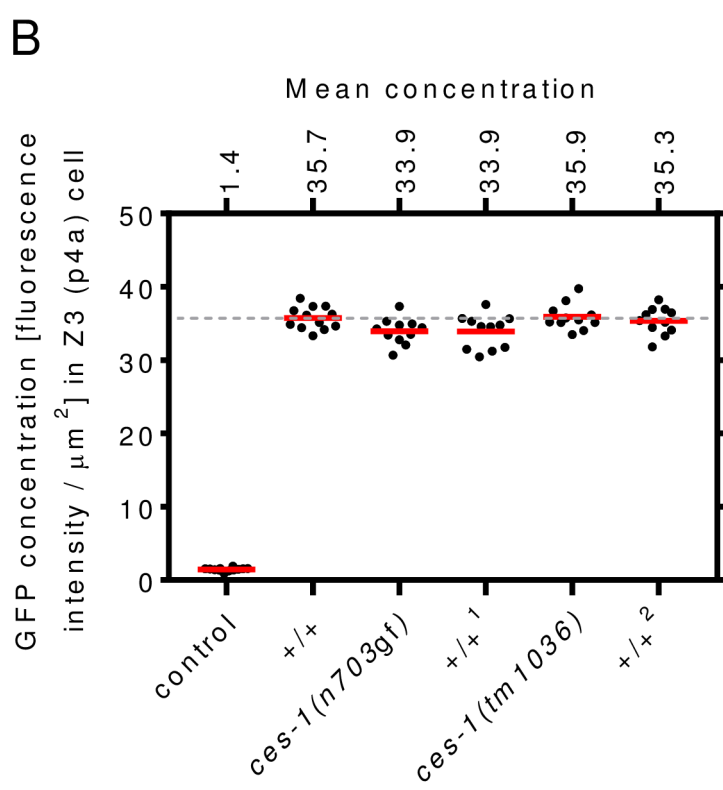
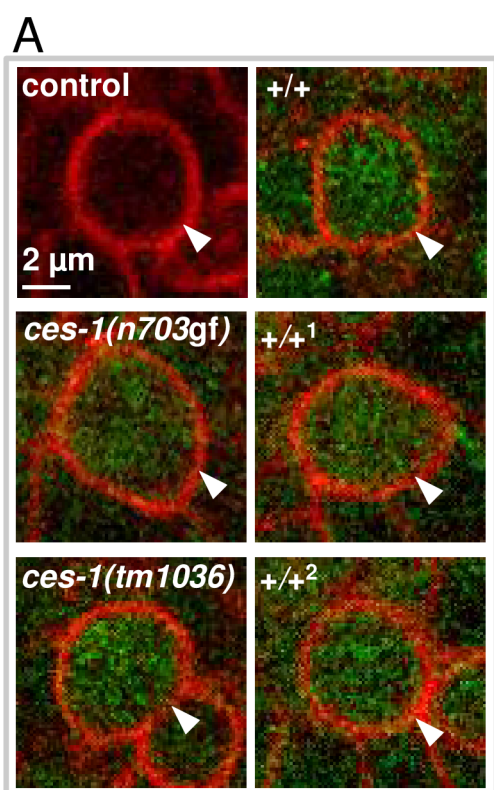
- Alessi, D. R., K. Sakamoto, and J. R. Bayascas, 2006 LKB1-dependent signaling pathways. *Annu. Rev. Biochem.* 75: 137–163.
- Audhya, A., F. Hyndman, I. X. McLeod, A. S. Maddox, J. R. Yates, III *et al.*, 2005 A complex containing the Sm protein CAR-1 and the RNA helicase CGH-1 is required for embryonic cytokinesis in *Caenorhabditis elegans*. *J. Cell Biol.* 171: 267–279.
- Bailey, T. L., M. Boden, F. A. Buske, M. Frith, C. E. Grant *et al.*, 2009 MEME SUITE: tools for motif discovery and searching. *Nucleic Acids Res.* 37: W202–W208.
- Barrallo-Gimeno, A., and M. A. Nieto, 2009 Evolutionary history of the Snail/Scratch superfamily. *Trends Genet.* 25: 248–252.
- Brenner, S., 1974 The genetics of *Caenorhabditis elegans*. *Genetics* 77: 71–94.
- Chakraborty, S., E. J. Lambie, S. Bindu, T. Mikeladze-Dvali, and B. Conradt, 2015 Engulfment pathways promote programmed cell death by enhancing the unequal segregation of apoptotic potential. *Nat. Commun.* 6: 10126.
- Chien, S. C., E. M. Brinkmann, J. Teuliere, and G. Garriga, 2013 *Caenorhabditis elegans* PIG-1/MELK acts in a conserved

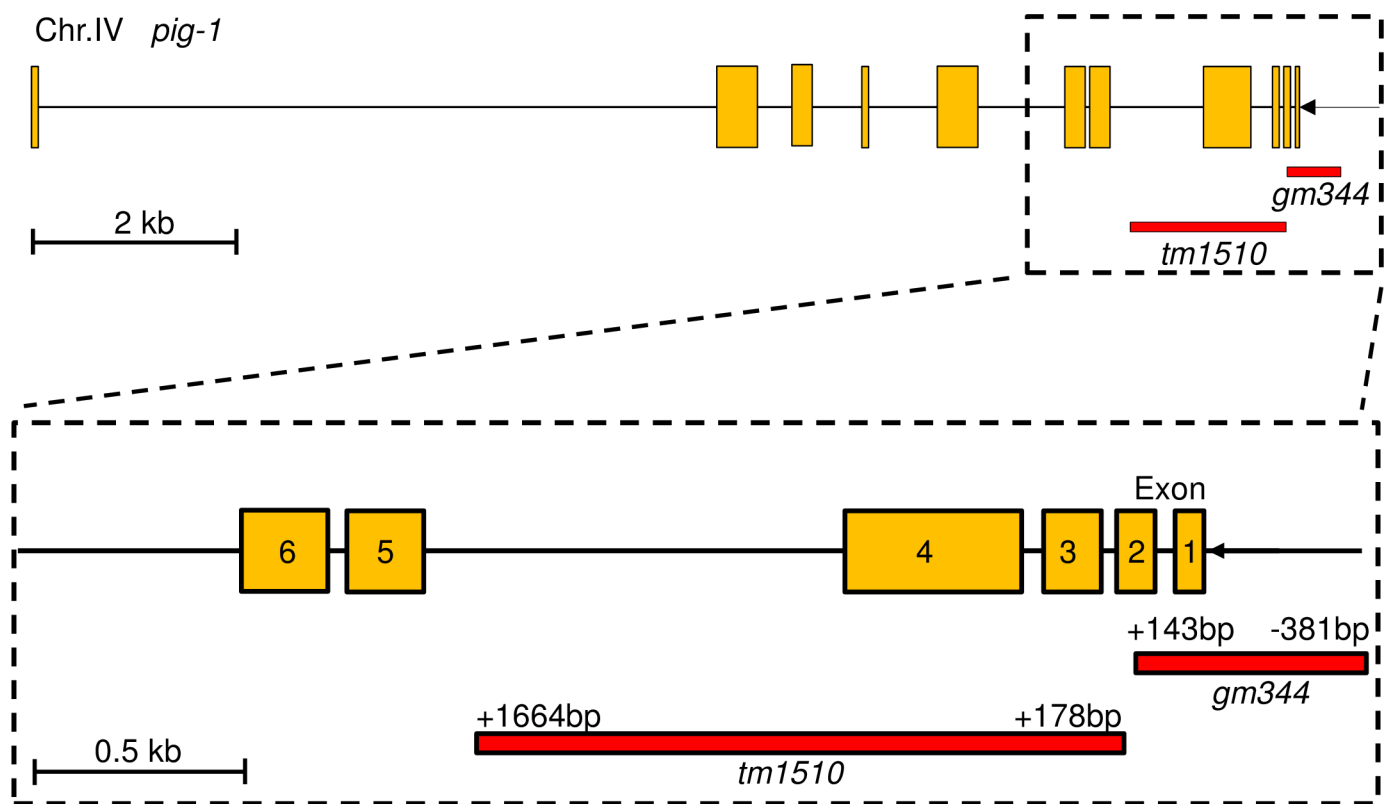
- PAR-4/LKB1 polarity pathway to promote asymmetric neuroblast divisions. *Genetics* 193: 897–909.
- Conradt, B., and H. R. Horvitz, 1998 The *C. elegans* protein EGL-1 is required for programmed cell death and interacts with the Bcl-2-like protein CED-9. *Cell* 93: 519–529.
- Conradt, B., Y. C. Wu, and D. Xue, 2016 Programmed cell death during *Caenorhabditis elegans*. *Dev. Genet.* 203: 1533–1562.
- Cordes, S., C. A. Frank, and G. Garriga, 2006 The *C. elegans* MELK ortholog PIG-1 regulates cell size asymmetry and daughter cell fate in asymmetric neuroblast divisions. *Development* 133: 2747–2756.
- Denning, D. P., V. Hatch, and H. R. Horvitz, 2012 Programmed elimination of cells by caspase-independent cell extrusion in *C. elegans*. *Nature* 488: 226–230.
- Desgrosellier, J. S., J. Lesperance, L. Seguin, M. Gozo, S. Kato *et al.*, 2014 Integrin α v β 3 drives slug activation and stemness in the pregnant and neoplastic mammary gland. *Dev. Cell* 30: 295–308.
- Ellis, R. E., and H. R. Horvitz, 1991 Two *C. elegans* genes control the programmed deaths of specific cells in the pharynx. *Development* 112: 591–603.
- Feng, G., P. Yi, Y. Yang, Y. Chai, D. Tian *et al.*, 2013 Developmental stage-dependent transcriptional regulatory pathways control neuroblast lineage progression. *Development* 140: 3838–3847.
- Frokjaer-Jensen, C., M. W. Davis, M. Ailion, and E. M. Jorgensen, 2012 Improved Mos1-mediated transgenesis in *C. elegans*. *Nat. Methods* 9: 117–118.
- Frokjaer-Jensen, C., M. W. Davis, M. Sarov, J. Taylor, S. Flibotte *et al.*, 2014 Random and targeted transgene insertion in *Caenorhabditis elegans* using a modified Mos1 transposon. *Nat. Methods* 11: 529–534.
- Ganguly, R., A. Mohyeldin, J. Thiel, H. I. Kornblum, M. Beullens *et al.*, 2015 MELK—a conserved kinase: functions, signaling, cancer, and controversy. *Clin. Transl. Med.* 4: 11.
- Gerstein, M. B., Z. J. Lu, E. L. Van Nostrand, C. Cheng, B. I. Arshinoff *et al.*, 2010 Integrative analysis of the *Caenorhabditis elegans* genome by the modENCODE project. *Science* 330: 1775–1787.
- Gladden, J. M., and B. J. Meyer, 2007 A ONECUT homeodomain protein communicates X chromosome dose to specify *Caenorhabditis elegans* sexual fate by repressing a sex switch gene. *Genetics* 177: 1621–1637.
- Guenther, C., and G. Garriga, 1996 Asymmetric distribution of the *C. elegans* HAM-1 protein in neuroblasts enables daughter cells to adopt distinct fates. *Development* 122: 3509–3518.
- Guo, W., Z. Keckesova, J. L. Donaher, T. Shibue, V. Tischler *et al.*, 2012 Slug and Sox9 cooperatively determine the mammary stem cell state. *Cell* 148: 1015–1028.
- Hatzold, J., and B. Conradt, 2008 Control of apoptosis by asymmetric cell division. *PLoS Biol.* 6: e84.
- Hirose, T., and H. R. Horvitz, 2013 An Sp1 transcription factor coordinates caspase-dependent and -independent apoptotic pathways. *Nature* 500: 354–358.
- Horner, M. A., S. Quintin, M. E. Domeier, J. Kimble, M. Labouesse *et al.*, 1998 pha-4, an HNF-3 homolog, specifies pharyngeal organ identity in *Caenorhabditis elegans*. *Genes Dev.* 12: 1947–1952.
- Horvay, K., T. Jarde, F. Casagrande, V. M. Perreau, K. Haigh *et al.*, 2015 Snail regulates cell lineage allocation and stem cell maintenance in the mouse intestinal epithelium. *EMBO J.* 34: 1319–1335.
- Huang da, W., B. T. Sherman, and R. A. Lempicki, 2009 Systematic and integrative analysis of large gene lists using DAVID bioinformatics resources. *Nat. Protoc.* 4: 44–57.
- Hwang, W. L., J. K. Jiang, S. H. Yang, T. S. Huang, H. Y. Lan *et al.*, 2014 MicroRNA-146a directs the symmetric division of Snail-dominant colorectal cancer stem cells. *Nat. Cell Biol.* 16: 268–280.
- Kim, J., I. Kawasaki, and Y. H. Shim, 2010 cdc-25.2, a *C. elegans* ortholog of cdc25, is required to promote oocyte maturation. *J. Cell Sci.* 123: 993–1000.
- Lambie, E. J., and B. Conradt, 2016 Deadly dowry: how engulfment pathways promote cell killing. *Cell Death Differ.* 23: 553–554.
- Landt, S. G., G. K. Marinov, A. Kundaje, P. Kheradpour, F. Pauli *et al.*, 2012 ChIP-seq guidelines and practices of the ENCODE and modENCODE consortia. *Genome Res.* 22: 1813–1831.
- Langmead, B., and S. L. Salzberg, 2012 Fast gapped-read alignment with Bowtie 2. *Nat. Methods* 9: 357–359.
- Li, Q. H., J. B. Brown, H. Y. Huang, and P. J. Bickel, 2011 Measuring reproducibility of high-throughput experiments. *Ann. Appl. Stat.* 5: 1752–1779.
- Lin, Y., X. Y. Li, A. L. Willis, C. Liu, G. Chen *et al.*, 2014 Snail1-dependent control of embryonic stem cell pluripotency and lineage commitment. *Nat. Commun.* 5: 3070.
- Lizcano, J. M., O. Goransson, R. Toth, M. Deak, N. A. Morrice *et al.*, 2004 LKB1 is a master kinase that activates 13 kinases of the AMPK subfamily, including MARK/PAR-1. *EMBO J.* 23: 833–843.
- Maddox, A. S., B. Habermann, A. Desai, and K. Oegema, 2005 Distinct roles for two *C. elegans* anillins in the gonad and early embryo. *Development* 132: 2837–2848.
- Melendez, A., and I. Greenwald, 2000 *Caenorhabditis elegans* lin-13, a member of the LIN-35 Rb class of genes involved in vulval development, encodes a protein with zinc fingers and an LXCXE motif. *Genetics* 155: 1127–1137.
- Mello, C., and A. Fire, 1995 DNA transformation. *Methods Cell Biol.* 48: 451–482.
- Metzstein, M. M., and H. R. Horvitz, 1999 The *C. elegans* cell death specification gene *ces-1* encodes a snail family zinc finger protein. *Mol. Cell* 4: 309–319.
- Metzstein, M. M., M. O. Hengartner, N. Tsung, R. E. Ellis, and H. R. Horvitz, 1996 Transcriptional regulator of programmed cell death encoded by *Caenorhabditis elegans* gene *ces-2*. *Nature* 382: 545–547.
- Nakano, I., A. A. Paucar, R. Bajpai, J. D. Dougherty, A. Zewail *et al.*, 2005 Maternal embryonic leucine zipper kinase (MELK) regulates multipotent neural progenitor proliferation. *J. Cell Biol.* 170: 413–427.
- Narasimhan, K., S. A. Lambert, A. W. Yang, J. Riddell, S. Mnaimneh *et al.*, 2015 Mapping and analysis of *Caenorhabditis elegans* transcription factor sequence specificities. *ELife* 4: 06967.
- Nieto, M. A., R. Y. Huang, R. A. Jackson, and J. P. Thiery, 2016 *Emt*. *Cell* 166: 21–45.
- Pacquelet, A., P. Uhart, J. P. Tassin, and G. Michaux, 2015 PAR-4 and anillin regulate myosin to coordinate spindle and furrow position during asymmetric division. *J. Cell Biol.* 210: 1085–1099.
- Puisieux, A., T. Brabletz, and J. Caramel, 2014 Oncogenic roles of EMT-inducing transcription factors. *Nat. Cell Biol.* 16: 488–494.
- Reece-Hoyes, J. S., B. Deplancke, M. I. Barrasa, J. Hatzold, R. B. Smit *et al.*, 2009 The *C. elegans* Snail homolog CES-1 can activate gene expression in vivo and share targets with bHLH transcription factors. *Nucleic Acids Res.* 37: 3689–3698.
- Reinke, V., M. Krause, and P. Okkema, 2013 Transcriptional regulation of gene expression in *C. elegans*. *WormBook*, ed. The *C. elegans* Research Community, *WormBook*, doi/10.1895/wormbook.1.45.2, <http://www.wormbook.org>
- Rembold, M., L. Ciglar, J. O. Yanez-Cuna, R. P. Zinzen, C. Girardot *et al.*, 2014 A conserved role for Snail as a potentiator of active transcription. *Genes Dev.* 28: 167–181.
- Robinson, J. T., H. Thorvaldsdottir, W. Winckler, M. Guttman, E. S. Lander *et al.*, 2011 Integrative genomics viewer. *Nat. Biotechnol.* 29: 24–26.
- Saito, R., Y. Tabata, A. Muto, K. Arai, and S. Watanabe, 2005 Melk-like kinase plays a role in hematopoiesis in the zebra fish. *Mol. Cell Biol.* 25: 6682–6693.
- Saito, R., H. Nakauchi, and S. Watanabe, 2012 Serine/threonine kinase, Melk, regulates proliferation and glial differentiation of retinal progenitor cells. *Cancer Sci.* 103: 42–49.

- Sarov, M., S. Schneider, A. Pozniakovski, A. Roguev, S. Ernst *et al.*, 2006 A recombineering pipeline for functional genomics applied to *Caenorhabditis elegans*. *Nat. Methods* 3: 839–844.
- Sarov, M., J. I. Murray, K. Schanze, A. Pozniakovski, W. Niu *et al.*, 2012 A genome-scale resource for in vivo tag-based protein function exploration in *C. elegans*. *Cell* 150: 855–866.
- Sulston, J. E., E. Schierenberg, J. G. White, and J. N. Thomson, 1983 The embryonic cell lineage of the nematode *Caenorhabditis elegans*. *Dev. Biol.* 100: 64–119.
- Tang, Y., T. Feinberg, E. T. Keller, X. Y. Li, and S. J. Weiss, 2016 Snail/Slug binding interactions with YAP/TAZ control skeletal stem cell self-renewal and differentiation. *Nat. Cell Biol.* 18: 917–929.
- Tassan, J. P., 2011 Cortical localization of maternal embryonic leucine zipper kinase (MELK) implicated in cytokinesis in early xenopus embryos. *Commun. Integr. Biol.* 4: 483–485.
- Theilmann, M., J. Hatzold, and B. Conradt, 2003 The Snail-like CES-1 protein of *C. elegans* can block the expression of the BH3-only cell-death activator gene *egl-1* by antagonizing the function of bHLH proteins. *Development* 130: 4057–4071.
- Woodruff, J. B., O. Wueseke, V. Viscardi, J. Mahamid, S. D. Ochoa *et al.*, 2015 Centrosomes. Regulated assembly of a supramolecular centrosome scaffold in vitro. *Science* 348: 808–812.
- Yan, B., N. Memar, J. Gallinger, and B. Conradt, 2013 Coordination of cell proliferation and cell fate determination by CES-1 snail. *PLoS Genet.* 9: e1003884.
- Ye, X., W. L. Tam, T. Shibue, Y. Kaygusuz, F. Reinhardt *et al.*, 2015 Distinct EMT programs control normal mammary stem cells and tumour-initiating cells. *Nature* 525: 256–260.
- Zeitlinger, J., R. P. Zinzen, A. Stark, M. Kellis, H. Zhang *et al.*, 2007 Whole-genome ChIP-chip analysis of Dorsal, Twist, and Snail suggests integration of diverse patterning processes in the *Drosophila* embryo. *Genes Dev.* 21: 385–390.
- Zhang, Y., T. Liu, C. A. Meyer, J. Eeckhoutte, D. S. Johnson *et al.*, 2008 Model-based analysis of ChIP-Seq (MACS). *Genome Biol.* 9: R137.
- Zhong, M., W. Niu, Z. J. Lu, M. Sarov, J. I. Murray *et al.*, 2010 Genome-wide identification of binding sites defines distinct functions for *Caenorhabditis elegans* PHA-4/FOXA in development and environmental response. *PLoS Genet.* 6: e1000848.

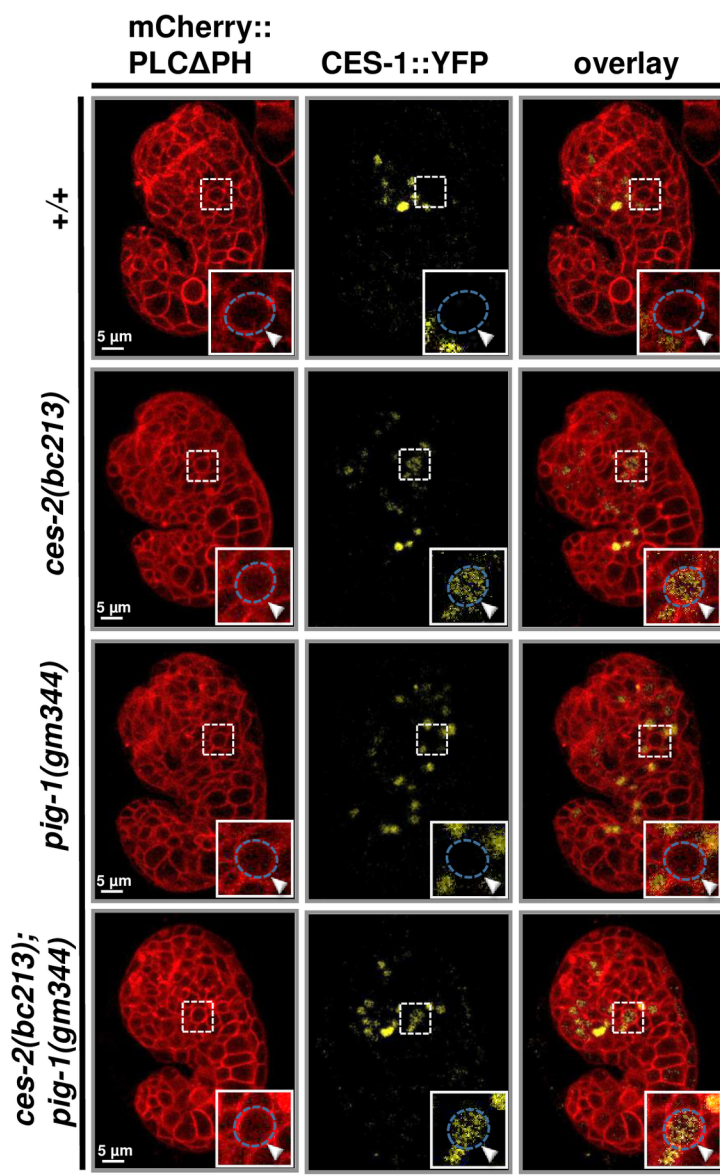
Communicating editor: O. Hobert







A



B

| Genotype | transgene (single copy) | NSMnb | | | NSM-NSMsc | | | | | | |
|-----------------------------------|----------------------------|-------|----|----|-----------|----|---|---|---|---|----|
| | | ● | ○ | n | ○ | ○ | ● | ● | ○ | ○ | ● |
| +/+ | $P_{ces-1}ces-1::yfp$ | 0 | 15 | 15 | 15 | 0 | 0 | 0 | 0 | 0 | 15 |
| <i>ces-2(bc213)</i> | $P_{ces-1}ces-1::yfp$ | 23 | 0 | 23 | 0 | 23 | 0 | 0 | 0 | 0 | 23 |
| <i>pig-1(gm344)</i> | $P_{ces-1}ces-1::yfp$ | 0 | 16 | 16 | 16 | 0 | 0 | 0 | 0 | 0 | 16 |
| <i>ces-2(bc213); pig-1(gm344)</i> | $P_{ces-1}ces-1::yfp$ | 22 | 0 | 22 | 0 | 22 | 0 | 0 | 0 | 0 | 22 |

1 **Supporting Information Captions**

2

3 **Table S1. Number of ChIP-seq reads.**

4 ChIP-seq analysis for CES-1 binding. The numbers of total and unique ChIP-seq reads
5 are shown for the two experiment repeats and their corresponding control.

6

7 **Table S2. Potential CES-1 Snail target genes.**

8 List of the 3,199 potential CES-1 target genes identified by ChIP-seq. See text for details.

9

10 **Table S3. GO analysis of target genes of 11 *C. elegans* transcription factors.**

11 GO analysis results for PHA-4, NHR-2, BLMP-1, ELT-3, LIN-13, CEH-39, GEI-11,
12 MED-1, CES-1, MEP-1 and LSY-2. GO analysis was performed at biological process
13 level 4 using DAVID6.8. See text for details.

14

15 **Table S4. Programmed cell death - potential CES-1 Snail targets.**

16 List of potential CES-1 target genes that are related to programmed cell death
17 (GO:0012501).

18

19 **Table S5. Asymmetric cell division – potential CES-1 Snail targets.**

20 List of potential CES-1 target genes that are related to asymmetric cell division
21 (GO:0008356).

22

23 **Fig S1. *ces-1* Snail expression during embryogenesis.**

24 DIC and epifluorescence images of wild-type (+/+) embryos carrying the integrated

25 transgene *wgIs174* ($P_{ces-1ces-1}::gfp$) at different stages of development. Expression of *gfp*
 26 was first observed in the ABplpapaap/ABprpapaap lineages (red arrows) during the bean
 27 stage of embryogenesis. During the 1.5-fold stage, the expression was observed in many
 28 cells in the area of the developing pharynx, most of which are neurons (red arrows).

29

30 **Figure S2. GFP level of *pig-1* transcriptional reporter in Z3.**

31 **(A)** Confocal images of representative Z3 cells at metaphase in control, wild-type (+/+,
 32 +/+¹, +/+²), *ces-1(n703gf)* and *ces-1(tm1036)* animals. Control animal is transgenic for
 33 *ltIs44* ($P_{pie-1mCherry}::ph^{PLC\delta}$) transgene. Wild-type (+/+, +/+¹, +/+²), *ces-1(n703gf)* and
 34 *ces-1(tm1036)* animals are transgenic for *bcSi43* ($P_{pig-1gfp}$) and *ltIs44* ($P_{pie-1mCherry}::ph^{PLC\delta}$)
 35 transgenes. +/+¹ indicates a strain from which *ces-1(n703gf)* was
 36 outcrossed. +/+² indicates a strain from which *ces-1(tm1036)* was outcrossed. White arrow
 37 heads indicate Z3. Scale bar represents 2 μ m. **(B)** GFP concentration [fluorescence
 38 intensity/ μ m²] in Z3 in control animals (control) and in animals carrying the transgene $P_{pig-1gfp}$
 39 (*bcSi43*) in various genetic backgrounds (+/+, *ces-1(n703gf)*, +/+¹, *ces-1(tm1036)*,
 40 +/+²) (n=11-13). Each dot represents the GFP concentration in one Z3. Red horizontal lines
 41 indicate mean concentrations, which are stated on top. Grey dotted line indicates the mean
 42 concentration in wild type (+/+).

43

44 **Figure S3. Schematic representation of the *pig-1* MELK transcription unit on**
 45 **Chromosome IV.**

46 (Top) The entire *pig-1* transcription unit is shown with the two deletion alleles *gm344* and
 47 *tm1510*. (Bottom) Detail of exons 1-6 of the *pig-1* transcription unit. *gm344* is a 524 bp
 48 deletion that removes parts of the 5' UTR, exon 1 and parts of exon 2. *tm1510* is a 1486 bp

49 deletion that removes parts of exon 2 and exon 3 and 4.

50

51 **Figure S4. Loss of *pig-1* MELK does not affect the expression of *ces-1* Snail in the**
52 **NSM neuroblast lineage.**

53 (A) Confocal images of wild type (+/+), *ces-2(bc213)*, *pig-1(gm344)* and *ces-2(bc213);*
54 *pig-1(gm344)* embryos transgenic for the integrated single-copy transgene (MosSCI allele)
55 $P_{ces-1ces-1::yfp}$ (*bcSi50*) and the integrated transgene $P_{pie-1mCherry::plc\delta ph}$ (*ltIs44*). A
56 higher magnification of the NSMnb is inserted at the bottom right corner of each image.
57 Blue circles mark membrane boundaries of NSMnbs at metaphase and white arrowheads
58 point to NSMnbs. The right column of confocal images are two-channel overlay
59 projections of single plane confocal images of representative embryos of a given genotype
60 shown in the two left columns. Scale bar represents 5 μ m. (B) Summary of $P_{ces-1ces-1::yfp}$
61 (*bcSi50*) expression in the NSM neuroblast lineage in different genetic backgrounds. The
62 NSMnb, the NSM and the NSMsc are indicated as circles. The yellow color indicates
63 detectable CES-1::YFP signal in the NSMnb (at metaphase), the NSM or NSMsc
64 (immediately post NSMnb division). n number of NSM neuroblast lineages analyzed.

65

Table S1. Summary of CES-1 ChIP-seq raw data.

| | | Total reads | Uniquely mapped reads (%) |
|-----------------|---------|-------------|---------------------------|
| Repeat1 | sample | 7,354,875 | 6,142,087 (83%) |
| Repeat1_control | control | 2,897,835 | 2,767,203 (95%) |
| Repeat2 | sample | 7,460,381 | 6,224,070 (83%) |
| Repeat2_control | control | 4,062,244 | 3,865,241 (95%) |

Supplemental Table S2 and Table S3 are not shown in this dissertation since they are excel files and contains lots of information, which would be more than 700 pages if I print them. Therefore, I cannot present them here. While these data are available online, please visit the following GENETICS website:

Table S2-Number of ChIP-seq reads. (.docx):

<http://www.genetics.org/content/206/4/2069.supplemental>

Table S3-Potential CES-1 Snail target genes. (.xlsx):

<http://www.genetics.org/content/206/4/2069.supplemental>

Table S4. CES-1 target genes for GOterm programmed cell death

| | |
|--|----------|
| GO:0012501~programmed cell death | |
| Count | Pvalue |
| 202 | 2.25E-18 |
| Target gene with this GOterm: | |
| <p><i>ifg-1, nud-1, lin-53, ubl-1, ubq-2, H28O16.1, ubq-1, T26G10.1, crt-1, his-61, cars-1, tba-1, his-65, mrg-1, C23G10.8, his-57, mpk-1, vha-12, wts-1, dcr-1, imb-3, lpin-1, lin-41, C08B11.3, ify-1, Y57G11C.15, his-47, icd-1, vars-2, pbs-2, mdt-15, npp-20, mes-2, unc-3, skr-1, F43G9.12, R186.8, mep-1, R186.3, rfp-1, cmd-1, let-607, vps-4, Y49E10.23, pcn-1, nsf-1, pbs-5, misc-1, tpxl-1, met-1, mdt-19, cnt-1, unc-32, fcd-2, rab-1, pcf-11, agef-1, C13B9.3, fem-2, gld-3, ape-1, rab-5, snr-6, snx-6, snr-1, eef-1A.1, F09F7.3, W04A4.5, eef-2, Y54F10AR.1, rla-0, cdl-1, F59E10.3, hrp-2, abl-1, ced-5, C14A4.11, ced-2, apb-1, dlc-1, cct-7, aps-3, lgg-1, daf-16, daf-21, Y76B12C.6, Y37D8A.18, lgc-46, ect-2, hsp-1, unc-51, ire-1, him-17, eat-3, dnj-10, etr-1, arf-1.2, rpl-20, rpl-18, mcd-1, atp-3, aex-3, eif-3.I, rpl-17, rpl-15, Y48G8AL.7, sca-1, rpl-13, rpl-12, mog-5, snap-1, F09E5.2, Y105E8A.25, sop-2, eif-3.C, eif-3.E, npp-7, rpl-4, fis-2, gcn-1, rpl-6, K12H4.4, mtp-18, eor-1, eor-2, syx-5, clpp-1, hpl-1, rpl-39, C45G9.5, nmt-1, sec-5, bir-1, nmy-2, rpl-31, sec-23, bec-1, rpl-35, T27F7.4, T05H10.1, pdi-2, pig-1, sel-12, rpl-25.2, act-4, rps-6, rps-5, rps-3, xnp-1, rps-1, hda-1, F43D9.3, F20D6.11, czw-1, pod-1, T14G10.5, C53A5.6, brc-1, knl-2, rps-0, rpn-7, F32D8.5, rpn-3, rba-1, F32D8.13, R05D3.8, T13H5.8, tig-2, bmk-1, rpm-1, let-526, eel-1, rps-23, eif-1, rps-28, cap-1, rps-26, hif-1, ubc-9, cyc-2.1, rps-19, usp-48, rps-11, cgh-1, dad-1, his-68, F14B4.3, rps-16, F38E11.5, rps-17, atad-3, crn-1, hel-1, cct-5, cct-6, lpd-2, T09E8.1, cct-1, let-70, ppk-1, arp-11, kin-19</i></p> | |

Table S5. CES-1 target genes for GOterm asymmetric cell division

| | |
|---|----------|
| GO:0008356~asymmetric cell division | |
| Count | Pvalue |
| 19 | 9.70E-04 |
| Target gene with this GOterm: <i>arf-3,dnj-11,arf-6,wrn-1,par-3,ham-1,par-2,ama-1,par-5,mig-5,par-1,pig-1,rab-5,nmy-2,lit-1,cnt-2,mom-5,cam-1,csnk-1</i> | |

Corrigendum for Wei *et al.*, *GENETICS* 206 (4) 2069-2084.

GENETICS, Vol 206, 2069-2084, August 2017, Copyright © 2017 Genetics Society of America.

CORRIGENDUM

In the article by H. Wei, B. Yan, J. Gagneur, and B. Conradt (*GENETICS* 206: 2069-2084) entitled “*Caenorhabditis elegans* CES-1 Snail Represses *pig-1* MELK Expression To Control Asymmetric Cell Division”, scholarship funding for H. W. was not included. The following sentence has been added to the Acknowledgments section:

H. W. was supported by a predoctoral fellowship from the China Scholarship Council (<https://www.csc.edu.cn/>).

Caenorhabditis elegans *ced-3* Caspase Is Required for Asymmetric Divisions That Generate Cells Programmed To Die

Nikhil Mishra, Hai Wei, and Barbara Conradt¹

Faculty of Biology, Center for Integrated Protein Science Munich, Ludwig-Maximilians-University Munich, 82152 Planegg-Martinsried, Germany

ORCID IDs: 0000-0002-6425-5788 (N.M.); 0000-0002-7338-4899 (H.W.); 0000-0002-3731-4308 (B.C.)

ABSTRACT Caspases have functions other than in apoptosis. Here, we report that *Caenorhabditis elegans* CED-3 caspase regulates asymmetric cell division. Many of the 131 cells that are “programmed” to die during *C. elegans* development are the smaller daughter of a neuroblast that divides asymmetrically by size and fate. We have previously shown that CED-3 caspase is activated in such neuroblasts, and that before neuroblast division, a gradient of CED-3 caspase activity is formed in a *ced-1* MEGF10 (multiple EGF-like domains 10)-dependent manner. This results in the nonrandom segregation of active CED-3 caspase or “apoptotic potential” into the smaller daughter. We now show that CED-3 caspase is necessary for the ability of neuroblasts to divide asymmetrically by size. In addition, we provide evidence that a *pig-1* MELK (maternal embryonic leucine zipper kinase)-dependent reciprocal gradient of “mitotic potential” is formed in the QL.p neuroblast, and that CED-3 caspase antagonizes this mitotic potential. Based on these findings, we propose that CED-3 caspase plays a critical role in the asymmetric division by size and fate of neuroblasts, and that this contributes to the reproducibility and robustness with which the smaller daughter cell is produced and adopts the apoptotic fate. Finally, the function of CED-3 caspase in this context is dependent on its activation through the conserved *egl-1* BH3-only, *ced-9* Bcl-2, and *ced-4* Apaf-1 pathway. In mammals, caspases affect various aspects of stem cell lineages. We speculate that the new nonapoptotic function of *C. elegans* CED-3 caspase in asymmetric neuroblast division is relevant to the function(s) of mammalian caspases in stem cells.

KEYWORDS caspase; nonapoptotic function; asymmetric cell division; neuroblasts; *C. elegans*; *pig-1* MELK

DURING embryonic and postembryonic *Caenorhabditis elegans* development, 131 somatic cells reproducibly die (Sulston and Horvitz 1977; Sulston *et al.* 1983). Genetic screens resulted in the identification of four genes that can mutate to block most of these cell deaths and that define a conserved apoptotic cell death pathway (*egl-1* BH3-only, *ced-9* Bcl-2, *ced-4* Apaf-1, and *ced-3* caspase) (Horvitz 2003; Conradt *et al.* 2016). Interestingly, most of the cells that are programmed to die during development are generated through divisions that are asymmetric by fate and size, and

that produce a smaller daughter that is programmed to die. The apoptotic death of the smaller daughter is triggered through the transcriptional upregulation (and, hence, increase in expression) in that cell of *egl-1* BH3-only, which induces apoptosome formation, and the maturation and activation of the protease CED-3 caspase. Active CED-3 caspase cleaves specific substrates and thereby induces the killing, dismantling, and phagocytosis of the cell in a cell-autonomous manner. For example, CED-3 caspase cleaves and activates the lipid scramblase CED-8 Xkr8, which results in the exposure of the “eat-me signal” phosphatidylserine (PS) on the surface of the dying cell (Stanfield and Horvitz 2000; Suzuki *et al.* 2013). This signal is recognized by receptors on neighboring cells, namely CED-1 MEGF10 (multiple EGF-like domains 10), which leads to receptor clustering and the activation of two conserved parallel engulfment pathways in the engulfing cell (Zhou *et al.* 2001; Venegas and Zhou 2007). Recently, we demonstrated that active CED-3 caspase is already present in the mother of at least

Copyright © 2018 by the Genetics Society of America

doi: <https://doi.org/10.1534/genetics.118.301500>

Manuscript received August 12, 2018; accepted for publication September 4, 2018; published Early Online September 7, 2018.

Available freely online through the author-supported open access option.

Supplemental material available at Figshare: <https://doi.org/10.25386/genetics.7058609>.

¹Corresponding author: Faculty of Biology, Center for Integrated Protein Science Munich, Ludwig-Maximilians-University Munich, LMU Biocenter, Großhaderner St. 2, 82152 Planegg-Martinsried, Germany. E-mail: conradt@bio.lmu.de

one cell programmed to die, the embryonic neurosecretory motor neuron (NSM) neuroblast, which divides to give rise to the larger NSM, which survives and differentiates into a serotonergic motor neuron, and the smaller NSM sister cell (NSMsc), which dies (Chakraborty *et al.* 2015; Lambie and Conratt 2016). Furthermore, this active CED-3 caspase causes the clustering and activation (in a *ced-8* Xkr8- and PS-independent manner) of CED-1 MEGF10 and the two engulfment pathways in the two dorsal neighbors of the NSM neuroblast. This activation of the engulfment pathways in turn is necessary for the formation and/or maintenance of a gradient of CED-3 caspase activity in the NSM neuroblast, and the nonrandom segregation of active CED-3 caspase into the smaller NSMsc, where it promotes the robust and swift execution of apoptotic cell death (Chakraborty *et al.* 2015; Lambie and Conratt 2016).

The formation of a gradient of CED-3 caspase activity in the mother of a cell programmed to die has so far only been demonstrated in the embryonic NSM neuroblast lineage. For this reason, the generality of this phenomenon has so far been unclear. In addition, whether active CED-3 caspase plays a role in the mother other than promoting its own enrichment in one part of the cell, has been unknown. To address these questions, we examined the postembryonic QL.p neuroblast lineage. Our results support the notion that the formation of a gradient of CED-3 caspase activity is a general phenomenon. Furthermore, we provide evidence that the *ced-3* caspase gene plays an active role in the asymmetric division of mothers. Specifically, we provide evidence that *ced-3* caspase is required for their ability to divide asymmetrically by size and fate, and, hence, to produce the smaller daughter, which is programmed to die.

Materials and Methods

Strains and genetics

All *C. elegans* strains analyzed were maintained at 25° on Nematode Growth Medium, unless otherwise specified (Brenner 1974). The following mutations and transgenes were used in this study: LGI: *ced-1(e1735)* (Hedgecock *et al.* 1983); LGIII: *ced-4(n1162)* (Ellis and Horvitz 1986), *ced-6(n1813)* (Ellis *et al.* 1991), *unc-119(ed3)* (Maduro and Pilgrim 1995) and *rdvIs1* (P_{egl-17} *mCherry::his-24*, P_{egl-17} *myristoylated mCherry*, P_{egl-17} *mig-10::yfp*) (Ou *et al.* 2010); LGIV: *ced-2(n1994)* (Ellis *et al.* 1991), *ced-3(n717)* (Ellis and Horvitz 1986), *ced-3(n2433)* (Shaham *et al.* 1999), *ced-3(n2427)* (Shaham *et al.* 1999), *pig-1(gm344)* (Cordes *et al.* 2006), and *bcSi82* (P_{toe-2} *mKate2::tac-1*) (this study); and LGV: *egl-1(n3330)* (Sherrard *et al.* 2017), *bzIs190* (P_{mec-4} *gfp*) (M. Driscoll (Rutgers University), personal communication), *ltIs44* (P_{pie-1} *mCherry::ph^{PLC}*) (Audhya *et al.* 2005), and *enIs1* (P_{ced-1} *ced-1ΔC::gfp*) (Zhou *et al.* 2001). Additional transgenes used in this study are: *bclIs133* (P_{toe-2} *gfp*) (this study), *bcEx1277* (P_{hyp7} *ced-1::gfp*) (this study), and *bcEx1334* (P_{toe-2} *ced-1::mKate2*) (this study).

Cloning

pBC1565 (P_{toe-2} *gfp*): The *toe-2* promoter (P_{toe-2}) (2117 bp immediately upstream of the *toe-2* start site) was amplified

by PCR using N2 genomic DNA, and restriction sites for AgeI and SacI were introduced at the ends of the PCR product. Primers used to amplify P_{toe-2} were SacI P_{toe-2} -F (5'-aaaa GAGCTCttatctgtaccacaaattcc-3') and AgeI P_{toe-2} -R (5'-aaaaACCGGTttttgacctgaggacatgatg-3'). The resulting PCR product and plasmid pBC1408 (P_{ces-2} *gfp::unc-54 3' UTR* in pBlue-script) were digested with AgeI and SacI (which drops out P_{ces-2} from pBC1408), and the PCR product cloned into the pBC1408 backbone using T4 ligation to obtain pBC1565 (P_{toe-2} *gfp*).

pBC1591 (P_{hyp7} *gfp*) and pBC1681 (P_{hyp7} *ced-1::gfp*): The promoter of gene *Y37A1B.5* (P_{hyp7}) (2910 bp immediately upstream of the *Y37A1B.5* start site) (Hunt-Newbury *et al.* 2007) was amplified by PCR using N2 genomic DNA, and restriction sites for AgeI and SacI were introduced at the ends of the PCR product. Primers used to amplify P_{hyp7} were P_{hyp7} -F (5'-aaaGAGCTCaaactttattagacgtcgcaattt-3') and P_{hyp7} -R (5'-aaaACCGGTtttggttttggattttgatc-3'). The PCR product obtained (P_{hyp7}) was used to replace P_{toe-2} in pBC1565 using restriction digest with AgeI and SacI, and T4 ligation to generate plasmid pBC1591 (P_{hyp7} *gfp*). A *ced-1* minigene was amplified from plasmid pZZ610 (P_{ced-1} *ced-1::gfp*, Zhou *et al.* 2001) by PCR using the primers AgeI *ced-1*-F (5'-aaaACCGG Tattgctctcattctccttgctac-3') and *ced-1*-R (5'-ttttctaccg tactgaattct-3'). The resulting PCR product and pBC1591 were digested with AgeI, and the *ced-1* minigene was inserted by T4 ligation into the linearized pBC1591 to obtain plasmid pBC1681 (P_{hyp7} *ced-1::gfp*).

pBC1805 (P_{toe-2} *ced-1::mKate2*): pBC1805 was cloned by Gibson cloning (Gibson *et al.* 2009). Primers pBSK P_{toe-2} -F (5'-ATCCCCCGGGCTGCAGGAATTCGATTTATCTGTACCACA AATTCCTTG-3') and *ced-1* P_{toe-2} -R (5'-GAATGAGACGCATT TTTGACCTGAGGACATG-3') were used to amplify P_{toe-2} using pBC1565 as a template. A *ced-1* minigene was amplified in two parts: fragment 1 was amplified using primers *P_{toe-2}ced-1_fwd* (5'-CCTCAGGTCAAAAATGCGTCTCAATCTCCTTG-3') and *ced-1_mini_1_rev* (5'-ccgggtcacagttGGCTCCATTTT CACAGTC-3'), whereas fragment 2 was amplified using the primers *ced-1_mini_2_fwd* (5'-tgaaaatggagccAACTGTGA CCCGGAATC-3') and *ced-1_mini_2_rev* (5'-ccttgatgagct cggaTTTTTCTACCGGTACTTGAATTC-3'). pZZ610 was used as a template for the amplification by PCR of both fragments (Zhou *et al.* 2001). *mKate2::tbb-2 3' UTR* was amplified from plasmid pEZ167 (P_{mec-5} *fkbp12::mKate2::tbb-2 3' UTR*; E. Zanin (LMU Munich), personal communication, Turek *et al.* 2013) as template with the help of the primers *mK_tbb-2_fwd* (5'-accgtagaataaaTCCGAGCTCATCAAGGAG-3') and *mK_tbb-2_rev* (5'-ggtcgacggtatcgataagcttgatCAATGAG ACTTTTTCTITGGC-3'). EcoRV-digested pBluescript II KS(+) was used as backbone and all the above fragments were assembled using Gibson assembly to obtain pBC1805 (P_{toe-2} *ced-1::mKate2*).

pBC1807 (P_{toe-2} *mKate2::tac-1*): pBC1807 was generated by Gibson assembly (Gibson *et al.* 2009). P_{toe-2} was amplified

using the primers NM1 (5'-gagctctggtaccctctagtcaggTTATC TGTACCACAAATTCCTTG-3') and NM2 (5'-tgagctcggacatTT TTAGCTGAGGACATG-3'), and pBC1565 as a template. *mKate2::tac-1* was obtained by PCR amplification using plasmid TMD34 (*P_{mex-5}mKate2::tac-1::tbb-2 3' UTR*; T. Mikeladze-Dvali, (LMU Munich) personal communication) as a template, and the primers NM3 (5'-cctcaggtcaaaaATGTCGG AGCTCATCAAG-3') and NM4 (5'-aattctacgaatgTTATGC ATCCGTCGAAATAAC-3'). Similarly, pBC1565 was used as a template to amplify the *unc-54 3' UTR* using primers NM5 (5'-gacggatgataaCATTCGTAGAATTCCTCAACTG-3') and NM6 (5'-agtcgtaatacactcacttaaggAAACAGTTATGTTTGGTATAT TGG-3'). These fragments were introduced into *StuI*-digested pCFJ909 (Frøkjær-Jensen *et al.* 2014) using Gibson assembly to obtain pBC1807 (*P_{toe-2}mKate2::tac-1*).

Microinjection

bcls133 (P_{toe-2}gfp): pBC1565 (20 ng/μl) + pRF4 (80 ng/μl) was injected into the gonads of young N2 adult hermaphrodites and extrachromosomal array was integrated by UV irradiation to obtain *bcls133*, which was 5× backcrossed with N2.

bcEx1277 (P_{hyp7}ced-1::gfp): pBC1681 (51 ng/μl) + IR101 (10 ng/μl) (*P_{rps-0}HygR::gpd-2/gpd-3::mCherry::unc-54 3' UTR*, Radman *et al.* 2013) was injected into the gonads of young *ced-1(e1735); ced-3(n2427); bcls133* adult hermaphrodites to obtain *ced-1(e1735); ced-3(n2427); bcls133; bcEx1277*.

bcEx1334 (P_{toe-2}ced-1::mKate2): *bcEx1334* was generated by injecting pBC1805 (26 ng/μl) + pCFJ90 (*P_{myo-2}::mCherry::unc-54 3' UTR*; Frøkjær-Jensen *et al.* 2008) (2.6 ng/μl) + pBluescript II KS(+) (60 ng/μl) into the gonads of young *ced-1(e1735); ced-3(n2427); bcls133* adult hermaphrodites to obtain *ced-1(e1735); ced-3(n2427); bcls133; bcEx1334*.

bcSi82 (P_{toe-2}mKate2::tac-1): *bcSi82* was generated by miniMOS integration of pBC1807 (*P_{toe-2}mKate2::tac-1*) into HT1593 [*unc-119(ed3)*] animals (Frøkjær-Jensen *et al.* 2014). First, 10 ng/μl of pBC1807 was injected into the gonads of HT1593 animals along with pCFJ601 (50 ng/μl), pGH8 (10 ng/μl), pCFJ90 (2.5 ng/μl), and pCFJ104 (5 ng/μl) (Frøkjær-Jensen *et al.* 2014). Worms were allowed to starve for 1 week, after which wild-type movers were examined for integration.

Extra PVM neurons

Posterior ventral mechanosensory (PVM) neurons were visualized using the transgene *P_{mec-4}gfp (bzIs190)*, which labels all mechanosensory neurons (Mitani *et al.* 1993). Fourth larval stage (L4) larvae of the desired genotype were anesthetized in a drop of sodium azide solution (30 mM in M9 buffer) on a 2% agarose pad on a glass slide. A 100×/1.3 NA oil-immersion objective lens on a Zeiss ([Carl Zeiss], Thornwood, NY) Imager.M2 epifluorescence microscope was used to visualize PVM neurons.

QL.pp survival

QL.pp survival was determined using the transgene *P_{toe-2}gfp (bcls133)*, which labels cells of the Q lineages (Gurling *et al.* 2014). In wild-type animals, QL.pp dies within ~17 hr post-egg laying during the first larval stage (L1 stage) (at 25°) (Sulston and Horvitz 1977). To avoid false positives due to delayed cell death, we used larvae of the second larval stage (L2 larvae) (25–30 hr postegg laying) for analysis. Larvae were anesthetized in a drop of levamisole solution (10 mM in M9 buffer) on a 2% agarose pad on a glass slide. *P_{toe-2}gfp* was visualized with the help of a 100X/1.3 NA oil-immersion objective lens on a Zeiss Imager.M2 epifluorescence microscope. We only considered those worms for assessing QL.pp survival in which QL.pa had divided and its daughters had formed visible neurite extensions at the time of counting. Thus, we ensured that slow-growing strains were not analyzed at an earlier developmental time point. Importantly, upon failure of death, QL.aa, which is produced in the vicinity of QL.p, migrates toward the tail, and therefore away from QL.pp. As a result, it does not interfere with our determination of QL.pp survival.

Division of “undead” QL.pps

The division of undead QL.pps was determined using the transgene *P_{toe-2}gfp (bcls133)*. L2 larvae were prepared similarly as for QL.pp survival. Animals were assessed after QL.pa had divided to form PVM and SDQL neurons with visible neurite outgrowths.

Live imaging of QL.p and QL.a divisions

The transgene *P_{toe-2}gfp (bcls133)* was used to identify QL.p and QL.a, and to analyze their asymmetric divisions. L1 larvae were immobilized in 1 μl polybead microsphere suspension (0.1 μm diameter, 2.5% w/v, catalog number 00876; Polysciences, Warrington, PA) on a 10% agarose pad (agarose was dissolved in 67% M9 buffer). A glass coverslip was placed on the agar pad and the empty space around the agarose pad underneath the coverslip was filled with paraffin oil to prevent dehydration. Image Z-stacks were acquired every 3 min with a 1-μm step size using a 63×/1.4 NA oil-immersion objective lens on the UltraVIEW VoX spinning disk microscope (Perkin Elmer [Perkin Elmer-Cetus], Norwalk, CT).

QL.p and QL.a daughter cell sizes

Q-lineage cells are relatively flat cells. As a result, single-plane cell areas provide a fair estimation of cell sizes (*i.e.*, area is directly proportional to cell volume) (Cordes *et al.* 2006). Therefore, the image Z-stacks acquired of the daughters of QL.p and QL.a using the transgene *P_{toe-2}gfp (bcls133)* (see *Live imaging of QL.p and QL.a divisions*) were converted to obtain maximum-intensity Z-projections. Cell sizes were estimated by circumscribing the cells and measuring their areas with Fiji (Schindelin *et al.* 2012; Schneider *et al.* 2012).

Determination of QL.p cleavage furrow position

Images of QL.p undergoing cytokinesis were obtained from the movies generated to assess QL.p daughter cell sizes. The

position of the cleavage furrow was determined by measuring its distance from the anterior periphery of QL.p and dividing it by the total length of the cell (Figure 5D). Distances were measured using Fiji (Schindelin *et al.* 2012; Schneider *et al.* 2012).

Localization studies for CED-1ΔC::GFP

CED-1 localization was analyzed using the transgene $P_{ced-1}ced-1\Delta C::gfp$ (*enIs1*) (Zhou *et al.* 2001). L1 larvae were anesthetized with levamisole (0.1 mM in M9 buffer), mounted on 3% agarose pads on glass slides, and examined using 63×/1.4 NA oil-immersion objectives on a Leica SP5 inverted confocal microscope. Q-lineage cells were identified with the help of the transgene $P_{egl-17}mCherry::his-24$, $P_{egl-17}myristoylated\ mCherry$, $P_{egl-17}mig-10::yfp$ (*rdvIs1*) (Ou *et al.* 2010).

TAC-1 ratio

The TAC-1 ratio was determined using the transgenes $P_{toe-2}mKate2::tac-1$ (*bcSi82*) and $P_{toe-2}gfp$ (*bcls133*). L1 larvae of the desired genotypes were grown at 20° and immobilized in 1 μl polybead microsphere suspension, and slides prepared as described earlier for live imaging of QL.p and QL.a divisions. Image Z-stacks were acquired every 5 min with a 0.5-μm step size using a 100×/1.4 NA oil-immersion objective lens on the UltraVIEW VoX spinning disk microscope (Perkin Elmer). The time point at which QL.p was at metaphase was used to determine the amount of TAC-1 associated with the two centrosomes. Quantification of the amount of centrosome-associated TAC-1 was performed as described previously (Chakraborty *et al.* 2015). A region of the same size on the slide but outside the animal was considered as background noise, and its intensity was subtracted from the measured intensities of centrosome-associated TAC-1.

NSM neuroblast daughter cell sizes

The NSM and NSMsc were identified using the transgene $P_{pie-1}mCherry::ph^{PLC\delta}$ (*ltIs44*), and their sizes determined as described (Chakraborty *et al.* 2015; Wei *et al.* 2017). All images were acquired using a Leica TCS SP5 II confocal microscope. All strains were incubated at 20° overnight before imaging.

Embryonic lethality

Five L4 larvae of each genotype were singled on seeded NGM plates. These were allowed to lay eggs for 30 hr at 20°. Two-days later, the numbers of larvae and dead eggs were determined.

Statistical analysis

Proportions were compared using Fisher's Exact Test, and the obtained *P*-values were adjusted using the Benjamini and Hochberg test for multiple comparisons (Fisher 1935; Yoav 1995). Wherever applicable, data were tested for normal distribution using the D'Agostino and Pearson normality test (D'Agostino and Pearson 1993). When data

were found to be distributed normally, the Student's *t*-test or parametric one-way ANOVA were performed to determine statistical significance between groups assuming that the groups had unequal SD, and Tukey's or the Benjamini and Hochberg multiple comparisons test was applied (Student 1908; Fisher 1921; Tukey 1949). When comparing the amounts of TAC-1 on the anterior and posterior centrosomes (where all posterior TAC-1 levels were set to 1), we used the Wilcoxon signed-rank test to determine if the groups were statistically different (Wilcoxon 1945). The Mann-Whitney test was used to compare the ratios of QL.a daughter cell sizes in wild-type animals with those in *ced-3(n717)* animals (Mann 1947).

Data availability

All reagents and strains generated for this study are available from the authors upon request. The authors affirm that all data necessary for confirming the conclusions of the article are present within the article and figures. Supplemental material available at Figshare: <https://doi.org/10.25386/genetics.7058609>.

Results

A ced-1 MEGF10-dependent, but pig-1 MELK-independent, gradient of CED-3 caspase activity is present in the postembryonic QL.p neuroblast

During the L1 stage of postembryonic *C. elegans* development, the neuroblast QL.p divides asymmetrically by size and fate to produce a larger anterior daughter, QL.pa, which survives, and a smaller posterior daughter, QL.pp, which is programmed to die (Sulston and Horvitz 1977; Cordes *et al.* 2006) (Figure 1, wild-type). The observation that defects in the asymmetric division of QL.p by size can affect the fate of its daughters (especially the fate of QL.pp) indicates that daughter cell size and daughter cell fate are functionally coupled (Cordes *et al.* 2006; Singhvi *et al.* 2011; Gurling *et al.* 2014; Teuliere *et al.* 2014; Teuliere and Garriga 2017). To determine whether a gradient of CED-3 caspase activity forms in QL.p prior to its division, we used a reporter for the protein TAC-1 ($P_{toe-2}mKate2::tac-1$). TAC-1 is a component of the pericentriolar material and a substrate of CED-3 caspase (Bellanger and Gonczy 2003; Le Bot *et al.* 2003; Srayko *et al.* 2003; Chakraborty *et al.* 2015). We have previously shown that in the embryonic NSM neuroblast, the amount of TAC-1 associated with the centrosome that is inherited by the larger daughter, which survives, is greater (by 1.30-fold) than the amount of TAC-1 associated with the centrosome that is inherited by the smaller daughter, which is programmed to die (Chakraborty *et al.* 2015). This "TAC-1 asymmetry" is dependent on a functional *ced-3* caspase gene as well as a CED-3 caspase cleavage site in the TAC-1 protein and, hence, reflects a gradient of CED-3 caspase activity along the cleavage axis of the NSM neuroblast. Furthermore, the establishment and/or maintenance of this gradient of CED-3 caspase activity in the NSM neuroblast is dependent

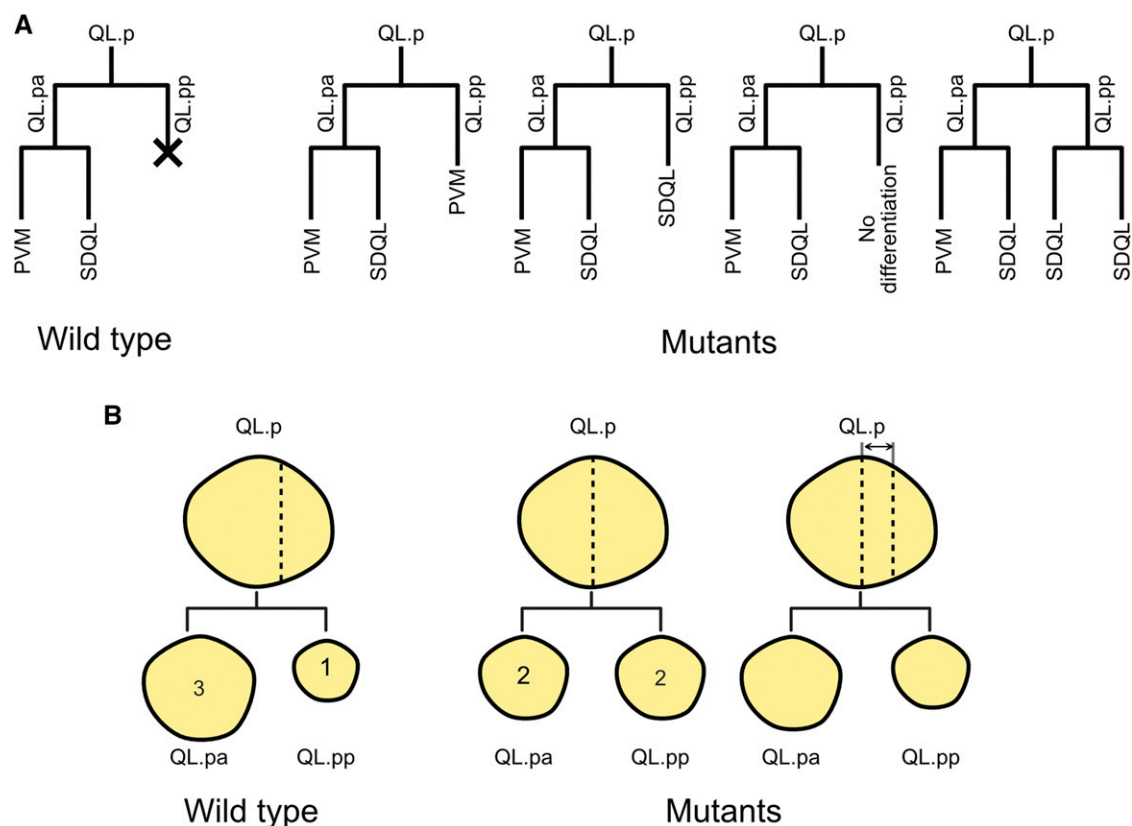


Figure 1 The *C. elegans* QL.p neuroblast lineage. (A) Schematic representation of the postembryonic QL.p neuroblast lineage in wild-type (left) and mutant (right) worms. Vertical and horizontal lines represent individual cells and cell divisions, respectively. “X” denotes a cell death. (B) Schematic representation of the cell sizes of the QL.p neuroblast and its daughter cells in wild-type (left) and mutant (right) worms. In wild-type worms, QL.pa is nearly three times as large as its sister, QL.pp. However, in mutants with defects in the asymmetric division by size of QL.p, QL.pa and QL.pp can be of similar sizes.

on the two conserved *C. elegans* engulfment pathways (Chakraborty *et al.* 2015). We found that at QL.p metaphase, the amount of TAC-1 associated with the anterior centrosome is 1.25-fold greater than that associated with the posterior centrosome (Figure 2, A and B). Furthermore, this asymmetry is lost in the background of a strong loss-of-function (lf) mutation of *ced-3* caspase, *n717*, or a strong lf mutation of the engulfment gene *ced-1* MEGF10, *e1735* (ratios of 0.97 and 0.99, respectively) (Figure 2, A and C). The gene *pig-1* encodes a PAR-1-like kinase orthologous to mammalian MELK (maternal embryonic leucine zipper kinase) and is important for the asymmetric division of QL.p. Specifically, the loss of *pig-1* MELK causes QL.p to divide symmetrically by size (Cordes *et al.* 2006) (see below). Interestingly, we found that TAC-1 asymmetry at QL.p metaphase is not affected by a strong lf mutation of *pig-1* MELK, *gm344* (ratio of 1.28) (Figure 2, A and C). Therefore, a *ced-1* MEGF10-dependent gradient of CED-3 caspase activity is also formed in QL.p prior to its division. This gradient is along the anterior–posterior axis and presumably results in the nonrandom segregation of active CED-3 caspase into the smaller posterior daughter QL.pp, which is programmed to die. *pig-1* MELK is not required for the formation of this CED-3 caspase activity gradient.

However, because of its role in the asymmetric division of QL.p by size, its loss nevertheless probably affects the concentration of active CED-3 caspase in QL.pp (the concentration is probably less than that in wild-type; see below).

Consistent with the notion that *ced-1* MEGF10 and the engulfment pathways play an instructive role in the establishment and/or maintenance of this gradient of CED-3 caspase activity, we found that an asymmetric contact exists between QL.p and a neighboring cell that exhibits detectable levels of CED-1 MEGF10 on its cell surface (Figure 3, Supplemental Material, Figure S1 and File S1). Specifically, QL.p is in contact with the syncytial cell hyp7, which is part of the hypodermis that covers large parts of the animal and which, after QL.p division, engulfs the QL.pp corpse (Sulston and Horvitz 1977). Using a CED-1 MEGF10 reporter (*P_{ced-1}ced-1ΔC::gfp*) (Zhou *et al.* 2001), we detected CED-1 MEGF10 on what appears to be the entire surface of hyp7 (Figure 3, Figure S1, and File S1). However, we found that while there is almost uniform contact between hyp7 and the lateral side of QL.p, there is an asymmetric contact between hyp7 and the medial side of QL.p. More specifically, the posterior, but not the anterior, part of QL.p’s medial side contacts hyp7. Therefore, a cell surface that contains detectable levels of CED-1

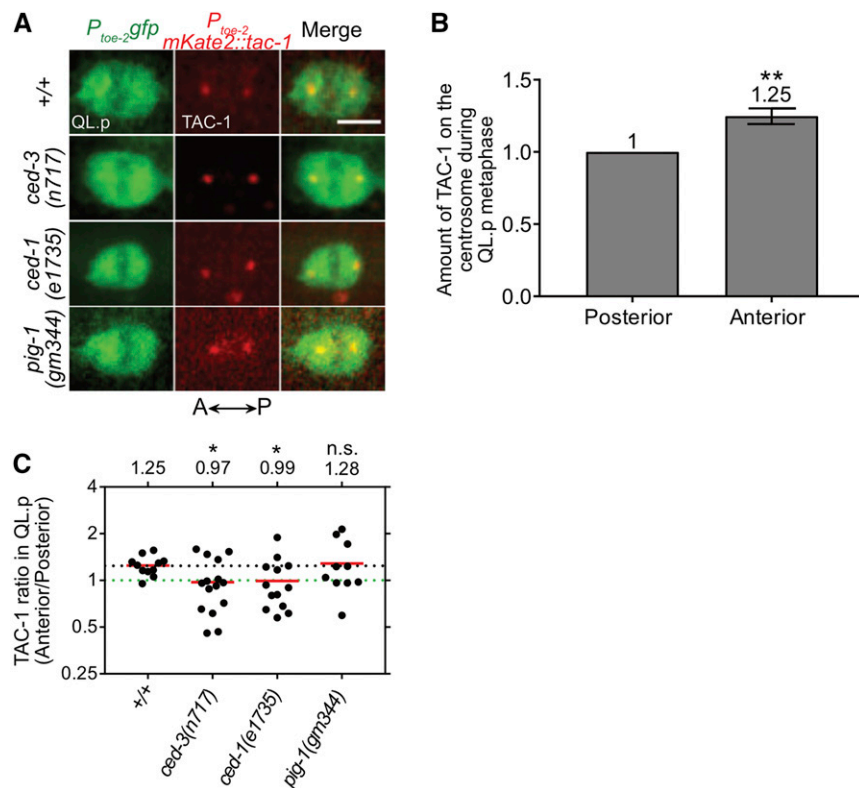


Figure 2 A *ced-1* MEGF10-dependent gradient of CED-3 caspase activity exists in QL.p at metaphase. (A) Representative images of centrosome-associated mKate2::TAC-1 in QL.p at metaphase in the indicated genotypes. Bar, 3 μ m. QL.p was identified using *P_{toe-2}gfp* (*bcls133*) and TAC-1 was visualized using *P_{toe-2}mKate2::tac-1* (*bc5182*). (B) Bar graph showing the comparison of total mKate2::TAC-1 signals associated with the anterior and posterior centrosomes during QL.p metaphase in wild-type animals. Total “Anterior” TAC-1 signal was normalized to the total “Posterior” TAC-1 signal, which was set to 1 for each animal. Wilcoxon signed-rank test was used to determine statistical significance. ** $P < 0.01$, $n = 11$ QL.ps. (C) Dot plot showing the spread of the TAC-1 ratios in QL.p (Anterior/Posterior) among animals of each genotype. The horizontal red lines indicate the mean for each genotype (also mentioned above the spread for each group). The dotted black line represents the mean for wild-type (+/+). The dotted green line represents the ratio 1. Each dot represents the TAC-1 ratio for one animal. Statistical significance was determined using the Student’s *t*-test and Benjamini and Hochberg multiple comparisons correction. * $P < 0.05$, $n \geq 10$ QL.ps. n.s., not significant.

MEGF10 apposes the part of QL.p that will later form the smaller daughter, QL.pp, which is programmed to die, but not the part of QL.p that will later form the larger daughter, QL.pa, which survives (schematically represented in the drawing in the lower left hand corner of Figure 3; this drawing was compiled based on the images shown in Figure 3 and in Figure S1). We propose that this asymmetry in the presentation of CED-1 MEGF10 on apposing cell surfaces (and, hence, in the activation of CED-1 MEGF10 and the engulfment pathways) is critical for the establishment of a gradient of CED-3 caspase activity along the anterior–posterior axis of QL.p.

The loss of *ced-1* MEGF10 promotes the appearance of extra PVM neurons

The larger daughter, QL.pa, not only survives but also divides to generate the neurons PVM and SDQL (Figure 1A, wild-type). To determine the possible function of the *ced-1* MEGF10-dependent gradient of CED-3 caspase activity in QL.p, we analyzed the number of PVM neurons generated by this lineage. A block in apoptotic cell death prevents the death of QL.pp, and this can lead to the presence of two, rather than one, PVM neurons in L4 larvae (Figure 1A, Mutants). For example, using a PVM-specific reporter (Mitani *et al.* 1993), an extra PVM neuron is detected in 0% of wild-type animals but in 2% of *ced-3(n717)* animals (Chien *et al.* 2013) (Figure 4, A and B). In contrast, a compromised apoptotic cell death pathway, such as in animals homozygous for the weak *ced-3* lf mutation *n2427*, does not lead to the presence of an extra PVM neuron. We found that in a

ced-3(n2427), but not wild-type, background, *ced-1(e1735)* causes the presence of an extra PVM neuron in 3% of the animals (Figure 4B). We also analyzed *ced-1(e1735)* in the background of *pig-1(gm344)*. In an otherwise wild-type background, the loss of *pig-1* MELK causes the presence of an extra PVM neuron in 30% of the animals (Cordes *et al.* 2006) (Figure 4B). We found that *ced-1(e1735)* as well as *ced-3(n2427)* significantly enhanced this phenotype to 58 or 70%, respectively. Furthermore, we found that 96% of the triple-mutant animals had an extra PVM neuron. Therefore, the loss of *ced-1* MEGF10 (and, hence, the loss of the gradient of active CED-3 caspase in QL.p) promotes the presence of extra PVM neurons in a background in which the apoptotic cell death pathway is compromised as well as in a background in which QL.p divides symmetrically. Furthermore, in a background in which QL.p divides symmetrically [*i.e.*, in *pig-1(gm344)*], the enhancements of the extra PVM neuron phenotype, either through compromising the apoptotic cell death pathway or through the loss of *ced-1* MEGF10, are additive.

ced-1 MEGF10 is not required for the asymmetric division of QL.p by size

The presence of an extra PVM neuron can be the result of a defect in the asymmetric division of QL.p by size, the asymmetric division of QL.p by fate, or a combination thereof. To determine which of these processes is affected by *ced-1(e1735)*, we analyzed them individually. To analyze the asymmetric division of QL.p by size, we used a GFP reporter that is expressed in QL.p and its daughters (*P_{toe-2}gfp*)

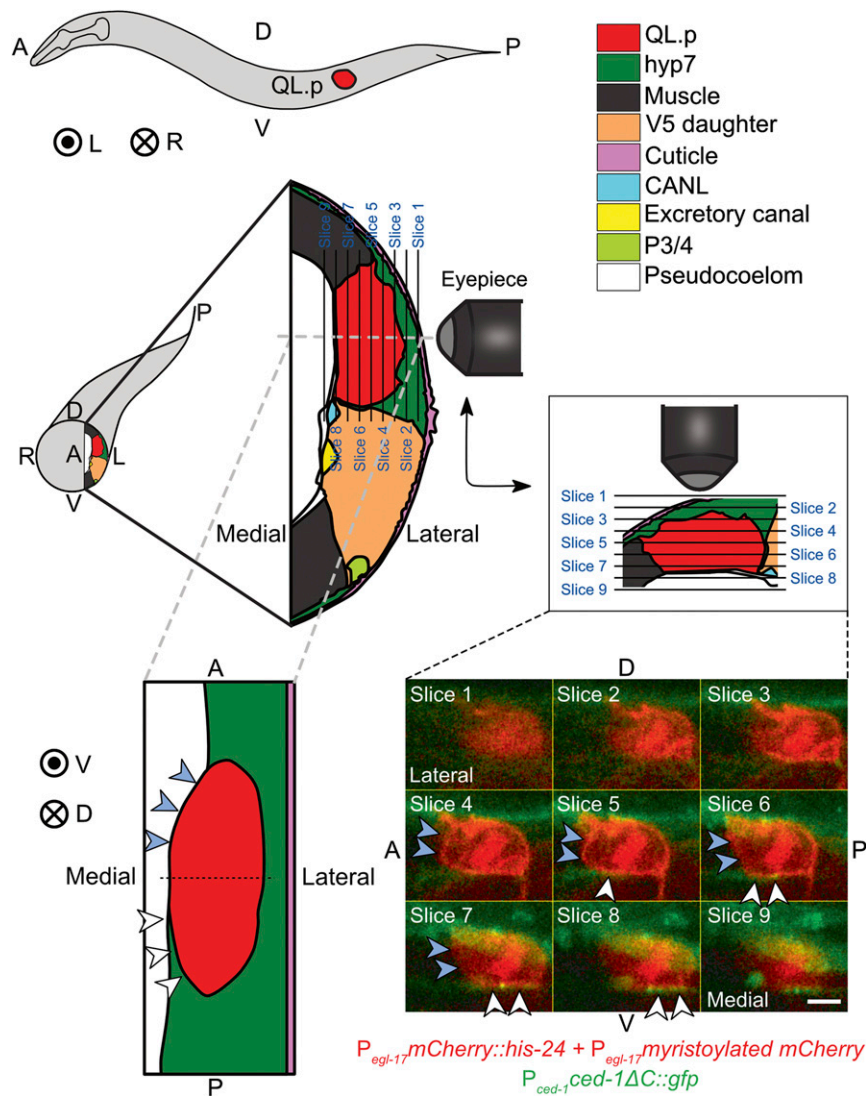


Figure 3 Asymmetric presence of CED-1 MEGF10 around QL.p. Schematic of an L1 larva with the location of QL.p indicated is shown top-left. A: anterior, P: posterior, D: dorsal, V: ventral, L: left, and R: right. Concentric circles represent the direction projecting toward the reader, while the circle with a cross represents the direction projecting away from the reader. The schematic below the L1 larva represents a transverse section through the larva at the position where QL.p is localized. The section is enlarged in the adjoining image on the right. This and another section (bottom-left) shown were drawn based on fluorescence images and images of electron microscopy sections available on WormAtlas (<http://www.wormatlas.org/>). The key for cell colors is at the top-right. Larvae were imaged from the side, and individual image slices were acquired while gradually moving from the left to the middle of the worm. QL.p was labeled with the transgene $P_{egl-17}mCherry::his-24$, $P_{egl-17}myristoylated\ mCherry$, $P_{egl-17}mig-10::yfp\ (rdvls1)$ and $hyp7$ with the transgene $P_{ced-1}ced-1\Delta C::gfp\ (enl51)$ (see *Materials and Methods* for details). The diagram in the middle-right represents the orientation of the image planes, images for which have been shown at the bottom-right. In these images, white arrowheads indicate a contact between CED-1ΔC::GFP and QL.p, whereas blue arrowheads indicate the lack of contact. Bar, 2 μm. It can be seen in the images for slices 4–9 that CED-1ΔC::GFP is in contact with the posterior part of QL.p but not with its anterior part. The coronal section (bottom-left) has been created based on the fluorescence images (slices shown at the bottom-right) and the images of the electron microscopy sections. It can be seen in this diagram that while $hyp7$ almost entirely envelops the posterior part of QL.p, it only forms contact with the left side of the anterior part.

(Gurling *et al.* 2014), and acquired image stacks of QL.p in developing L1 larvae every 3 min. The first stack acquired after the completion of QL.p cytokinesis was then used to estimate the sizes of the two daughter cells (Figure 5A) (Q-lineage cells are relatively flat cells. Hence, measurements of their areas of maximum intensity projection images provide reliable approximations of their cell sizes (Cordes *et al.* 2006)). In wild-type animals, QL.p divides asymmetrically by size to produce the larger QL.pa and the smaller QL.pp with a size ratio of QL.pa to QL.pp of ~ 3.0 (Figure 1B, wild-type; Figure 5, B and C). As was reported previously (Cordes *et al.* 2006), in $pig-1(gm344)$ animals, QL.p divides symmetrically to produce two cells of similar sizes with a size ratio of QL.pa to QL.pp of 1.1 (Figure 5, B and C). Using this assay, we did not observe a significant effect of $ced-1(e1735)$ on the asymmetric division by size of QL.p in a wild-type or $ced-3(n2427)$ background. Therefore, the loss of $ced-1$ MEGF10 does not promote the presence of additional PVM neurons by affecting the asymmetric division by size of QL.p.

***ced-1* MEGF10 promotes the apoptotic fate of QL.pp**

QL.p divides asymmetrically by fate to produce QL.pa, which survives and divides to generate two neurons, PVM and SDQL (“mitotic fate”), and QL.pp, which is programmed to die by apoptosis (“apoptotic fate”) (Figure 1A). We tested whether the loss of $ced-1$ MEGF10 affects the ability of QL.pp to adopt the apoptotic fate. Using the $P_{toe-2}gfp$ reporter, we determined the fraction of QL.pps that inappropriately survive (regardless of whether they subsequently divided or not) (Figure 6A). In wild-type animals, QL.pp always dies. In contrast, in animals carrying strong *lf* mutations of $egl-1$ BH3-only, $n3330$, $ced-4$ Apaf-1, $n1162$, or $ced-3$ caspase, $n717$, QL.pp survives in almost all animals (Figure 6B). Furthermore, in animals homozygous for $ced-3(n2427)$, 37% of QL.pps survive. We found that while $ced-1(e1735)$ does not cause QL.pp survival in an otherwise wild-type background, it increases QL.pp survival in a $ced-3(n2427)$ background to 58%. Similarly, *lf* mutations of $ced-2$ CrkII or $ced-6$ GULP ($n1994$ and

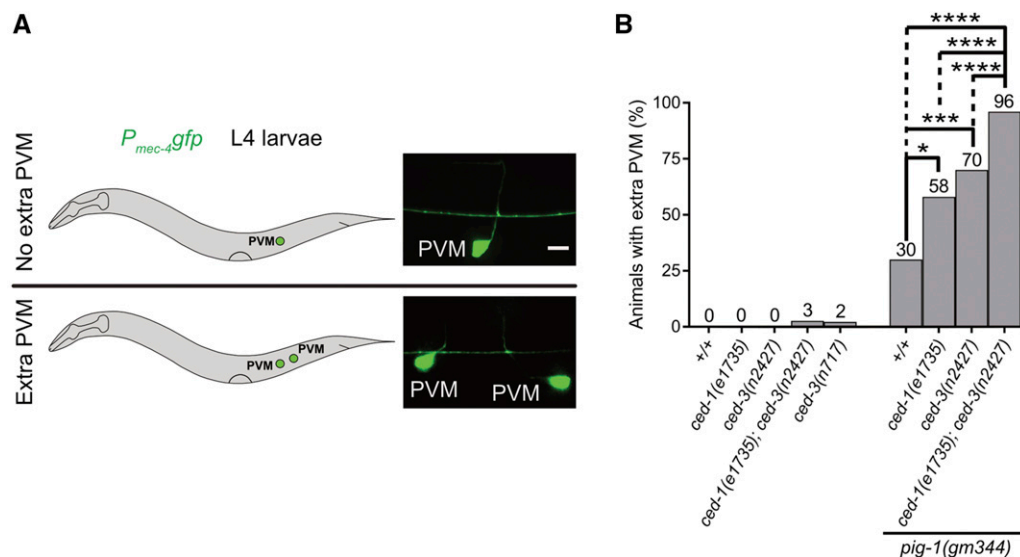


Figure 4 The loss of *ced-1* MEGF10 enhances the extra PVM phenotype of *ced-3(n2427)* animals. (A) Schematic representation of assay and representative images of L4 larvae with no extra PVM neuron (top), or with an extra PVM neuron (bottom). Bar, 5 μ m. PVM neurons were visualized using *P_{mec-4gfp}* (*bzIs190*) as reporter. (B) Bar graph showing the fraction of animals with extra PVM neurons for the indicated genotypes. Statistical test: Fisher's exact test with Benjamini and Hochberg multiple comparisons correction. * $P < 0.05$, *** $P < 0.001$, **** $P < 0.0001$, and $n > 50$ animals.

n1813, respectively), two other engulfment genes, also enhance the *ced-3(n2427)* phenotype. To determine in which cell or cells the engulfment genes act to enhance QL.pp survival, we performed rescue experiments using promoters that drive transgene expression specifically in the Q lineage (*toe-2* promoter) (Gurling *et al.* 2014) or in *hyp7* (“*hyp7* promoter”) (Hunt-Newbury *et al.* 2007). We found that the expression of a *ced-1* minigene under the control of the *hyp7* promoter, but not the *toe-2* promoter, rescues the *ced-1(e1735)* phenotype (Figure 6B). Therefore, in a background in which apoptotic cell death is compromised, the loss of *ced-1* MEGF10 or other engulfment genes increases the probability of QL.pp survival. Hence, the engulfment genes act to promote the apoptotic fate in QL.pp. Furthermore, in this context, *ced-1* MEGF10, and most probably the other engulfment genes, act in *hyp7* and therefore in a cell nonautonomous manner. Finally, based on our finding that a *ced-1* MEGF10-dependent gradient of CED-3 caspase activity is established in QL.p before its division, we propose that *ced-1* MEGF10 and the other engulfment genes promote the apoptotic fate of QL.pp by causing the non-random segregation of active CED-3 caspase into QL.pp.

***pig-1* MELK, *ced-1* MEGF10, and *ced-3* caspase interact to promote the apoptotic fate of QL.pp**

We also determined the effect of *ced-1(e1735)* on the ability of QL.pp to adopt the apoptotic fate in a background in which QL.p divides symmetrically by size, *i.e.*, in the *pig-1(gm344)* background. In *pig-1(gm344)* animals, 45% of QL.pps survive (Figure 6B). We found that the loss of *ced-1* MEGF10 enhances QL.pp survival in this background to 86% (Figure 6B). Similarly, *ced-3(n2427)* enhances QL.pp survival in *pig-1(gm344)* animals from 45 to 94%. Finally, in the triple mutant, 100% of QL.pps inappropriately survive. The loss of *pig-1* MELK does not affect the formation of the gradient of CED-3 caspase activity in QL.p (see above; Figure 2, A and C). However, since the size of QL.pp in *pig-1(gm344)* animals is

increased by a factor of ~ 2.0 , the loss of *pig-1* MELK probably results in a significant reduction of the concentration of active CED-3 caspase in QL.pp after QL.p division (since QL.p and its daughters are relatively flat cells, an increase by a factor of ~ 2.0 in cell size results in an increase by a factor of ~ 2.0 in cell volume as well; hence, the loss of *pig-1* potentially could reduce the concentration of active CED-3 caspase by as much as two-fold). Furthermore, the loss of *pig-1* MELK may also affect the concentration in QL.pp of factors other than CED-3 caspase. For example, the loss of *pig-1* MELK may cause a reduction in the concentration of other proapoptotic factors, such as transcriptional activators of *egl-1* BH3-only. Combined with a reduction in the concentration of active CED-3 caspase, this may be sufficient to cause 45% of the QL.pps to inappropriately survive. Abolishing the gradient of CED-3 caspase activity in QL.p [*i.e.*, *ced-1(e1735)*] or compromising the apoptotic cell death pathway [*i.e.*, *ced-3(n2427)*] is expected to reduce the concentration of active CED-3 caspase in QL.pp in *pig-1(gm344)* animals even further, thereby increasing the fraction of animals in which QL.pp inappropriately survives. Finally, in *ced-1(e1735); pig-1(gm344) ced-3(n2427)* triple mutants, the concentration of active CED-3 caspase in QL.pp is reduced below the threshold required to execute the apoptotic fate in 100% of the animals.

***pig-1* MELK, but not *ced-1* MEGF10, is required to restrict mitotic potential to QL.pa**

Next, we asked whether the loss of *ced-1* MEGF10 affects the ability of an undead QL.pp to inappropriately adopt the mitotic fate, *i.e.*, the fate normally adopted by QL.pa. Specifically, using *P_{toe-2gfp}*, we determined the fraction of undead QL.pps that divide (Figure 7A). Since in *ced-1(e1735)* animals QL.pp always dies, we addressed this question in the background of *ced-3(n2427)*. In *ced-3(n2427)* or *ced-1(e1735); ced-3(n2427)* animals, 37 or 58% of QL.pps inappropriately survive, respectively. We found that none of the

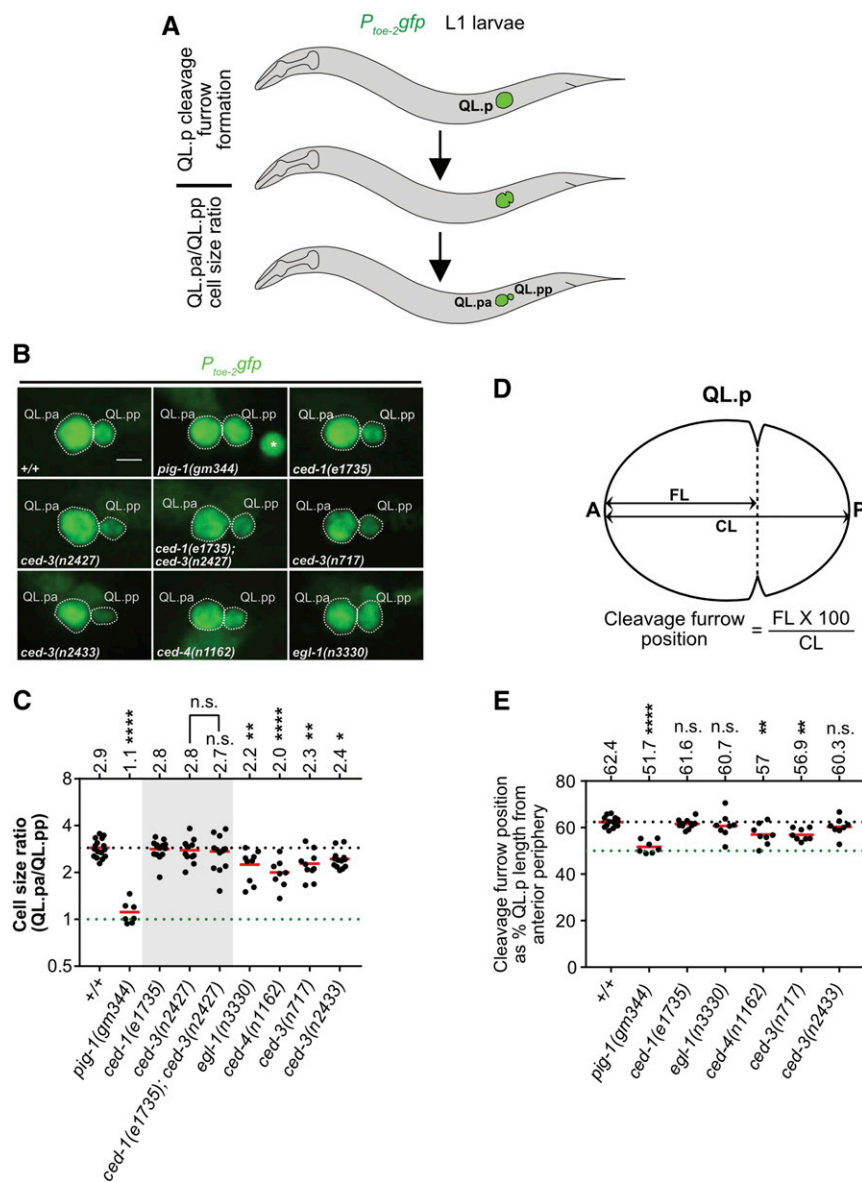


Figure 5 Genetic requirements for the asymmetric division by size of QL.p. (A) Schematic representation of the assays. The division of QL.p was monitored by live imaging. QL.p division asymmetry was assessed at two stages during mitosis, specifically during and after cytokinesis. During cytokinesis, we determined the position of the cleavage furrow. The first time point upon the completion of cytokinesis was used to estimate daughter cell sizes based on maximum intensity projection images, as described in the *Materials and Methods*. QL.p and its daughter cells were visualized using the transgene $P_{toe-2:gfp}$ (*bcls133*). (B) Representative images of QL.p daughters immediately after QL.p cytokinesis in the indicated genotypes. Bar, 3 μ m. In the image showing *pig-1(gm344)*, the asterisk (*) marks QL.aa present in the vicinity of QL.pa and QL.pp. (C) Dot plot showing cell size ratios (QL.pa/QL.pp) in the indicated genotype. Each dot represents the cell size ratio for one QL.p. The horizontal red lines indicate the means for the respective genotypes, which are also mentioned on top for each genotype. The dotted black line represents the mean in wild-type (+/+). The dotted green line represents the ratio 1. (D) Schematic representation of the method used to determine the position of the cleavage furrow during QL.p cytokinesis. We measured the distance of the cleavage furrow from the anterior periphery of QL.p (FL), and divided it by QL.p length (CL) to obtain the cleavage furrow position. (E) Dot plot showing the position of the cleavage furrow during QL.p cytokinesis. Each dot represents the position in one QL.p. The horizontal red lines indicate the means for the respective genotypes, which are also mentioned at the top for each genotype. The dotted green line represents the position corresponding to 50% CL, and the dotted black line represents the mean for wild-type animals. Statistical test: one-way ANOVA followed by Benjamini and Hochberg multiple comparisons correction. ** $P < 0.01$, **** $P < 0.0001$, and $n \geq 7$ QL.ps. Statistical test: one-way ANOVA followed by Benjamini and Hochberg multiple comparisons correction. * $P < 0.05$, ** $P < 0.01$, **** $P, 0.0001$, and $n \geq 7$ QL.ps. n.s., not significant.

undead QL.pps divide in either of these genetic backgrounds (Figure 7B). In contrast, in *pig-1(gm344)* animals, in which 45% of QL.pps inappropriately survive, 56% of undead QL.pps divide. Therefore, the loss of *pig-1* MELK, but not *ced-1* MEGF10, causes undead QL.pps to inappropriately adopt the mitotic fate. Hence, *pig-1* MELK, but not *ced-1* MEGF10, is required to restrict the mitotic potential to QL.pa. Based on this observation, we propose that a *pig-1* MELK-dependent, *ced-1* MEGF10-independent gradient of mitotic potential exists in QL.p prior to its division. Furthermore, we propose that this gradient is along the anterior–posterior axis of QL.p reciprocal to the gradient of CED-3 caspase activity (with a higher concentration in the anterior rather than posterior part of QL.p) and that during QL.p division, this gradient results in the nonrandom segregation of mitotic potential into QL.pa, instead of QL.pp (Figure 9). According to this model, the loss of this gradient in *pig-1(gm344)* animals should

result in the inappropriate presence of mitotic potential in QL.pp after QL.p division, and, hence, the ability of undead QL.pps to adopt the mitotic fate and divide. In support of this model, Garriga and co-workers found that while the loss of *pig-1* MELK or *strd-1* STRD1 causes similar defects in the asymmetric division by size of QL.p and QR.p, *pig-1* mutants have a more penetrant “extra neuron phenotype,” most likely as a result of the division of more undead QL.pps and QR.pps (Chien *et al.* 2013). Based on this observation, the authors proposed that *pig-1* may act in a *strd-1*-independent manner to affect the segregation of “fate determinants” during QL.p and QR.p division. Alternatively, the mitotic potential could be distributed throughout QL.p, and inherited into QL.pa and QL.pp proportional to cell size, but the small size of QL.pp ($\sim 1/3$ of QL.pa) may prevent its ability to divide. In that case, the loss of *pig-1* MELK would increase by a factor of ~ 2.0 both the size of QL.pp

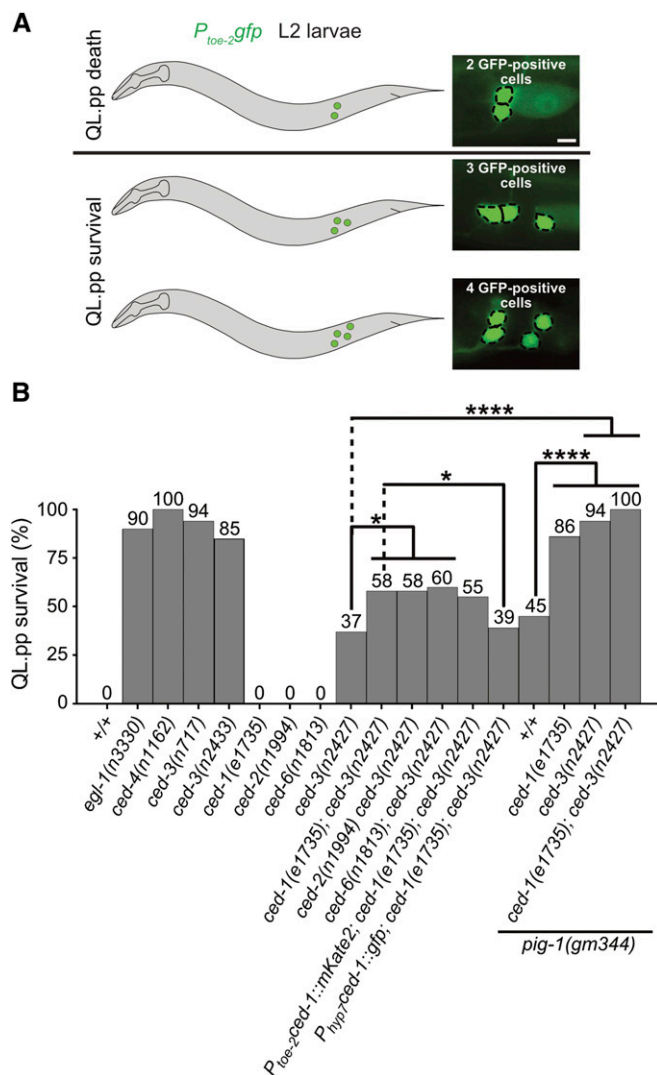


Figure 6 *pig-1* MELK, *ced-1* MEGF10, and *ced-3* caspase interact to promote the apoptotic fate in QL.pp. (A) Schematic representation of assay and representative images of L2 larvae showing two, three, or four cells of the QL.p lineage. Bar, 3 μ m. Cells were visualized using the transgene $P_{\text{toe-2}}\text{-}gfp$ (*bcls133*). For the purpose of this analysis, animals with three or four QL.p lineage cells were counted as an instance of “QL.pp survival,” and those with two QL.p lineage cells were counted as ones of “QL.pp death.” (B) Bar graph showing the fraction of animals in which QL.pp inappropriately survived for the indicated genotypes. Fisher’s exact test was used to determine statistical significance. Benjamini and Hochberg multiple comparisons correction was used to adjust individual *P* values. * $P < 0.05$, **** $P < 0.0001$, and $n > 50$ animals.

as well as the total amount of mitotic potential in QL.pp (with no change in its concentration), and this would lead to the inappropriate division of 56% of undead QL.pps. Finally, *pig-1* MELK may also act in QL.pp to antagonize the activity of mitotic potential, and this could lead to the division of undead QL.pps in animals lacking *pig-1*.

Surprisingly, we found that *ced-3(n2427)* significantly increases the fraction of undead QL.pps that divide in *pig-1(gm344)* animals (from 56 to 80%; Figure 7B). In contrast, *ced-1(e1735)* fails to do so in a *pig-1(gm344)*

(56 vs. 45%) or *pig-1(gm344) ced-3(n2427)* (80 vs. 87%) background. Based on this, we propose that CED-3 caspase antagonizes the activity of the mitotic potential. Furthermore, the finding that compromising the apoptotic cell death pathway [i.e., *ced-3(n2427)*] but not abolishing the gradient of CED-3 caspase activity in QL.p [i.e., *ced-1(e1735)*] increases the fraction of undead QL.pps that divide in *pig-1(gm344)* animals, indicates that it is CED-3 caspase activity *per se* rather than a gradient of CED-3 caspase activity that is capable of antagonizing the activity of the mitotic potential. Possibly, the functional interaction between CED-3 caspase and the mitotic potential could occur in QL.p (before the formation of the gradient of CED-3 Caspase activity) and not in QL.pp after QL.p division. Alternatively, the interaction could take place in QL.pp; in this case, *ced-3(n2427)* but not *ced-1(e1735)* would reduce the level of CED-3 caspase activity below the threshold necessary to antagonize the activity of the mitotic potential. Finally, the observation that *ced-3(n2427)* enhances the fraction of undead QL.pps that divide in *pig-1(gm344)*, but not in wild-type animals, provides additional support for the notion that a gradient of mitotic potential exists in QL.p and that during QL.p division, little or no mitotic potential is normally segregated into QL.pp.

***egl-1* BH3-only, *ced-4* Apaf-1, and *ced-3* caspase promote the ability of QL.p to divide asymmetrically by size**

Like *ced-1* MEGF10, the genes *egl-1* BH3-only, *ced-4* Apaf-1, and *ced-3* caspase are required for the formation of the gradient of CED-3 caspase activity in the NSM neuroblast and presumably also in QL.p. However, *egl-1* BH3-only, *ced-4* Apaf-1, and *ced-3* caspase, but not *ced-1* MEGF10, are required for the initial maturation and full activation of CED-3 caspase. We found that unlike *ced-1(e1735)*, *egl-1(n3330)*, *ced-4(n1162)*, and *ced-3(n717)* affect the ability of undead QL.pps to divide. Specifically, we found that in an otherwise wild-type background, these mutations cause between 2 and 11% of undead QL.pps to divide (Figure 7B). We also tested the *ced-3* mutation *n2433*, which is a missense mutation in the coding region of the *ced-3* gene and leads to the synthesis of CED-3 protein that lacks protease activity. We found that, similarly, *ced-3(n2433)* causes 4% of undead QL.pps to divide. Hence, the loss of CED-3 caspase activity *per se* rather than the loss of a gradient of CED-3 caspase activity can result in the inappropriate presence of mitotic potential in undead QL.pps after QL.p division. This suggests that it is the loss of *ced-3* caspase in QL.p rather than QL.pp that causes the inappropriate presence of mitotic potential in QL.pp. Therefore, we tested whether the loss of *egl-1* BH3-only, *ced-4* Apaf-1, or *ced-3* caspase affects the asymmetric division of QL.p by size and, hence, the partitioning of mitotic potential during QL.p division. We found that rather than exhibiting a cell size ratio of QL.pa to QL.pp of ~ 3.0 , in these mutants, cell size ratios observed range from 2.4 to 2.0, indicating that the cleavage plane has shifted anteriorly resulting in larger QL.pps (Figure 5, B and C) [it has previously been reported that the loss of *ced-4* affects the cell size ratio of QL.pa to QL.pp (Singhvi *et al.* 2011)]. To rule out

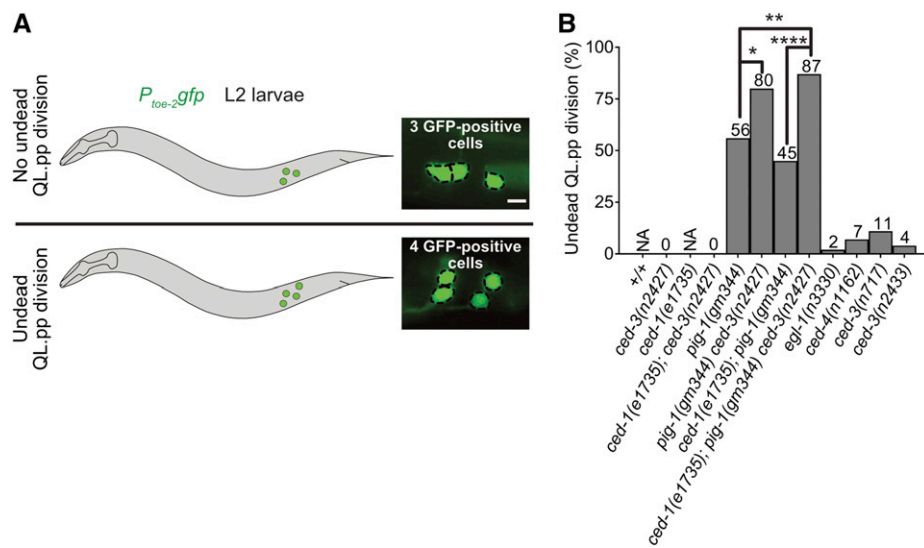


Figure 7 *pig-1* MELK and *ced-3* caspase interact to suppress the mitotic fate in QL.pp. (A) Schematic representation of assay and representative images of L2 larvae showing three or four QL.p lineage cells. Bar, 3 μ m. Cells were visualized using the reporter *P_{toe-2gfp}* (*bcls133*). Only those animals, in which QL.pp failed to die were considered for this analysis. Animals with four QL.p lineage descendants were considered to have had an instance of “undead QL.pp division,” whereas the ones with three QL.p lineage cells were counted as an instance of “no undead QL.pp division.” (B) Bar graph showing the fraction of undead QL.pps that divided for the indicated genotypes. Statistical test: Fisher’s exact test with Benjamini and Hochberg multiple comparisons correction. * $P < 0.05$, ** $P < 0.01$, **** $P < 0.0001$, and $n > 25$ animals. NA, not applicable.

that the changes in cell size ratios observed are a result of differences in the cell shape of undead QL.pps (and, hence, our ability to estimate QL.pp size rather than the asymmetry of the QL.p division), we determined the position of the cleavage furrow in QL.p in the different mutant backgrounds. To that end, we used the image stacks generated every 3 min of L1 larvae carrying the *P_{toe-2gfp}* reporter that we generated to determine the cell size ratio of QL.pa to QL.pp (Figure 5A), and used the last stack before QL.p division to determine the position of the cleavage furrow as outlined in Figure 5D. Using this approach, we found that in wild-type animals, the cleavage furrow is positioned at 62.4% QL.p length and in *pig-1(gm344)* animals at 51.7% QL.p length (Figure 5E). Considering that the cell size ratio of QL.pa to QL.pp is 2.9 in the wild-type and 1.1 in *pig-1(gm344)* animals, it is likely that small changes in cleavage furrow position may result in significant changes in QL.pa to QL.pp cell size ratio. Next, we analyzed animals lacking *egl-1* BH3-only, *ced-4* Apaf-1, or *ced-3* caspase, and found significant changes in cleavage furrow position in *ced-4(n1162)* and *ced-3(n717)* animals (57 and 56.9% of QL.p length, respectively). In addition, we found small changes in cleavage furrow position in *egl-1(n3330)* and *ced-3(n2433)*, but not *ced-1(e1735)*, animals. As mentioned above, small changes in cleavage furrow position may result in significant changes in QL.pa to QL.pp cell size ratio. The small changes in cleavage furrow position detected in *egl-1(n3330)* and *ced-3(n2433)* animals may therefore account for the significant changes in QL.pa to QL.pp cell size ratios observed in these animals (Figure 5, C and E).

Based on these observations, we conclude that the loss of *egl-1* BH3-only, *ced-4* Apaf-1, or *ced-3* caspase compromises the ability of QL.p to divide asymmetrically by size. Therefore, CED-3 caspase contributes to the asymmetric division by size of QL.p. Furthermore, we propose that through the observed shift in cleavage plane toward the anterior, mitotic potential is segregated inappropriately into QL.pp during QL.p division, and that this accounts for the small fraction

of undead QL.pps that divide in these mutants. Finally, the ability of CED-3 caspase to contribute to the asymmetric division by size of QL.p depends on its activation through *egl-1* BH3-only and *ced-4* Apaf-1, and, hence, the apoptotic cell death pathway.

The function of the apoptotic cell death pathway in asymmetric cell division by size is not restricted to the QL.p neuroblast

To determine whether the function of the apoptotic cell death pathway in asymmetric cell division by size is specific to the QL.p neuroblast, we analyzed the postembryonic QL.a neuroblast and the embryonic NSM neuroblast, both of which divide asymmetrically by size and fate to produce a smaller daughter that is programmed to die (Sulston *et al.* 1983; Hatzold and Conradt 2008). In wild-type animals, QL.a divides to generate a larger posterior daughter, QL.ap, and a smaller anterior daughter, QL.aa, with a cell size ratio of QL.ap to QL.aa of 2.67 (Ou *et al.* 2010) (Figure 8, A and B) (cells of the QL.a lineages are also relatively flat cells; therefore, cell size was determined as for QL.p daughters). We found that in *ced-3(n717)* animals, this ratio was reduced to 2.13. Furthermore, we observed an effect of the loss of *ced-3* caspase on the asymmetric division by size of the NSM neuroblast; however, only in the background of *pig-1(gm344)*. Specifically, the NSM neuroblast divides to produce a larger ventral daughter, the NSM, and a smaller dorsal daughter, the NSMsc, with a cell size ratio of NSM to NSMsc of 1.57 (Hatzold and Conradt 2008) (Figure 8, C and D) (since cells of the NSM neuroblast lineage are not flat cells, cell size was estimated as described in Figure 8C and in the *Materials and Methods*). As reported previously, in *pig-1(gm344)* animals, the NSM neuroblast divides symmetrically by size and generates two daughter cells of similar sizes, with a cell size ratio of NSM to NSMsc of 1.00 (Wei *et al.* 2017). In *ced-3(n717)* or *ced-4(n1162)* animals, the cell size ratio is not significantly different from that of wild-type

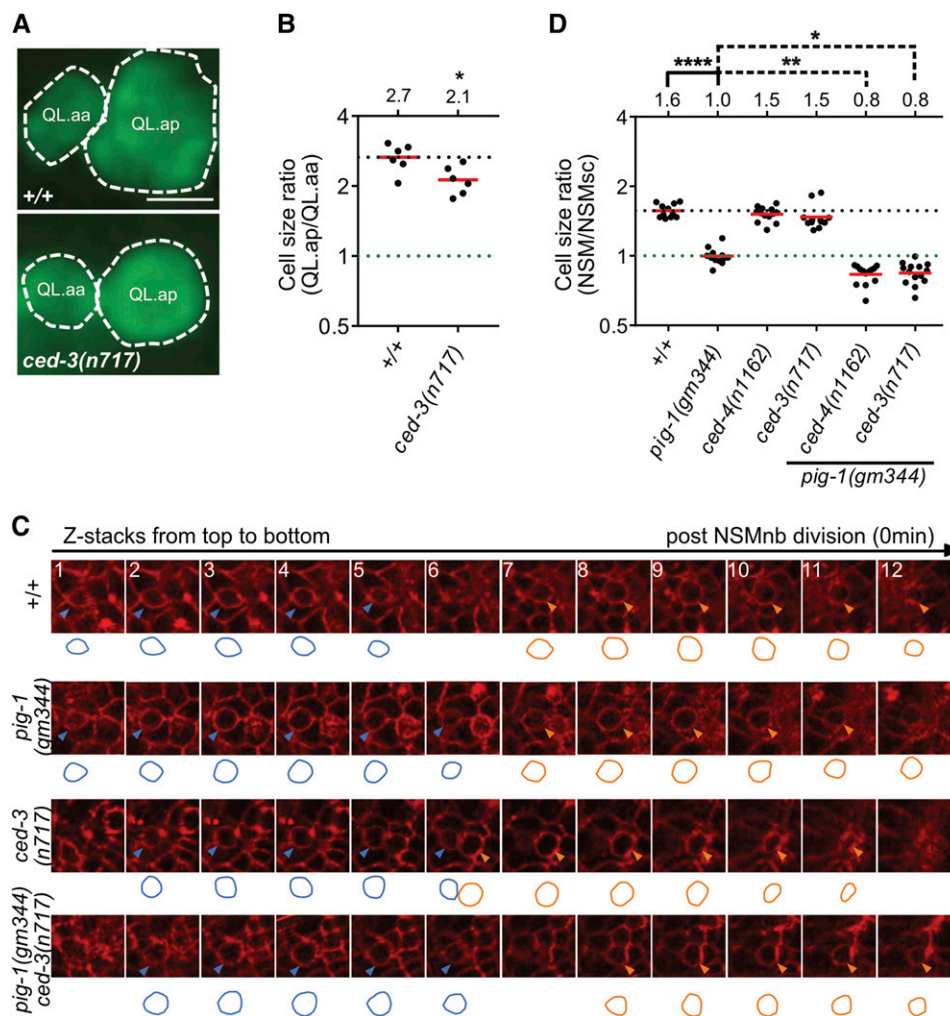


Figure 8 The apoptotic pathway promotes asymmetric cell division in other neuroblast lineages. (A) Representative images and (B) dot plot showing relative sizes of QL.a daughter cells in wild-type and *ced-3(n717)* animals. Bar, 3 μ m. Cells were visualized using the reporter $P_{\text{toe-2gfp}}$ (*bcls133*). Statistical test: Mann–Whitney test. * $P < 0.05$, $n = 6$ QL.as. (C) Representative images showing NSM (Neurosecretory motor neuron) neuroblast (NSMnb) daughter cells visualized with $P_{\text{pie-1mCherry::ph}^{\text{plc6}}}$ (*Itls44*). The circumferences of the daughter cells were traced and are shown below the respective images. Circumferences of NSM sister cells (NSMsc) are shown in blue and circumferences of NSM are shown in orange. (D) Dot plot showing cell size ratios (NSM/NSMsc) in the indicated genotypes. One-way ANOVA with Tukey's multiple comparisons test was used to determine statistical significance. * $P < 0.05$, ** $P < 0.01$, **** $P < 0.0001$, $n > 11$ NSM neuroblasts.

animals (1.47 and 1.51, respectively). However, in a *pig-1(gm344)* background, the cell size ratio of *ced-3(n717)* or *ced-4(n1162)* animals is significantly reduced compared to that of *pig-1(gm344)* animals (0.84 and 0.83, respectively). A reduction in the ratio below 1.0 is indicative of a reversal of polarity. Indeed, in these double-mutant animals, the NSM is smaller than the NSMsc. In summary, these results indicate that the function of the apoptotic cell death pathway in asymmetric neuroblast division, at least by size, is not restricted to the QL.p neuroblast.

Our finding that *ced-4(n1162)* and *ced-3(n717)* affect the asymmetric division of the NSM neuroblast in a *pig-1(gm344)*, but not wild-type, background suggests that in certain lineages, the apoptotic cell death pathway may act in parallel to *pig-1* MELK to affect cellular polarization. Therefore, we tested whether *ced-3(n717)* enhances embryonic lethality in *pig-1(gm344)* animals.

When grown at 20 $^{\circ}$, we observed 0% embryonic lethality among *ced-3(n717)* animals ($n = 1413$) and 8% embryonic lethality among *pig-1(gm344)* animals ($n = 1514$). However, in *pig-1(gm344) ced-3(n717)* double mutants, 43% of the animals arrested during embryonic development ($n = 397$). Therefore, the apoptotic cell death pathway may play a more

general role in cellular polarization and asymmetric cell division, and, in this context, act in parallel to *pig-1* MELK.

Discussion

The formation of reciprocal gradients of mitotic and apoptotic potential is critical for the asymmetric division of the QL.p neuroblast by fate

Based on results presented here, we propose that prior to QL.p division, reciprocal gradients of mitotic and apoptotic potential form in QL.p, and that these gradients result in the non-random segregation of mitotic potential into QL.pa and of apoptotic potential into QL.pp (Figure 9). We speculate that the mitotic potential in QL.pa promotes its ability to divide, and we provide evidence that the apoptotic potential in QL.pp promotes its ability to execute apoptotic cell death. Furthermore, while we know that apoptotic potential encompasses at least active CED-3 caspase, we do not know the molecular nature of the mitotic potential. However, we speculate that it encompasses factors involved in cell cycle control, and/or molecules or organelles required for energy production. We also provide evidence that distinct genetic pathways are responsible for the establishment and/or

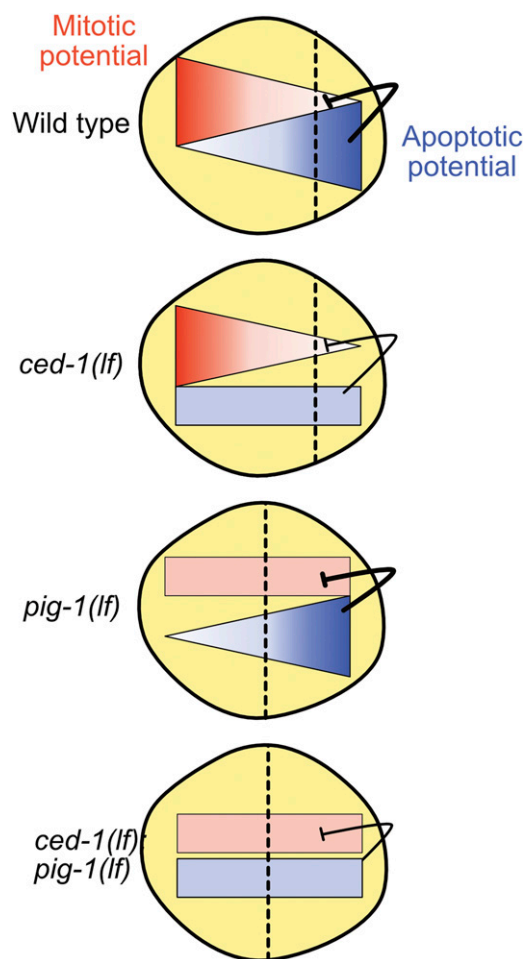


Figure 9 Working model. Schematic representation of QL.p neuroblast at metaphase. We propose that reciprocal gradients of mitotic (red) and apoptotic (blue) potential are present in QL.p along the anterior–posterior axis in wild-type animals. The gradient of apoptotic potential is dependent on *ced-1* MEGF10 function and the gradient of mitotic potential may be dependent on *pig-1* MELK function. See text for details.

maintenance of these two gradients in QL.p. Specifically, the two conserved *C. elegans* engulfment pathways are necessary for the gradient of CED-3 caspase activity but not the gradient of mitotic potential. Conversely, a *pig-1* MELK-dependent pathway is necessary for the gradient of mitotic potential but not the gradient of CED-3 caspase activity. How these distinct pathways control the two reciprocal gradients, and how these gradients are generated in the first place, remains to be determined. Interestingly, in the case of the gradient of CED-3 caspase activity, we found that there is a mechanistic difference in the symmetry-breaking event that orients this gradient along the dorsal–ventral axis in the NSM neuroblast and along the anterior–posterior axis in the QL.p neuroblast. In the case of the NSM neuroblast, all neighboring cells appear to present CED-1 MEGF10 on their cell surface; however, CED-1 MEGF10 clustering and activation specifically occurs on the cell surface of the two dorsal neighbors (Chakraborty *et al.* 2015). In contrast, in the case of QL.p, at least on the medial side, CED-1 MEGF10 is asymmetrically

presented and, for this reason, results in CED-1 MEGF10 activation only on the posterior side. Finally, the results presented here indicate that the formation of a gradient of CED-3 caspase activity in a mother of a cell programmed to die is not specific to the NSM neuroblast lineage. Based on this, we speculate that it represents a general phenomenon of cell death lineages in developing *C. elegans* animals.

The apoptotic cell death pathway is required for the asymmetric division by size and fate of the QL.p neuroblast

The asymmetric division of mothers of cells programmed to die is critical for the correct fate of their daughters and, in particular, for the correct fate of the daughters programmed to die. Hence, it has been postulated that asymmetric cell division regulates the apoptotic cell death pathway (Hatzold and Conradt 2008; Teuliere and Garriga 2017). We now demonstrate that the apoptotic cell death pathway contributes to the ability of mothers of cells programmed to die to divide asymmetrically. Specifically, we present evidence that the apoptotic cell death pathway is required for the asymmetric division of QL.p by size and, hence, the correct sizes of the daughter cells QL.pa and QL.pp. In addition, we present evidence that the apoptotic cell death pathway is also required for the asymmetric division of QL.p by fate. Specifically, by controlling the sizes of QL.pa and QL.pp, the apoptotic cell death pathway indirectly influences the relative amounts of mitotic potential or apoptotic potential that are segregated into either QL.pa or QL.pp during QL.p division. In addition, the apoptotic cell death pathway is required for the activation of CED-3 caspase in QL.p, which we propose antagonizes the mitotic potential. Hence, the apoptotic cell death pathway controls the total amount of apoptotic and mitotic potential present in QL.p, and, therefore, the amounts that can be segregated into QL.pa and QL.pp. Based on these new findings, we now postulate that not only does asymmetric cell division regulate the apoptotic cell death pathway, but that in the context of cell death lineages, the apoptotic cell death pathway regulates asymmetric cell division. Furthermore, this regulation of asymmetric cell division through the apoptotic cell death pathway is necessary for the production of smaller daughters that are programmed to die.

A new nonapoptotic function of the *C. elegans* apoptotic cell death pathway in asymmetric neuroblast division

The *C. elegans* apoptotic cell death pathway, and CED-3 caspase in particular, has been implicated in a number of nonapoptotic processes, which range from aging and neuronal regeneration to the control of the expression of specific genes, such as the heterochronic gene *lin-28* (Pinan-Lucarre *et al.* 2012; Weaver *et al.* 2014; Yee *et al.* 2014). Similarly, mammalian caspases have been shown to have various nonapoptotic functions during development (Nakajima and Kuranaga 2017). We now present evidence that the apoptotic cell death pathway is also involved in the asymmetric division of neuroblasts that generate a smaller daughter that is programmed to die. How CED-3 caspase affects the position of

the cleavage plane in these neuroblasts remains to be determined. In *C. elegans*, the positioning of the cleavage plane is best understood in the one-cell embryo, which, like QL.p, divides asymmetrically by size and fate (Rose and Gonczy 2014; Wu and Griffin 2017). In general, the cleavage plane is perpendicular to and centered on the middle of the mitotic spindle. As a result of unequal dynein-mediated pulling forces emanating from the anterior and posterior poles (with more pulling forces emanating from the posterior pole), in one-cell embryos, the spindle is shifted posteriorly along the anterior–posterior axis. As a result, the cleavage plane is shifted posteriorly as well, generating a larger anterior cell, AB, and a smaller posterior cell, P1. It has been shown previously that the spindle is shifted posteriorly in QL.p as well (Ou *et al.* 2010), and we speculate that this is also caused by unequal dynein-mediated pulling forces. However, whereas the loss of *pig-1* MELK causes QL.p to divide symmetrically rather than asymmetrically, it fails to do so in the one-cell embryo [however, the loss of *pig-1* MELK does synergize with the loss of *ani-1*, which encodes one of two *C. elegans* anillin genes, to affect the position of the cleavage plane in one-cell embryos (Pacquelet *et al.* 2015)]. This suggests that the function of *pig-1* MELK in the regulation of cleavage plane position differs between the one-cell embryo and the QL.p neuroblast lineage. Nevertheless, since the loss of *ced-3* caspase causes a partial defect in the posterior shift of the cleavage plane in QL.p, *ced-3* caspase may be necessary for the dynein-mediated pulling forces that emanate from the posterior pole. However, the finding that the loss of *ced-3* caspase also affects the asymmetric division by size of the QL.a neuroblast suggests that dynein-mediated pulling forces may not be the target of CED-3 caspase activity in this context. Specifically, like QL.p, the neuroblast QL.a divides asymmetrically by size and fate to generate a larger daughter, which survives, and a smaller daughter, which dies (in contrast to QL.p, the smaller daughter of QL.a is the anterior rather than the posterior daughter). However, rather than through a shift of the mitotic spindle along the anterior–posterior axis, it has been suggested that two daughter cells of different sizes are generated from QL.a through asymmetric myosin-mediated contractile forces during QL.a division (Ou *et al.* 2010). Hence, *ced-3* caspase may be required for general cellular polarization of QL.p and QL.a, and affect the position of the cleavage plane or myosin-mediated contractile forces indirectly. Consistent with the notion that *ced-3* caspase may be required for general cellular polarization, we found that in the embryonic NSM neuroblast lineage, the loss of *ced-3* caspase in a *pig-1* MELK mutant background causes a reversal of polarity. Finally, the finding that the loss of *ced-3* caspase enhances embryonic lethality in animals lacking *pig-1* MELK function suggests that *ced-3* caspase (and possibly the entire apoptotic cell death pathway) also functions in asymmetric cell division and cellular polarization in lineages other than cell death lineages, and that this may be crucial for normal animal development.

Interestingly, there is increasing evidence that mammalian caspases have functions in different types of embryonic and

adult stem cells (Baena-Lopez *et al.* 2017). Hence, our finding that *C. elegans* CED-3 caspase plays a role in cellular polarization, and the asymmetric division by size and fate of neuroblasts may very well be relevant to these nonapoptotic functions of mammalian caspases in stem cell lineages.

Acknowledgments

The authors thank E. Lambie, E. Zanin, and B. Weaver for comments on the manuscript; G. Garriga, D. Hall, and members of the Conrads laboratory for constructive discussions; M. Bauer, N. Lebedeva, and M. Schwarz for excellent technical support; R. Sherrard for constructing plasmid pBC1805; Z. Zhou for plasmid pZZ610; T. Mikeladze-Dvali for plasmid TMD34; H. Bringmann for the *mKate2* clone; Monica Driscoll for *bzIs190*; and E. Zanin for plasmid pEZ167. Some strains used in this study were provided by the *Caenorhabditis* Genetics Center (<https://cbs.umn.edu/cgc/home>), which is funded by the National Institutes of Health Office of Research Infrastructure Programs (P40 OD-010440). N.M. was supported by a predoctoral fellowship from the Studienstiftung des deutschen Volkes (<https://www.studienstiftung.de/>) and H.W. was supported by a predoctoral fellowship from the China Scholarship Council (<https://www.csc.edu.cn/>). This work was supported by the Deutsche Forschungsgemeinschaft (Center for Integrated Protein Science Munich; EXC 114).

Literature Cited

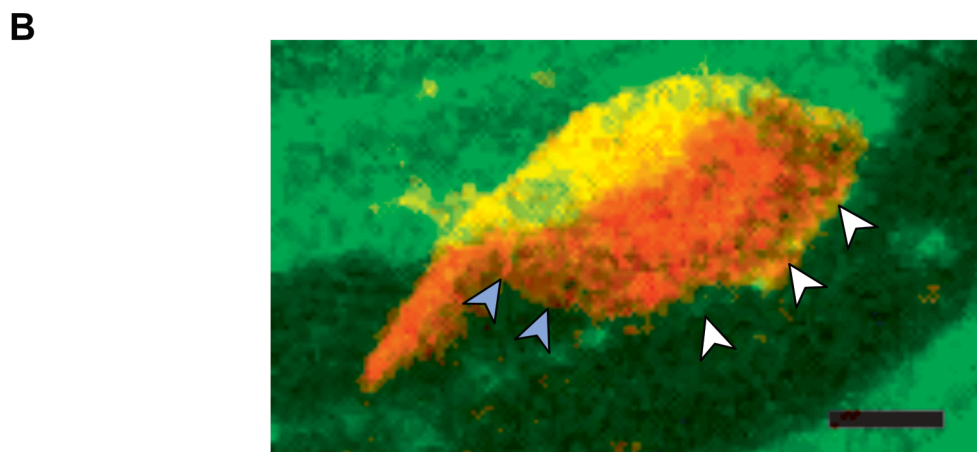
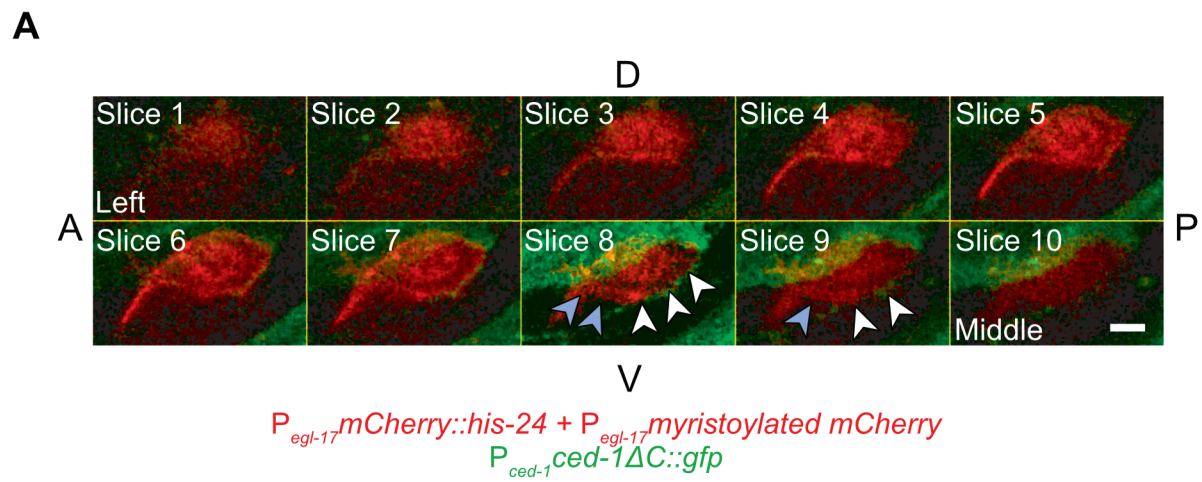
- Audhya, A., F. Hyndman, I. X. McLeod, A. S. Maddox, J. R. Yates, III *et al.*, 2005 A complex containing the Sm protein CAR-1 and the RNA helicase CGH-1 is required for embryonic cytokinesis in *Caenorhabditis elegans*. *J. Cell Biol.* 171: 267–279. <https://doi.org/10.1083/jcb.200506124>
- Baena-Lopez, L. A., L. Arthurton, D. C. Xu, and A. Galasso, 2017 Non-apoptotic Caspase regulation of stem cell properties. *Semin. Cell Dev. Biol.* 82: 118–126. <https://doi.org/10.1016/j.semcdb.2017.10.034>
- Bellanger, J. M., and P. Gonczy, 2003 TAC-1 and ZYG-9 form a complex that promotes microtubule assembly in *C. elegans* embryos. *Curr. Biol.* 13: 1488–1498. [https://doi.org/10.1016/S0960-9822\(03\)00582-7](https://doi.org/10.1016/S0960-9822(03)00582-7)
- Brenner, S., 1974 The genetics of *Caenorhabditis elegans*. *Genetics* 77: 71–94.
- Chakraborty, S., E. J. Lambie, S. Bindu, T. Mikeladze-Dvali, and B. Conrads, 2015 Engulfment pathways promote programmed cell death by enhancing the unequal segregation of apoptotic potential. *Nat. Commun.* 6: 10126. <https://doi.org/10.1038/ncomms10126>
- Chien, S. C., E. M. Brinkmann, J. Teuliere, and G. Garriga, 2013 *Caenorhabditis elegans* PIG-1/MELK acts in a conserved PAR-4/LKB1 polarity pathway to promote asymmetric neuroblast divisions. *Genetics* 193: 897–909. <https://doi.org/10.1534/genetics.112.148106>
- Conrads, B., Y. C. Wu, and D. Xue, 2016 Programmed cell death during *Caenorhabditis elegans*. *Dev. Genet.* 203: 1533–1562. <https://doi.org/10.1534/genetics.115.186247>
- Cordes, S., C. A. Frank, and G. Garriga, 2006 The *C. elegans* MELK ortholog PIG-1 regulates cell size asymmetry and daughter

- cell fate in asymmetric neuroblast divisions. *Development* 133: 2747–2756. <https://doi.org/10.1242/dev.02447>
- D'Agostino, R. P., and E. S. Pearson, 1993 Tests for departure from normality. Empirical results for the distributions of b_2 and $\sqrt{b_1}$. *Biometrika* 60: 613–622.
- Ellis, H. M., and H. R. Horvitz, 1986 Genetic control of programmed cell death in the nematode *C. elegans*. *Cell* 44: 817–829. [https://doi.org/10.1016/0092-8674\(86\)90004-8](https://doi.org/10.1016/0092-8674(86)90004-8)
- Ellis, R. E., D. M. Jacobson, and H. R. Horvitz, 1991 Genes required for the engulfment of cell corpses during programmed cell death in *Caenorhabditis elegans*. *Genetics* 129: 79–94.
- Fisher, R. A., 1921 On the probable error of a coefficient of correlation deduced from a small sample. *Metron* 1: 3–32.
- Fisher, R. A., 1935 *The Design of Experiments*. Macmillan, New York.
- Frøkjær-Jensen, C., M. W. Davis, C. E. Hopkins, B. J. Newman, J. M. Thummel *et al.*, 2008 Single-copy insertion of transgenes in *Caenorhabditis elegans*. *Nat. Genet.* 40: 1375–1383. <https://doi.org/10.1038/ng.248>
- Frøkjær-Jensen, C., M. W. Davis, M. Sarov, J. Taylor, S. Flibotte *et al.*, 2014 Random and targeted transgene insertion in *Caenorhabditis elegans* using a modified Mos1 transposon. *Nat. Methods* 11: 529–534. <https://doi.org/10.1038/nmeth.2889>
- Gibson, D. G., L. Young, R. Y. Chuang, J. C. Venter, C. A. Hutchison, III *et al.*, 2009 Enzymatic assembly of DNA molecules up to several hundred kilobases. *Nat. Methods* 6: 343–345. <https://doi.org/10.1038/nmeth.1318>
- Gurling, M., K. Talavera, and G. Garriga, 2014 The DEP domain-containing protein TOE-2 promotes apoptosis in the Q lineage of *C. elegans* through two distinct mechanisms. *Development* 141: 2724–2734. <https://doi.org/10.1242/dev.110486>
- Hatzold, J., and B. Conradt, 2008 Control of apoptosis by asymmetric cell division. *PLoS Biol.* 6: e84. <https://doi.org/10.1371/journal.pbio.0060084>
- Hedgecock, E. M., J. E. Sulston, and J. N. Thomson, 1983 Mutations affecting programmed cell deaths in the nematode *Caenorhabditis elegans*. *Science* 220: 1277–1279. <https://doi.org/10.1126/science.6857247>
- Horvitz, H. R., 2003 Nobel lecture. Worms, life and death. *Biosci. Rep.* 23: 239–303. <https://doi.org/10.1023/B:BIRE.0000019187.19019.e6>
- Hunt-Newbury, R., R. Viveiros, R. Johnsen, A. Mah, D. Anastas *et al.*, 2007 High-throughput in vivo analysis of gene expression in *Caenorhabditis elegans*. *PLoS Biol.* 5: e237. <https://doi.org/10.1371/journal.pbio.0050237>
- Lambie, E. J., and B. Conradt, 2016 Deadly dowry: how engulfment pathways promote cell killing. *Cell Death Differ.* 23: 553–554. <https://doi.org/10.1038/cdd.2015.170>
- Le Bot, N., M. C. Tsai, R. K. Andrews, and J. Ahringer, 2003 TAC-1, a regulator of microtubule length in the *C. elegans* embryo. *Curr. Biol.* 13: 1499–1505. [https://doi.org/10.1016/S0960-9822\(03\)00577-3](https://doi.org/10.1016/S0960-9822(03)00577-3)
- Maduro, M., and D. Pilgrim, 1995 Identification and cloning of unc-119, a gene expressed in the *Caenorhabditis elegans* nervous system. *Genetics* 141: 977–988.
- Mann, H. B. W., 1947 On a test of whether one of two random variables is stochastically larger than the other. *Ann. Math. Stat.* 18: 50–60. <https://doi.org/10.1214/aoms/1177730491>
- Mitani, S., H. Du, D. H. Hall, M. Driscoll, and M. Chalfie, 1993 Combinatorial control of touch receptor neuron expression in *Caenorhabditis elegans*. *Development* 119: 773–783.
- Nakajima, Y. I., and E. Kuranaga, 2017 Caspase-dependent non-apoptotic processes in development. *Cell Death Differ.* 24: 1422–1430. <https://doi.org/10.1038/cdd.2017.36>
- Ou, G., N. Stuurman, M. D'Ambrosio, and R. D. Vale, 2010 Polarized myosin produces unequal-size daughters during asymmetric cell division. *Science* 330: 677–680. <https://doi.org/10.1126/science.1196112>
- Pacquelet, A., P. Uhart, J. P. Tassan, and G. Michaux, 2015 PAR-4 and anillin regulate myosin to coordinate spindle and furrow position during asymmetric division. *J. Cell Biol.* 210: 1085–1099. <https://doi.org/10.1083/jcb.201503006>
- Pinan-Lucarre, B., C. V. Gabel, C. P. Reina, S. E. Hulme, S. S. Shevkoplyas *et al.*, 2012 The core apoptotic executioner proteins CED-3 and CED-4 promote initiation of neuronal regeneration in *Caenorhabditis elegans*. *PLoS Biol.* 10: e1001331. <https://doi.org/10.1371/journal.pbio.1001331>
- Radman, I., S. Greiss, and J. W. Chin, 2013 Efficient and rapid *C. elegans* transgenesis by bombardment and hygromycin B selection. *PLoS One* 8: e76019. <https://doi.org/10.1371/journal.pone.0076019>
- Rose, L., and P. Gonczy, 2014 Polarity establishment, asymmetric division and segregation of fate determinants in early *C. elegans* embryos (December 30, 2014), *WormBook*, ed. The *C. elegans* Research Community, *WormBook*, doi/10.1895/wormbook.1.30.2, <http://www.wormbook.org>.
- Schindelin, J., I. Arganda-Carreras, E. Frise, V. Kaynig, M. Longair *et al.*, 2012 Fiji: an open-source platform for biological-image analysis. *Nat. Methods* 9: 676–682. <https://doi.org/10.1038/nmeth.2019>
- Schneider, C. A., W. S. Rasband, and K. W. Eliceiri, 2012 NIH Image to ImageJ: 25 years of image analysis. *Nat. Methods* 9: 671–675. <https://doi.org/10.1038/nmeth.2089>
- Shaham, S., P. W. Reddien, B. Davies, and H. R. Horvitz, 1999 Mutational analysis of the *Caenorhabditis elegans* cell-death gene *ced-3*. *Genetics* 153: 1655–1671.
- Sherrard, R., S. Luehr, H. Holzkamp, K. McJunkin, N. Memar *et al.*, 2017 miRNAs cooperate in apoptosis regulation during *C. elegans* development. *Genes Dev.* 31: 209–222. <https://doi.org/10.1101/gad.288555.116>
- Singhvi, A., J. Teuliere, K. Talavera, S. Cordes, G. Ou *et al.*, 2011 The Arf GAP CNT-2 regulates the apoptotic fate in *C. elegans* asymmetric neuroblast divisions. *Curr. Biol.* 21: 948–954. <https://doi.org/10.1016/j.cub.2011.04.025>
- Srayko, M., S. Quintin, A. Schwager, and A. A. Hyman, 2003 *Caenorhabditis elegans* TAC-1 and ZYG-9 form a complex that is essential for long astral and spindle microtubules. *Curr. Biol.* 13: 1506–1511. [https://doi.org/10.1016/S0960-9822\(03\)00597-9](https://doi.org/10.1016/S0960-9822(03)00597-9)
- Stanfield, G. M., and H. R. Horvitz, 2000 The *ced-8* gene controls the timing of programmed cell deaths in *C. elegans*. *Mol. Cell* 5: 423–433. [https://doi.org/10.1016/S1097-2765\(00\)80437-2](https://doi.org/10.1016/S1097-2765(00)80437-2)
- Student, 1908 The probable error of a mean. *Biometrika* 6: 1–25.
- Sulston, J. E., and H. R. Horvitz, 1977 Post-embryonic cell lineages of the nematode, *Caenorhabditis elegans*. *Dev. Biol.* 56: 110–156. [https://doi.org/10.1016/0012-1606\(77\)90158-0](https://doi.org/10.1016/0012-1606(77)90158-0)
- Sulston, J. E., E. Schierenberg, J. G. White, and J. N. Thomson, 1983 The embryonic cell lineage of the nematode *Caenorhabditis elegans*. *Dev. Biol.* 100: 64–119. [https://doi.org/10.1016/0012-1606\(83\)90201-4](https://doi.org/10.1016/0012-1606(83)90201-4)
- Suzuki, J., D. P. Denning, E. Imanishi, H. R. Horvitz, and S. Nagata, 2013 Xk-related protein 8 and CED-8 promote phosphatidylserine exposure in apoptotic cells. *Science* 341: 403–406. <https://doi.org/10.1126/science.1236758>
- Teuliere, J., and G. Garriga, 2017 Size matters: how *C. elegans* asymmetric divisions regulate apoptosis. *Results Probl. Cell Differ.* 61: 141–163. https://doi.org/10.1007/978-3-319-53150-2_6
- Teuliere, J., S. Cordes, A. Singhvi, K. Talavera, and G. Garriga, 2014 Asymmetric neuroblast divisions producing apoptotic cells require the cytoskeleton GRP-1 in *Caenorhabditis elegans*. *Genetics* 198: 229–247. <https://doi.org/10.1534/genetics.114.167189>
- Tukey, J. W., 1949 Comparing individual means in the analysis of variance. *Biometrics* 5: 99–114. <https://doi.org/10.2307/3001913>
- Turek, M., I. Lewandrowski, and H. Bringmann, 2013 An AP2 transcription factor is required for a sleep-active neuron to

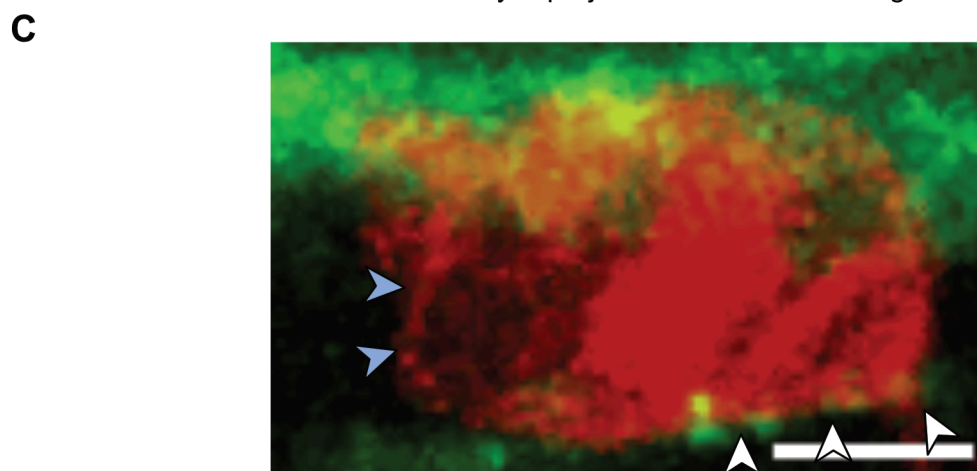
- induce sleep-like quiescence in *C. elegans*. *Curr. Biol.* 23: 2215–2223. <https://doi.org/10.1016/j.cub.2013.09.028>
- Venegas, V., and Z. Zhou, 2007 Two alternative mechanisms that regulate the presentation of apoptotic cell engulfment signal in *Caenorhabditis elegans*. *Mol. Biol. Cell* 18: 3180–3192. <https://doi.org/10.1091/mbc.e07-02-0138>
- Weaver, B. P., R. Zabinsky, Y. M. Weaver, E. S. Lee, D. Xue *et al.*, 2014 CED-3 caspase acts with miRNAs to regulate non-apoptotic gene expression dynamics for robust development in *C. elegans*. *Elife* 3: e04265. <https://doi.org/10.7554/eLife.04265>
- Wei, H., B. Yan, J. Gagneur, and B. Conradt, 2017 *Caenorhabditis elegans* CES-1 snail represses pig-1 MELK expression to control asymmetric cell division. *Genetics* 206: 2069–2084. <https://doi.org/10.1534/genetics.117.202754>
- Wilcoxon, F., 1945 Individual comparisons by ranking methods. *Biom. Bull.* 1: 80–83. <https://doi.org/10.2307/3001968>
- Wu, Y., and E. E. Griffin, 2017 Regulation of cell polarity by PAR-1/MARK kinase. *Curr. Top. Dev. Biol.* 123: 365–397. <https://doi.org/10.1016/bs.ctdb.2016.11.001>
- Yee, C., W. Yang, and S. Hekimi, 2014 The intrinsic apoptosis pathway mediates the pro-longevity response to mitochondrial ROS in *C. elegans*. *Cell* 157: 897–909. <https://doi.org/10.1016/j.cell.2014.02.055>
- Yoav, B. H. Y., 1995 Controlling the false discovery rate: a practical and powerful approach to multiple testing. *J. R. Stat. Soc. B* 57: 289–300.
- Zhou, Z., E. Hartwig, and H. R. Horvitz, 2001 CED-1 is a transmembrane receptor that mediates cell corpse engulfment in *C. elegans*. *Cell* 104: 43–56. [https://doi.org/10.1016/S0092-8674\(01\)00190-8](https://doi.org/10.1016/S0092-8674(01)00190-8)

Communicating editor: M. Sundaram

Figure S1



Maximum intensity Z-projection of all slices in Fig. S1C.



Maximum intensity Z-projection of all slices in Fig. 3

Supplemental File S1 is not shown in this dissertation since it is an avi file. Therefore, I cannot present it here. While this movie is available online, please visit the following GENETICS website:

File S1: <https://doi.org/10.25386/genetics.7058609>

Legends

Figure S1: CED-1 is in asymmetric contact with QL.p.

(A) Individual image planes along the lateral-medial axis showing the localization of CED-1 Δ C::GFP around QL.p. QL.p was labelled with the transgene $P_{egl-17}mCherry::his-24$, $P_{egl-17}myristoylated\ mCherry$, $P_{egl-17}mig-10::yfp$ (*rdvIs1*) and hyp 7 with the transgene $P_{ced-1}ced-1\Delta C::gfp$ (*enIs1*) (see ‘Materials and Methods’ for details). Images were acquired as explained for Fig. 3. It can be seen in the images for slices 8 and 9 that CED-1 Δ C::GFP is in contact with the posterior part of QL.p (white arrowheads) but not with its anterior part (blue arrowheads). A: Anterior, P: Posterior, D: Dorsal, V: Ventral. Scale bar: 2 μ m. (B-C) Maximum-intensity Z-projections generated using image planes shown in Fig. S1A (B) and in Fig. 3 (C). Scale bar: 2 μ m. White arrowheads indicate contact between CED-1 Δ C::GFP and QL.p, whereas blue arrowheads indicate the lack of contact.

Part III

***pig-1* MELK and *ced-3* Caspase cooperate to control the cell polarity in the *C. elegans* NSM neuroblast**

Discussion

C. elegans ces-1 encodes an ortholog of Snail, which belongs to the family of C2H2 zinc-finger transcription factors. According to previous studies on *ces-1* Snail, *ces-1* Snail is involved in controlling cell polarity and cell cycle progression in the NSMnb during embryogenesis (Hatzold & Conradt, 2008). In 2013, the mechanism of how *ces-1* Snail affects cell cycle progression in the NSMnb was revealed (Yan, Memar, Gallinger, & Conradt, 2013). According to this study, *ces-1* Snail was found to act as an upstream transcriptional repressor of *cdc-25.2*, while *cdc-25.2* acts together with *cya-1* to control the cell cycle progression in the NSMnb. However, it was yet unknown how *ces-1* Snail controls cell polarity in the NSMnb. In order to elucidate this mechanism, our goal was to find direct downstream targets of *ces-1* Snail, which have roles in controlling cell polarity in the NSMnb.

To this end, we analyzed the CES-1 ChIP-seq data that was acquired from the modENCODE Project (Gerstein et al., 2010) and identified more than three thousand (3417 reproducible sites) CES-1 binding sites throughout the whole genome. From the reproducible binding sites that were located upstream of transcriptional start sites (TSS), 3199 genes were identified as potential CES-1 target genes. Further, I identified *pig-1* among the genes that were related to asymmetric cell division and cell fate. *pig-1* has been reported to be associated with the asymmetric cell division and cell fate in the HSN/PHB and the QL.p lineages in *C. elegans* (Cordes, Frank, & Garriga, 2006). In addition, *ham-1*, which encodes a protein containing a winged helix DNA binding motif, acts as a transcriptional activator of *pig-1* to influence asymmetric cell division in the Q.a lineage (Feng et al., 2013). According to my study, *pig-1* MELK is a direct target of CES-1 Snail in the NSMnb lineage. A gain-of-function (gf) mutation of *ces-1* reduces the transcription of *pig-1*, and loss-of-function (lf) mutation of *ces-1* significantly increases the transcriptional level of *pig-1* when compared to wild-type. Moreover, *pig-1* MELK acts downstream of *ces-1* Snail to control the asymmetric positioning and the orientation of the NSMnb cleavage plane, as well as the fate and the kinetics of NSMsc death. Moreover, *ced-3*, which encodes the *C. elegans* Caspase and which executes cell death in most of the cell death lineages, also plays a role in controlling the asymmetric positioning of the NSMnb cleavage plane and functions in parallel to *pig-1* MELK.

It has been shown that Snail TFs play important roles during Epithelial to Mesenchymal Transition (EMT) (Batlle et al., 2000; Cano et al., 2000; Nieto, Sargent, Wilkinson, & Cooke,

1994), which is a noteworthy process in tumorigenesis. The mammalian MELK kinase was shown to be involved in various processes, such as cell cycle regulation, cell proliferation and carcinogenesis (Du et al., 2014; Nakano et al., 2005; Vulsteke et al., 2004). According to previous studies in different organisms, no direct interaction was reported between Snail family members and MELK kinases, which is involved in regulating cell polarity. In my study, it is elucidated for the first time that Snail and MELK act in the same pathway to control cell polarity and cell death. However, the exact mechanisms of how *ces-1* Snail and *pig-1* MELK function in the process of asymmetric cell division and cell death remain elusive. Therefore, studying the interrelationships between *ces-1* and *pig-1* are important for us to understand these biological processes, and could provide insights for understanding human diseases.

1. CES-1 Snail acts as a transcriptional repressor of *pig-1* MELK in the NSM neuroblasts

In order to find downstream targets of CES-1 that might be involved in controlling cell polarity in the NSMnb, we analyzed the CES-1 ChIP-seq data that was generated by the modENCODE project and obtained more than three thousand potential target genes of *ces-1* (Gerstein et al., 2010). Since a chromatin immuno-precipitation combined with microarray analysis (ChIP-on-ChIP) of Snail TF has been performed in *D. melanogaster* (Zeitlinger et al., 2007), we compared our potential CES-1 targets with the orthologs of potential target genes obtained from *D. melanogaster* Snail. Many of them are conserved in some fundamental processes such as cell adhesion, which means that these Snail factors have some conserved functions across various species (Nieto, Huang, Jackson, & Thiery, 2016). On the other hand, certain potential targets of CES-1 Snail were specific to *C. elegans* indicating that Snail TFs may also have distinct roles in different species.

It has been reported that the BH3-only gene *egl-1* and the Cdc25 phosphatase gene *cdc-25.2* are two direct targets of CES-1 Snail in the NSMnb lineage (Thellmann, 2003; Yan et al., 2013). However, neither *egl-1* nor *cdc-25.2* were among the more than three thousand potential targets that were identified in our ChIP-seq analysis. Based on previous studies, the binding site of CES-1 Snail in the *egl-1* cis-regulatory region is located ~ 3 kb downstream of the *egl-1* transcription unit. The binding site of CES-1 Snail in the regulatory region of *cdc-25.2* is located ~ 4.8-6.5 kb upstream of the *cdc-25.2* TSS. Therefore, the criteria that we used to identify potential CES-1 binding sites was to check for binding sites that lie within the transcription unit or ~ 2 kb upstream or downstream of the transcriptional start sites. This might affect the identification of potential targets whose regulatory regions are further away than 2 kb, such as *egl-1* and *cdc-25.2*. Moreover, by analysis of the CES-1 ChIP-seq data, ~ 20 % of the binding

sites cannot be identified as potential target genes of *ces-1*, which suggests that we might miss potential targets and that *egl-1* and *cdc-25.2* may exist among them.

Through analysis of the CES-1 ChIP-seq data, we identified three CES-1 binding motifs, which consist of CAGC(T/A)GC, AAT(T/G/C)(A/C/G)AAT and AGACG(C/G)A G. As mentioned in my results, a strong CES-1 binding peak arises at - 200 bp upstream of the *pig-1* start codon and spans more than 100 base pairs centered on this - 200 bp site. I checked the *pig-1* genomic DNA sequence in this region and found sequences that are similar to one of the three CES-1 motifs. This suggests that CES-1 may inhibit the transcription of *pig-1* by binding multiple sites within these 100 base pairs in the *pig-1* upstream regulatory region. Therefore, the precise binding motifs of CES-1 Snail in this region needs to be studied more extensively. The Ou lab found that *ham-1* acts as a transcriptional activator of *pig-1* to influence cell polarity in Q.a by promoting the transcription of *pig-1* (Feng et al., 2013). Based on HAM-1 ChIP-seq data, which was also acquired from the modENCODE project, a strong HAM-1 binding peak appears upstream of the *pig-1* start codon, which spans from -42 bp to -266 bp. The overlap of these two binding peaks between CES-1 and HAM-1 suggests that CES-1 and HAM-1 may compete with each other for binding to the same motif or disrupt the binding affinity of each other through influencing some neighboring motifs in the upstream regulatory region of *pig-1*. On the other hand, it is possible that CES-1 and HAM-1 have distinct roles in different neuroblasts. The Garriga lab reported that no defect of NSMsc survival was observed in *ham-1* lf mutants, but they only quantified the survival rate of the NSMsc using a NSM reporter (Teuliere, Kovacevic, Bao, & Garriga, 2018). More details of the asymmetric division of the NSMnb should be investigated, such as the asymmetric position and the orientation of the NSMnb cleavage plane. For instance, *ham-1* (lf) does not affect asymmetric division in the Q.p lineage as well, but it indeed influences the expression level of *pig-1* in Q.p (Feng et al., 2013).

In addition, the Horvitz lab discovered that *sptf-3*, which encodes a Sp1 family transcription factor, directly drives the expression of *pig-1* to influence the cell death of the M4 and the AQR sister cells (Hirose & Horvitz, 2013). SPTF-3 has a glutamine-rich domain and three C2H2 zinc finger domains. Through ChIP-seq analysis, a consensus CGCCC binding motif of SPTF-3 was identified, which is quite different from the CES-1 binding motifs. The SPTF-3 binding peak in *pig-1* upstream regulatory region overlaps with the peak of CES-1 and HAM-1 as well. Hence, SPTF-3 might also affect the binding affinity of CES-1 or HAM-1 in the *pig-1* upstream regulatory region. Whether HAM-1 or SPTF-3 function as positive transcriptional regulators in the NSMnb lineage needs to be further investigated in the future. Moreover, the precise locus of *ces-1* binding motifs in the *pig-1* upstream regulatory region are unknown. Considering that

the CES-1 binding peak in *pig-1* upstream regulatory regions covers ~100 base pairs, I propose that CES-1 may regulate *pig-1* through multiple sites.

Taken together, I propose that *ces-1* and *ham-1* may have similar or distinct roles in regulating the expression levels of *pig-1* to promote establishment of cell polarity in the NSM neuroblasts. Because of the overlap of their binding peaks in the upstream regulatory region of *pig-1*, *ham-1* is possible to play roles in the NSM neuroblasts. Future studies will reveal whether they act together to control cell polarity in the NSMnb. If this is the case, I then want to determine what elements CES-1 and HAM-1 bind to to regulate the transcription of *pig-1*.

2. Regulators of PIG-1 MELK activity have similar functions in the NSM neuroblast

Above, I discussed how *pig-1* is regulated at the transcriptional level. However, post-transcriptional regulators and post-translational regulators may also play critical roles in the regulation of PIG-1 activity by controlling translation progression or by influencing protein activity.

In mammals, it has been reported that LKB1 acts upstream to phosphorylate MELK and this phosphorylation is crucial for functions of MELK protein (Lizcano et al., 2004). The activity of LKB1 depends on the combination of a pseudokinase, STRAD, and an adaptor, MO25, and this combination promotes the stability and activity of the LKB1 kinase and the translocation from the nucleus to the cytoplasm (Baas et al., 2003; Boudeau et al., 2003). In *C. elegans*, their orthologs are *par-4*, *strd-1* and *mop-25.1/25.2*, respectively. Based on a study from the Garriga lab, this phosphorylation mechanism is also conserved in larval development of *C. elegans* and the function of *pig-1* in Q.p asymmetric division depends on *par-4*, *strd-1* and *mop-25.2* pathway. In the Q.p lineage, *par-4*, *strd-1* and *mop-25.2* were found to act together to play an important role in phosphorylating the Threonine 169 residue of PIG-1 protein. Mutations of this site influence the function of PIG-1 in controlling the asymmetric division of the Q.p (Chien, Brinkmann, Teuliere, & Garriga, 2013; Hirose & Horvitz, 2013). According to my studies, this mechanism is also conserved in the NSMnb. Loss-of-function mutations of these genes not only disrupt the asymmetric positioning of the cleavage plane but also affect the orientation of the cleavage plane in the NSMnb. Interestingly, I only observed defects when I knocked-down both *mop-25.1* and *mop-25.2* by RNAi (by injection) while I did not observe any defects when *mop-25.1* or *mop-25.2* was knocked-down alone. This suggests that *mop-25.1* and *mop-25.2* have redundant roles in the NSM neuroblast, but not in the Q.p cell where only *mop-25.2* is necessary. Therefore, I propose that *mop-25.1* acts together with *mop-25.2* to promote cell polarity establishment during embryogenesis, but that *mop-25.2* alone plays a major role in this process

post-embryogenesis. This could be due to different expression levels or distinct protein activities of MOP-25.1 and MOP-25.2 in different neuroblasts.

In addition to these upstream regulators of MELK, various microRNAs (miRNAs) have been shown to play critical roles in regulating the translation of MELK mRNA. For example, the role of *hsa-miR-145-3p* in regulating MELK has been found to be crucial for prostate cancer (PCa) (Atala, 2016; Matakı et al., 2016). Since malignant transformation of a normal stem cell often is accompanied with a high level of MELK expression, *hsa-miR-145-3p* could inhibit tumorigenesis through directly repressing MELK overexpression (Goto et al., 2017). In addition, *hsa-miR-214-3p* has been shown to mediate cell cycle progression and cell proliferation in hepatocellular carcinoma by retaining the expression of MELK (Lee et al., 2013). On the other hand, it has been shown that *hsa-miR27a-5p* acts together with *hsa-miR34b-3p* to inhibit carcinogenesis by regulating MELK expression (Mizuno et al., 2017). These mechanisms could potentially also be conserved in *C. elegans*. According to the prediction of microRNA targets of *pig-1* from the TargetScanWorm website, *miR-253*, which encodes a non-protein coding microRNA and is classified into the *mir-220* family of microRNAs with human *mir-220* (Kaufman & Miska, 2010), could be a direct regulator of *pig-1* through binding to its 3' terminal UTR. According to the prediction from the website, it has a conserved seed match across *C. elegans*, *C. briggsae*, *C. remanei*, *C. brenneri*, *C. japonica* and *C. pacificus*, which consists of 7 nucleotides, CUACUAA. However, the precise function of *mir-253* is not yet known. In addition, no miRNAs have yet been reported to be involved in the post-transcriptional regulation of *pig-1* MELK in worms. Therefore, studying the function and mechanism of *miR-253* in the NSMnb or other neuroblasts may shed light on how miRNAs are involved in mediating cell polarity establishment and reveal the post-transcriptional regulation of *pig-1*.

3. *ces-1* Snail is involved in various developmental processes

As mentioned in the result section, we selected 10 other TFs of *C. elegans* for which the ChIP-seq data sets are available from the modENCODE project to do a Gene Ontology (GO) analysis together with CES-1 Snail. Among the top 50 of the most highly enriched biological processes, processes related to larval development, embryonic development and system development are highly enriched in the case of all these TFs. This suggests that these TFs may have some redundant roles in regulating these fundamental biological processes. It is possible that these TFs have similar functions like *ces-1* in the NSMnb or other neuroblast lineages. Due to redundant roles between these TFs, it could be one of the reasons why the loss of *ces-1* alone does not cause strong defects during embryogenesis and post-embryogenesis. In addition, apart

from the top 12 biological processes that are enriched for most TFs in the GO analysis, CES-1 involves in all the other 38 biological processes and contributes an average role to these processes based on the p-value, which is different for the other 10 TFs. This suggests that CES-1 may have broad and some distinct functions during *C. elegans* development. However, how CES-1 contributes to these biological processes is unknown. Because RNA-seq method is able to reveal the presence and expression quantity of total RNAs in a biological organism or in a single cell. Therefore, using CES-1 ChIP-seq data together with a CES-1 RNA-seq data set would help to further discover new potential downstream targets of CES-1 and advance our understanding of how CES-1 Snail contributes in diverse biological processes.

In addition to *pig-1* MELK, the other two reported targets of CES-1 in the NSMnb lineage are *egl-1* and *cdc-25.2* (Thellmann, 2003; Yan et al., 2013). Each of them functions in different pathways to ensure normal development during embryogenesis. *egl-1* acts as a pro-apoptotic factor to promote the activation of the *ced-3* Caspase in the conserved cell death pathway (Conradt & Horvitz, 1998). *cdc-25.2* encodes a putative homolog of CDC25 protein phosphatase, which acts together with *cya-1* to control cell cycle progression in the NSMnb (Yan et al., 2013). As I mentioned above, more than 3000 genes were identified through the CES-1 ChIP-seq analysis, which suggests that CES-1 has many more potential direct targets that could affect the NSMnb developmental process or other biological progressions in other lineages. The most well-known cell polarity pathway in *C. elegans* involves the PAR complex, which was initially discovered because of its role in early embryogenesis in *C. elegans* (Kemphues, Priess, Morton, & Cheng, 1988). Interestingly, CES-1 binding peaks were identified in genes encoding some PAR complex components, such as PAR-3 and PAR-6 (Etemad-Moghadam, Guo, & Kemphues, 1995; Hung & Kemphues, 1999). This suggests that PAR components could be involved in the regulation of NSMnb polarity through a *ces-1*-dependent pathway. These PAR components could act in parallel or act together with PIG-1 to mediate cell polarity establishment in the NSMnb. In addition, certain components related to the Ras pathway and Wnt signaling pathway were also identified in the CES-1 ChIP data. The Ras superfamily encodes a class of proteins named small GTPases, which are involved in diverse processes like cell growth, cell differentiation and cell survival (Barbacid, 1987; Giehl, 2005; Malumbres & Barbacid, 2003). It is possible that *ces-1* influences the apoptotic fate of the small daughter (NSMsc) and the differentiation of the large daughter (NSM) by affecting the expression level of Ras components. The Wnt signaling pathway plays important roles in signal transductions between neighboring cells, and members of the Wnt family play roles in influencing cell specification, cell migration, cell proliferation etc (Nüsslein-volhard & Wieschaus, 1980; Reya & Clevers, 2005; Rijsewijk et al., 1987). Considering that CES-1 is

strongly expressed in the NSMnb neighboring cells, I therefore propose that Wnt signaling from the NSMnb neighboring cells may play critical roles in promoting NSMnb polarity establishment and additional developmental processes in the two daughter cells (NSM and NSMsc). Since only ~ 2% of the NSMsc abnormally survive in *pig-1* lf mutants and ~ 90% of the NSMsc abnormally survive in *ces-1* gf mutants, I propose that targets of CES-1 that belong to the Wnt signaling or Ras pathway may function in parallel or act together with *pig-1* to control the cell fate of the NSMsc.

4. *pig-1* MELK is involved in various developmental processes

In *C. elegans*, *pig-1* encodes the sole ortholog of MELK and plays roles in controlling the position of the cleavage plane and the cell fate in the HSN/PHB and the Q.p lineages (Cordes et al., 2006). Based on my study, *pig-1* not only affects the asymmetric position of the cleavage plane but also influences the orientation of the cleavage plane in the NSM neuroblasts. Loss of *pig-1* disrupts the polarity of the NSMnb and affects the kinetics of the NSMsc death, while loss of *pig-1* only represents a very low penetrance on the NSMsc survival rate. This suggests that *pig-1* plays major roles in controlling asymmetric cell division but only plays a minor role in influencing the distribution of cell-fate determinants. One explanation could be that only a few cell-fate determinants are disrupted due to the lack of *pig-1*. In this case, the NSMsc still inherits enough apoptotic potential and initiates cell death.

In addition to the effect on cell polarity and cell fate, *pig-1* seems to have more roles especially during embryogenesis. Using a null allele of *pig-1*, *gm344*, I observed a high penetrance of embryonic lethality at 20 °C and this defect is even significantly enhanced by the weak loss of *ced-3* mutation, *n2427* (Figure 10). Moreover, the embryonic lethality caused by loss of *pig-1* seems to depend on temperature. Compared to the penetrance of embryonic lethality at 25 °C, *gm344* exhibits a much lower penetrance if it is incubated at 20 °C or 15 °C. A similar phenotype is also observed for the double mutant of *pig-1(gm344) ced-3(n2427)*. On the other hand, the Rose lab reported that the kinases *par-1* and *pig-1* act in parallel to influence the asymmetric cell division in the EMS (Liro, Morton, & Rose, 2018). According to their study, they observed a similar phenotype of embryonic and larval lethality in *pig-1(gm344)* animals at 19.5 and 25 °C. Moreover, they observed a significant enhancement when *gm344* was crossed into the background of a temperature-sensitive (ts) *par-1* mutation, *zu310*, which is similar to what I observed in the double mutant of *pig-1(gm344) ced-3(n2427)*. It suggests that *ced-3* may act together or in parallel with *par-1* to enhance this developmental defect that is caused by the loss of *pig-1*. Taken together, it seems that *pig-1* MELK plays various roles during embryogenesis in addition to controlling cell polarity in some neuroblasts.

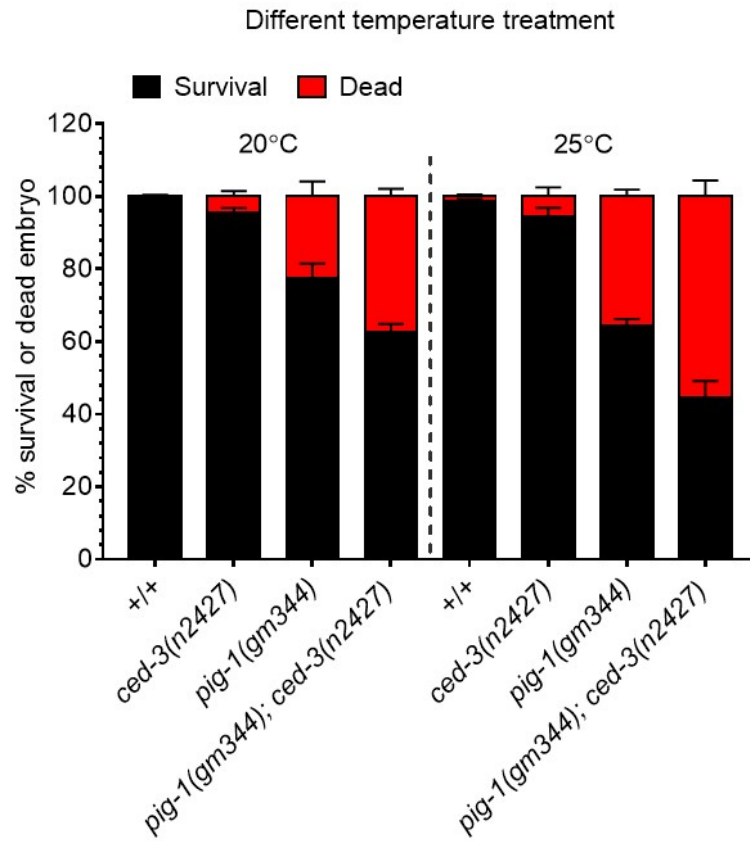


Figure 10. Percent embryonic lethality in *pig-1* and *ced-3* If mutants at different temperatures. In addition to influencing the NSMnb cell polarity, loss of *pig-1* also results in embryonic lethality. This defect is enhanced by a weak loss of *ced-3* allele and displays a temperature sensitivity.

5. *pig-1* MELK may play a role in influencing cell cycle progression in the NSMnb lineage

In the NSMnb, *ces-1* was reported to be involved in regulating cell cycle progression by controlling the transcription of *cdc-25.2* (Yan et al., 2013), which encodes a CDC25-like phosphatase. In mammalian cells, CDC-25 has three isoforms: CDC25A, CDC25B and CDC25C (Galaktionov & Beach, 1991; Nagata, Igarashi, Jinno, Suto, & Okayama, 1991; Sadhu, Reed, Richardson, & Russell, 1990). All of them are important for the checkpoint of cell cycle progression. They promote cell division by dephosphorylating cyclin dependent protein kinases (CDK) (Kaldis, 1999; Kristjánisdóttir & Rudolph, 2004). Misregulation of CDC25 phosphatase results in genomic instability or even carcinogenesis (Branzei & Foiani, 2008; Kastan & Bartek, 2004; Meikrantz & Schlegel, 1995). Therefore, understanding the activation mechanisms of CDC25 is important for cancer therapy. In view of previous discoveries, CDC25 phosphatases themselves are highly controlled via various mechanisms, such as transcriptional regulation, subcellular or intracellular localization, binding to other partners etc. Among these mechanisms, phosphorylation of CDC25 plays an essential role in inhibition or activation of its phosphatase activity (Gabrielli, Clark, McCormack, & Ellem, 1997; Hoffmann, Clarke, Marcote, Karsenti, & Draetta, 1993; Izumi & Maller, 1993; Mailand et al., 2002). Interestingly, it has been reported that MELK is one of the upstream kinases that regulates the CDC25B activity by phosphorylating conserved serine sites. This phosphorylation of CDC25B on centrosomes is crucial for mitotic entry (Mirey et al., 2005; Schmitt et al., 2006). Similar to MELK localization in mammalian cells, *pig-1* is also observed to localize to centrosomes during the division of the one-cell embryo, which hints at the possibility that *pig-1* plays a similar role in controlling cell cycle progression by regulating the ortholog of CDC25B in *C. elegans*. Based on this hypothesis, I used a strong *ced-3* lf allele, *n717*, which results in 100 % NSMsc survival, and crossed it with a *pig-1* null allele, *gm344*, to investigate whether *pig-1* affects the number of NSM cells. In *ced-3(n717)* animals, 100 % larvae have 4 NSM-like cells using the NSM reporter *bcIs66* ($P_{\text{tph-1his-24}}::\text{gfp}$), whereas in the double mutant of *pig-1(gm344) ced-3(n717)*, ~84 % larvae show 4 NSM signals and ~16 % larvae show < 4 NSM signals. This suggests that *pig-1* may inhibit the 100 % NSMsc survival of *ced-3(n717)* through influencing the cell cycle progression by mediating the phosphorylation of CDC-25.2 in the NSMnb. However, it is very difficult to track the NSMnb when embryo starts to twitch after the two-fold stage. In addition, it could be possible that the NSMnb in the *pig-1(gm344) ced-3(n717)* embryo may divide very late post the two-fold stage. Therefore, I cannot completely conclude that the ~16 % larvae showing < 4 NSM signals are due to the defect of the NSMnb division. Moreover, *cdc-25.2* was reported to act together with *cya-1* to control cell division progression in the NSMnb. I then checked the number of the NSM signals in the triple mutant of *cya-1(bc416); pig-1(gm344)*

ced-3(n717) by using the NSM reporter *bclIs66*. I observed ~ 64 % larvae to have 4 NSM signals. Thus, the phenotype of the *pig-1(gm344) ced-3(n717)* double mutant was enhanced by the loss of *cya-1*. Therefore, *pig-1* seems to act in parallel with *cya-1* to influence cell cycle progression in the NSMnb. Moreover, the NSM neuroblasts took much longer time to divide in the *pig-1(gm344)* or the *pig-1(gm344) ced-3(n717)* animals compared to wild-type. In addition, among tracking development process of ten NSM neuroblasts, one NSMnb did not divide when this embryo reached the comma stage. These data suggest that *pig-1* MELK may act through a conserved manner, which is similar to the mechanism in mammalian cells, to promote NSMnb cell cycle progression by phosphorylating CDC-25.2 on some conserved serine residues to regulate its activity.

6. The correct asymmetric positioning of the NSMnb cleavage plane depends on CED-3 Caspase activity

The most well-known function of *ced-3* Caspase is to execute cell death in cells destined to die (Shaham & Horvitz, 1996; Xue, Shaham, & Horvitz, 1996; Yuan & Horvitz, 1990). However, *ced-3* also seems to play non-killing roles important for embryogenesis or post-embryogenesis. For example, CED-3 acts with the miRNA-induced-silencing complex (miRISC) to regulate the levels of non-apoptotic proteins, such as LIN-14, LIN-28 and DISL-2 to mediate developmental processes in *C. elegans* (Weaver, Weaver, Mitani, & Han, 2017; Weaver et al., 2014). In addition, it has also been reported that CED-3 plays roles in influencing aging and neural regeneration (Pinan-Lucarre et al., 2012; Yee, Yang, & Hekimi, 2014). Based on my study, I found that *ced-3* Caspase affects the localization of the NSMnb cleavage plane in a *pig-1* lf background, which means CED-3 or pro-CED-3 has a role in mediating asymmetric cell division. Because the activation of *ced-3* Caspase depends on the upstream factors *egl-1* and *ced-4* in vivo, loss of *egl-1* or *ced-4* blocks cell death that is executed by *ced-3* Caspase. To confirm that this process is dependent on active CED-3 but not pro-CED-3, I checked the position of the cleavage plane in *egl-1* (lf) and *ced-4* (lf) mutants in a *pig-1* lf background. A similar phenotype was observed between *pig-1* (lf) *ced-3* (lf) double mutants, *ced-4* (lf); *pig-1* (lf) double mutants or *pig-1* (lf); *egl-1* (lf) double mutants. In wild-type embryos, the NSMnb cleavage plane usually localizes to the dorsal-lateral side and in *pig-1* lf mutants, the asymmetric localization of the cleavage plane shifts to the middle of the NSMnb and gives rise to a symmetric division. Interestingly, the loss of the cell death components (*egl-1*, *ced-4*, *ced-3*) along with *pig-1* MELK shifts the cleavage plane from the dorsal-lateral to the ventral-medial side. This opposite localization of the NSMnb cleavage plane ultimately results in a smaller NSM and a larger NSMsc. This suggest that active *ced-3* plays a role in controlling the correct positioning of the cleavage plane in the NSMnb. However, the detailed mechanisms through

which *ced-3* Caspase regulates the positioning of the cleavage plane are unknown. It has been reported that CED-3::GFP is present in the mother cell (the NSMnb) and that it promotes a gradient of apoptotic potential through an engulfment pathway-dependent manner (Chakraborty, Lambie, Bindu, Mikeladze-Dvali, & Conratt, 2015). However, the other functions of CED-3 in the mother cell (the NSMnb) are still unclear. Using a full-length CED-3::GFP reporter, I observed that CED-3::GFP clustered around the cleavage plane during the NSMnb asymmetric division (Figure 11). I hereby propose that, the active CED-3 may activate or inhibit some components localized on the cleavage plane or that inactive Caspase pro-CED-3 may physically interact with other components to regulate asymmetric cell division in the NSMnb. Because I cannot distinguish between pro-CED-3 and active CED-3 by using the full-length CED-3::GFP reporter, a direct detector or reporter of active CED-3 needs to be developed to answer this question. On the other hand, to reveal the mechanism through which CED-3 regulates asymmetric cell division, performing a Yeast Two Hybrid screen of active CED-3 could help us to find new interesting potential targets of CED-3 Caspase that are involved in regulating cell polarity and cell fate. On the other hand, we cannot exclude the possibility that pro-CED-3 may play important roles during this process since the pro-domain of CED-3 could also play certain roles during embryogenesis. Therefore, an additional pro-CED-3 Yeast Two Hybrid screen is also important for answering whether pro-CED-3 plays roles in regulating the asymmetric division of the NSMnb.

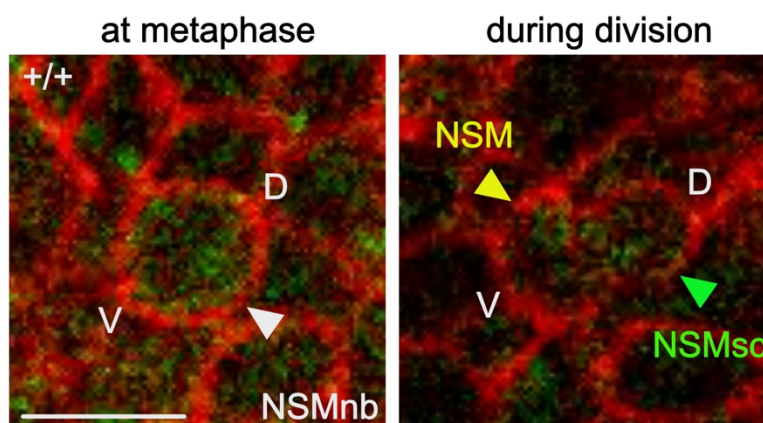


Figure 11. Expression of CED-3::GFP in the NSMnb lineage. Using a single-copy of *ced-3::gfp* transgene, fluorescence signals of CED-3::GFP are observed at the NSMnb metaphase and in the NSMnb division progression. CED-3::GFP seems to cluster around the cleavage furrow in the progression of asymmetric division in the NSMnb. V means ventral side and D means dorsal side. The NSM is marked in yellow and the NSMsc is marked in green. Error bar indicates 5 μ m.

7. *pig-1* MELK influences the kinetics of the NSMsc death through indirectly influencing the activity of CED-3 Caspase

It has been reported that the asymmetric division of the NSMnb is critical for the correct fate of its daughter cells, and in particular, for the small daughter NSMsc that is destined to die (Hatzold & Conradt, 2008). Therefore, asymmetric cell division somehow influences the apoptotic cell death pathway. In the NSMnb lineage, the apoptotic fate of the NSMsc depends on *ced-3* Caspase, loss of *ced-3* results in 100 % survival of the NSMsc. However, disruption of the asymmetric NSMnb division that is caused by the loss of *pig-1* only results in 2 % survival of the NSMsc. This suggests that *pig-1* may only play a minor role or affect certain components that are involved in regulating the apoptotic cell death pathway. Since the NSMsc takes longer time (~ 30 min) to die in *pig-1* (lf) animals compared to wild type (~ 22 min), it seems that *pig-1* influences the apoptotic kinetics through repressing the activity of *ced-3* Caspase. Because of this repression, the NSMsc needs longer time to encounter enough active *ced-3* Caspase to execute cell death. In view of previous studies, no physical interaction between *pig-1* and *ced-3* is reported. Therefore, I propose that *pig-1* indirectly represses the activity of *ced-3* Caspase in the NSMsc. To test this, it could be helpful to compare the distribution of upstream regulators of *ced-3* Caspase in the NSMnb lineage in wild-type and *pig-1* (lf) animals. Since *pig-1* encodes a MELK kinase, the phosphatase activity of *pig-1* MELK could affect various targets that are involved in diverse biological processes, which makes it difficult to find a direct target of *pig-1* that mediates the activity of *ced-3* Caspase.

8. *pig-1* MELK and *ced-3* Caspase cooperate to regulate asymmetric cell division in the NSMnb

Asymmetric cell division is very important to generate diversity during animal development because it gives rise to two daughter cells with different fates. The asymmetric positioning of the cleavage plane is one of the crucial processes during this event. In *C. elegans*, the mechanisms of positioning of the cleavage plane is well studied in one-cell stage embryos (Rose & Gonczy, 2014). Centrosome and spindle positioning are two crucial steps for the correct positioning of the cleavage plane. The positioning of the mitotic spindle at the end of anaphase specifies the cleavage furrow, while the correct positioning of the anaphase spindle depends on the position of two centrosomes prior to mitosis. In these processes, microtubules and microtubule-associated proteins such as dynein and members of the dynein complex, generate the major pulling forces from the anterior and posterior poles for centrosome movement (Galli & van den Heuvel, 2008; Morin & Bellaïche, 2011). Therefore, checking the position of the two centrosomes and the localization of dynein in the NSMnb could reveal more details of how

pig-1 MELK and *ced-3* Caspase cooperate to control the asymmetric positioning of the cleavage plane. However, due to the very small size, the spherical cell shape and the lack of a specific marker for the NSMnb lineage, many techniques cannot be applied in this lineage to obtain more data to elucidate detailed mechanisms of how the asymmetric cleavage plane is established in the NSMnb.

Moreover, it has been reported that centrosome and spindle positioning are correlated with anterior-posterior polarity, which ensure coordination with the asymmetric distribution of cell-fate determinants during asymmetric cell division (Betschinger & Knoblich, 2004; C. R. Cowan & Hyman, 2007; Carrie R. Cowan & Hyman, 2004; Galli & van den Heuvel, 2008). Therefore, checking the localization of components that are involved in establishing and maintaining the cell polarity or gradients of cell-fate determinants in one-cell stage embryos may provide more hints to understand how *pig-1* and *ced-3* contribute to asymmetric cell division in the NSMnb or other neuroblasts. For example, *ect-2* (GEF) and *nmy-2* (non-muscle myosin II) play important roles in symmetry breaking and in generating flows of cortical materials (such as PARs). Interestingly, the Gartner lab found that the phosphorylation of two serine residues in NMY-2 is decreased in *pig-1* (lf) animals (Offenburger, Bensaddek, Murillo, Lamond, & Gartner, 2017), which indicates that NMY-2 may be phosphorylated by PIG-1. This is important since it has been shown that NMY-2 activity depends on its phosphorylation status (Guo & Kemphues, 1996). Therefore, I propose that *pig-1* may regulate NSMnb polarity by influencing the activity of NMY-2, which generates different cortical contractions from anterior to posterior. Apart from these two factors, it would be interesting to check the localizations and functions of PAR components (such as *par-1* and *par-4*) in the NSMnb lineages in the future.

In addition, more evidence shows that mammalian Caspases have non-killing functions in different types of stem cells (Baena-Lopez, Arthurton, Xu, & Galasso, 2018). Therefore, my finding that CED-3 Caspase plays roles in mediating the asymmetric cell division of the NSM neuroblasts could be relevant to those non-killing functions of mammalian Caspases.

References:

- Ai E., D. S. Poole, and A. R. Skop, 2011 Long astral microtubules and RACK-1 stabilize polarity domains during maintenance phase in *Caenorhabditis elegans* embryos. *PLoS One*. <https://doi.org/10.1371/journal.pone.0019020>
- Albertson D. G., and J. N. Thomson, 1976 The pharynx of *Caenorhabditis elegans*. *Philos. Trans. R. Soc. Lond. B. Biol. Sci.* <https://doi.org/10.1098/rstb.1976.0085>
- Alison M. G. Robertson, and J. N. Thomson, 1982 Morphology of programmed cell death in the ventral nerve cord of *C. elegans* larvae. *Development* 1982 67: 89-100.
- Atala A., 2016 Regulation of UHRF1 by Dual-Strand Tumor-Suppressor MicroRNA-145 (miR-145-5p and miR-145-3p): Inhibition of Bladder Cancer Cell Aggressiveness. *J. Urol.* <https://doi.org/10.1016/j.juro.2016.07.048>
- Baas A. F., J. Boudeau, G. P. Sapkota, L. Smit, R. Medema, *et al.*, 2003 Activation of the tumour suppressor kinase LKB1 by the STE20-like pseudokinase STRAD. *EMBO J.* <https://doi.org/10.1093/emboj/cdg292>
- Badouel C., I. Chartrain, J. Blot, and J. P. Tassan, 2010 Maternal embryonic leucine zipper kinase is stabilized in mitosis by phosphorylation and is partially degraded upon mitotic exit. *Exp. Cell Res.* 316: 2166–2173. <https://doi.org/10.1016/j.yexcr.2010.04.019>
- Baena-Lopez L. A., L. Arthurton, D. C. Xu, and A. Galasso, 2018 Non-apoptotic Caspase regulation of stem cell properties. *Semin. Cell Dev. Biol.* <https://doi.org/10.1016/j.semcdb.2017.10.034>
- Barbacid M., 1987 Ras genes. *Annual Review of Biochemistry.* <https://doi.org/10.1146/annurev.bi.56.070187.004023>
- Barrallo-gimeno A., and M. A. Nieto, Evolutionary history of the Snail / Scratch superfamily. 25: 248–252.
- Barrallo-Gimeno A., 2005 The Snail genes as inducers of cell movement and survival: implications in development and cancer. *Development.* <https://doi.org/10.1242/dev.01907>
- Battle E., E. Sancho, C. Francí, D. Domínguez, M. Monfar, *et al.*, 2000 The transcription factor Snail is a repressor of E-cadherin gene expression in epithelial tumour cells. *Nat. Cell Biol.* <https://doi.org/10.1038/35000034>
- Betschinger J., and J. A. Knoblich, 2004 Dare to be different: Asymmetric cell division in *Drosophila*, *C. elegans* and vertebrates. *Curr. Biol.*
- Bienkowska D., and C. R. Cowan, 2012 Centrosomes can initiate a polarity axis from any position within one-cell *C. Elegans* embryos. *Curr. Biol.* <https://doi.org/10.1016/j.cub.2012.01.064>
- Blanco M. J., G. Moreno-Bueno, D. Sarrio, A. Locascio, A. Cano, *et al.*, 2002 Correlation of Snail expression with histological grade and lymph node status in breast carcinomas. *Oncogene.* <https://doi.org/10.1038/sj.onc.1205416>

- Bloss T. A., E. S. Witze, and J. H. Rothman, 2003 Suppression of CED-3-independent apoptosis by mitochondrial β NAC in *Caenorhabditis elegans*. *Nature*.
- Blot J., I. Chartrain, C. Roghi, M. Philippe, and J. P. Tassan, 2002 Cell cycle regulation of pEg3, a new *Xenopus* protein kinase of the KIN1/PAR-1/MARK family. *Dev. Biol.* <https://doi.org/10.1006/dbio.2001.0525>
- Boudeau J., A. F. Baas, M. Deak, N. A. Morrice, A. Kieloch, *et al.*, 2003 MO25 α/β interact with STRAD α/β enhancing their ability to bind, activate and localize LKB1 in the cytoplasm. *EMBO J.* <https://doi.org/10.1093/emboj/cdg490>
- Bouillet P., and A. Strasser, 2002 BH3-only proteins –evolutionarily conserved pro-apoptotic Bcl-2 family members essential for initiating programmed cell death. *J Cell Sci.* <https://doi.org/11950875>
- Boulay J. L., C. Dennefeld, and A. Alberga, 1987 The *Drosophila* developmental gene snail encodes a protein with nucleic acid binding fingers. *Nature.* <https://doi.org/10.1038/330395a0>
- Branzei D., and M. Foiani, 2008 Regulation of DNA repair throughout the cell cycle. *Nat. Rev. Mol. Cell Biol.*
- Budirahardja Y., and P. Gonczy, 2008 PLK-1 asymmetry contributes to asynchronous cell division of *C. elegans* embryos. *Development.* <https://doi.org/10.1242/dev.019075>
- Byerly L., R. C. Cassada, and R. L. Russell, 1976 The life cycle of the nematode *Caenorhabditis elegans*. I. Wild-type growth and reproduction. *Dev. Biol.* [https://doi.org/10.1016/0012-1606\(76\)90119-6](https://doi.org/10.1016/0012-1606(76)90119-6)
- Cano A., M. A. Pérez-Moreno, I. Rodrigo, A. Locascio, M. J. Blanco, *et al.*, 2000 The transcription factor Snail controls epithelial-mesenchymal transitions by repressing E-cadherin expression. *Nat. Cell Biol.* <https://doi.org/10.1038/35000025>
- Chakraborty S., E. J. Lambie, S. Bindu, T. Mikelandze-Dvali, and B. Conradt, 2015 Engulfment pathways promote programmed cell death by enhancing the unequal segregation of apoptotic potential. *Nat. Commun.* 6: 10126. <https://doi.org/10.1038/ncomms10126>
- Chen F., B. M. Hersh, B. Conradt, Z. Zhou, D. Riemer, *et al.*, 2000 Translocation of *C. elegans* CED-4 to nuclear membranes during programmed cell death. *Science.* <https://doi.org/10.1126/science.287.5457.1485>
- Chien S. C., E. M. Brinkmann, J. Teuliere, and G. Garriga, 2013 *Caenorhabditis elegans* PIG-1/MELK acts in a conserved PAR-4/LKB1 polarity pathway to promote asymmetric neuroblast divisions. *Genetics* 193: 897–909. <https://doi.org/10.1534/genetics.112.148106>
- Conradt B., and H. R. Horvitz, 1998 The *C. elegans* Protein EGL-1 is required for programmed cell death and interacts with the Bcl-2-like protein CED-9. *Cell.* [https://doi.org/10.1016/S0092-8674\(00\)81182-4](https://doi.org/10.1016/S0092-8674(00)81182-4)
- Corbo J. C., A. Erives, G. A. Di, A. Chang, and M. Levine, 1997 Dorsal-ventral patterning of the vertebrate neural tube is conserved in a protochordate. *Development* 124: 2335–2344.

- Cordes S., C. A. Frank, and G. Garriga, 2006 The *C. elegans* MELK ortholog PIG-1 regulates cell size asymmetry and daughter cell fate in asymmetric neuroblast divisions. *Development* 133: 2747–2756. <https://doi.org/10.1242/dev.02447>
- Cowan C. R., and A. A. Cowan, 2004 Centrosomes direct cell polarity independently of microtubule assembly in *C. elegans* embryos. *Nature*.
- Cowan C. R., and A. A. Hyman, 2004 Asymmetric cell division in *C. elegans*: cortical polarity and spindle positioning. *Annu. Rev. Cell Dev. Biol.* <https://doi.org/10.1146/annurev.cellbio.19.111301.113823>
- Cowan C. R., and A. A. Hyman, 2007 Acto-myosin reorganization and PAR polarity in *C. elegans*. *Development*. <https://doi.org/10.1242/dev.000513>
- Cuenca A. A., 2003 Polarization of the *C. elegans* zygote proceeds via distinct establishment and maintenance phases. *Development*. <https://doi.org/10.1242/dev.00284>
- Culetto E., 2000 A role for *Caenorhabditis elegans* in understanding the function and interactions of human disease genes. *Hum. Mol. Genet.* <https://doi.org/10.1093/hmg/9.6.869>
- Daniels B. R., T. M. Dobrowsky, E. M. Perkins, S. X. Sun, and D. Wirtz, 2010 MEX-5 enrichment in the *C. elegans* early embryo mediated by differential diffusion. *Development*. <https://doi.org/10.1242/dev.051326>
- Denning D. P., V. Hatch, and H. R. Horvitz, 2013 Both the Caspase CSP-1 and a Caspase-Independent Pathway Promote Programmed Cell Death in Parallel to the Canonical Pathway for Apoptosis in *Caenorhabditis elegans*. *PLoS Genet.* <https://doi.org/10.1371/journal.pgen.1003341>
- DeRenzo C., K. J. Reese, and G. Seydoux, 2003 Exclusion of germ plasm proteins from somatic lineages by cullin-dependent degradation. *Nature*. <https://doi.org/10.1038/nature01887>
- Du T., Y. Qu, J. Li, H. Li, L. Su, *et al.*, 2014 Maternal embryonic leucine zipper kinase enhances gastric cancer progression via the FAK/Paxillin pathway. *Mol. Cancer* 13: 100. <https://doi.org/10.1186/1476-4598-13-100>
- Ellis H. M., and H. R. Horvitz, 1986 Genetic control of programmed cell death in the nematode *C. elegans*. *Cell*. [https://doi.org/10.1016/0092-8674\(86\)90004-8](https://doi.org/10.1016/0092-8674(86)90004-8)
- Ellis R. E., and H. R. Horvitz, 1991 Two *C. elegans* genes control the programmed deaths of specific cells in the pharynx. *Development*.
- Etemad-Moghadam B., S. Guo, and K. J. Kemphues, 1995 Asymmetrically distributed PAR-3 protein contributes to cell polarity and spindle alignment in early *C. elegans* embryos. *Cell*. [https://doi.org/10.1016/0092-8674\(95\)90187-6](https://doi.org/10.1016/0092-8674(95)90187-6)
- Evans R. M., and S. M. Hollenbergt, 1988 Zinc fingers: Gilt by association. *Cell*.
- Feng G., P. Yi, Y. Yang, Y. Chai, D. Tian, *et al.*, 2013a Developmental stage-dependent transcriptional regulatory pathways control neuroblast lineage progression. 3847: 3838–3847.

<https://doi.org/10.1242/dev.098723>

- Feng G., P. Yi, Y. Yang, Y. Chai, D. Tian, *et al.*, 2013b Developmental stage-dependent transcriptional regulatory pathways control neuroblast lineage progression. *Development*. <https://doi.org/10.1242/dev.098723>
- Frank C. A., N. C. Hawkins, C. Guenther, H. R. Horvitz, and G. Garriga, 2005 *C. elegans* HAM-1 positions the cleavage plane and regulates apoptosis in asymmetric neuroblast divisions. *Dev. Biol.* <https://doi.org/10.1016/j.ydbio.2005.05.026>
- Gabrielli B. G., J. M. Clark, A. K. McCormack, and K. A. O. Ellem, 1997 Hyperphosphorylation of the N-terminal domain of cdc25 regulates activity toward cyclin B1/cdc2 but not cyclin A/cdk2. *J. Biol. Chem.* <https://doi.org/10.1074/jbc.272.45.28607>
- Galaktionov K., and D. Beach, 1991 Specific activation of cdc25 tyrosine phosphatases by B-type cyclins: Evidence for multiple roles of mitotic cyclins. *Cell*. [https://doi.org/10.1016/0092-8674\(91\)90294-9](https://doi.org/10.1016/0092-8674(91)90294-9)
- Galli M., and S. van den Heuvel, 2008 Determination of the Cleavage Plane in Early *C. elegans* Embryos. *Annu. Rev. Genet.* <https://doi.org/10.1146/annurev.genet.40.110405.090523>
- Ganguly R., A. Mohyeldin, J. Thiel, H. I. Kornblum, M. Beullens, *et al.*, 2015 MELK-a conserved kinase: functions, signaling, cancer, and controversy. *Clin. Transl. Med.* 4: 11. <https://doi.org/10.1186/s40169-014-0045-y>
- Geng X., Q. H. Zhou, E. Kage-Nakadai, Y. Shi, N. Yan, *et al.*, 2009 *Caenorhabditis elegans* caspase homolog CSP-2 inhibits CED-3 autoactivation and apoptosis in germ cells. *Cell Death Differ.* <https://doi.org/10.1038/cdd.2009.88>
- Gerstein M. B., Z. J. Lu, E. L. Van Nostrand, C. Cheng, B. I. Arshinoff, *et al.*, 2010 Integrative analysis of the *Caenorhabditis elegans* genome by the modENCODE project. *Science*. <https://doi.org/10.1126/science.1196914>
- Giehl K., 2005 Oncogenic Ras in tumour progression and metastasis. *Biol. Chem.*
- Goldstein B., and I. G. Macara, 2007 The PAR Proteins: Fundamental Players in Animal Cell Polarization. *Dev. Cell*.
- Goto Y., A. Kurozumi, T. Arai, N. Nohata, S. Kojima, *et al.*, 2017 Impact of novel miR-145-3p regulatory networks on survival in patients with castration-resistant prostate cancer. *Br. J. Cancer*. <https://doi.org/10.1038/bjc.2017.191>
- Grau Y., C. Carteret, and P. Simpson, 1984 Mutations and chromosomal rearrangements affecting the expression of snail, a gene involved in embryonic patterning in *Drosophila melanogaster*. *Genetics*.
- Griffin E. E., D. J. Odde, and G. Seydoux, 2011 Regulation of the MEX-5 Gradient by a Spatially Segregated Kinase/Phosphatase Cycle. *Theor. Econ.* 146: 955–968. <https://doi.org/10.1016/j.cell.2011.08.012>

- Guenther C., and G. Garriga, 1996 Asymmetric distribution of the *C. elegans* HAM-1 protein in neuroblasts enables daughter cells to adopt distinct fates. *Development*. <https://doi.org/S0896627302006785> [pii] ET - 2002/06/14
- Gumienny T. L., E. Lambie, E. Hartwig, H. R. Horvitz, and M. O. Hengartner, 1999 Genetic control of programmed cell death in the *Caenorhabditis elegans* hermaphrodite germline. *Development*. <https://doi.org/10.5167/uzh-1041>
- Guo S., and K. J. Kemphues, 1995 par-1, a gene required for establishing polarity in *C. elegans* embryos, encodes a putative Ser/Thr kinase that is asymmetrically distributed. *Cell*. [https://doi.org/10.1016/0092-8674\(95\)90082-9](https://doi.org/10.1016/0092-8674(95)90082-9)
- Guo S., and K. J. Kemphues, 1996 A non-muscle myosin required for embryonic polarity in *Caenorhabditis elegans*. *Nature*. <https://doi.org/10.1038/382455a0>
- Güven-Ozkan T., S. M. Robertson, Y. Nishi, and R. Lin, 2010 zif-1 translational repression defines a second, mutually exclusive OMA function in germline transcriptional repression. *Development*. <https://doi.org/10.1242/dev.055327>
- Hatzold J., and B. Conradt, 2008 Control of apoptosis by asymmetric cell division. *PLoS Biol.* 6: 771–784. <https://doi.org/10.1371/journal.pbio.0060084>
- Hawley S. a, J. Boudeau, J. L. Reid, K. J. Mustard, L. Udd, *et al.*, 2003 Complexes between the LKB1 tumor suppressor, STRAD alpha/beta and MO25 alpha/beta are upstream kinases in the AMP-activated protein kinase cascade. *J Biol.* <https://doi.org/10.1186/1475-4924-2-28>
- Hemavathy K., S. I. Ashraf, and Y. T. Ip, 2000 Snail/Slug family of repressors: Slowly going into the fast lane of development and cancer. *Gene*.
- Hengartner M. O., R. Ellis, and H. R. Horvitz, 1992 *Caenorhabditis elegans* gene ced-9 protects cells from programmed cell death. *Nature*. <https://doi.org/10.1038/356494a0>
- Hengartner M. O., and H. R. Horvitz, 1994 *C. elegans* cell survival gene ced-9 encodes a functional homolog of the mammalian proto-oncogene bcl-2. *Cell*. [https://doi.org/10.1016/0092-8674\(94\)90506-1](https://doi.org/10.1016/0092-8674(94)90506-1)
- Heyer B. S., J. Warsowe, D. Solter, B. B. Knowles, and S. L. Ackerman, 1997 New member of the Snf1/AMPK kinase family, Melk, is expressed in the mouse egg and preimplantation embryo. *Mol. Reprod. Dev.* 47: 148–156. [https://doi.org/10.1002/\(SICI\)1098-2795\(199706\)47:2<148::AID-MRD4>3.0.CO;2-M](https://doi.org/10.1002/(SICI)1098-2795(199706)47:2<148::AID-MRD4>3.0.CO;2-M)
- Heyer B. S., H. Kochanowski, and D. Solter, 1999 Expression of Melk, a new protein kinase, during early mouse development. *Dev. Dyn.* [https://doi.org/10.1002/\(SICI\)1097-0177\(199908\)215:4<344::AID-AJA6>3.0.CO;2-H](https://doi.org/10.1002/(SICI)1097-0177(199908)215:4<344::AID-AJA6>3.0.CO;2-H)
- Hird S. N., and J. G. White, 1993 Cortical and cytoplasmic flow polarity in early embryonic cells of *Caenorhabditis elegans*. *J. Cell Biol.* <https://doi.org/10.1083/jcb.121.6.1343>
- Hirose T., and H. R. Horvitz, 2013 An Sp1 transcription factor coordinates caspase-dependent and -

- independent apoptotic pathways. *Nature*. <https://doi.org/10.1038/nature12329>
- Hoffmann I., P. R. Clarke, M. J. Marcote, E. Karsenti, and G. Draetta, 1993 Phosphorylation and activation of human cdc25-C by cdc2--cyclin B and its involvement in the self-amplification of MPF at mitosis. *EMBO J*. <https://doi.org/10.1038/76479>
- Horvitz H. R., 1999 Genetic control of programmed cell death in the nematode *Caenorhabditis elegans*, in *Cancer Research*.
- Huang N. N., D. E. Mootz, A. J. M. Walhout, M. Vidal, and C. P. Hunter, 2002 MEX-3 interacting proteins link cell polarity to asymmetric gene expression in *Caenorhabditis elegans*. *Development*. <https://doi.org/10.1021/acsami.6b08089>
- Huang W., T. Jiang, W. Choi, S. Qi, Y. Pang, *et al.*, 2013 Mechanistic insights into CED-4-mediated activation of CED-3. *Genes Dev*. <https://doi.org/10.1101/gad.224428.113>
- Hung T. J., and K. J. Kemphues, 1999 PAR-6 is a conserved PDZ domain-containing protein that colocalizes with PAR-3 in *Caenorhabditis elegans* embryos. *Development*.
- Izumi T., and J. L. Maller, 1993 Elimination of cdc2 phosphorylation sites in the cdc25 phosphatase blocks initiation of M-phase. *Mol. Biol. Cell*. <https://doi.org/10.1091/mbc.4.12.1337>
- Jenkins N., J. R. Saam, and S. E. Mango, 2006 CYK-4/GAP provides a localized cue to initiate anteroposterior polarity upon fertilization. *Science*. <https://doi.org/10.1126/science.1130291>
- Kachur T. M., A. Audhya, and D. B. Pilgrim, 2008 UNC-45 is required for NMY-2 contractile function in early embryonic polarity establishment and germline cellularization in *C. elegans*. *Dev. Biol*. <https://doi.org/10.1016/j.ydbio.2007.11.028>
- Kaldis P., 1999 The cdk-activating kinase (CAK): From yeast to mammals. *Cell. Mol. Life Sci*.
- Kastan M. B., and J. Bartek, 2004 Cell-cycle checkpoints and cancer. *Nature*.
- Kataoka H., T. Murayama, M. Yokode, S. Mori, H. Sano, *et al.*, 2000 A novel snail-related transcription factor Smuc regulates basic helix-loop-helix transcription factor activities via specific E-box motifs. *Nucleic Acids Res*. <https://doi.org/10.1093/nar/28.2.626>
- Katoh M., and M. Katoh, 2005 Comparative genomics on SNAI1, SNAI2, and SNAI3 orthologs. *Oncol. Rep*.
- Kemphues K. J., J. R. Priess, D. G. Morton, and N. Cheng, 1988 Identification of genes required for cytoplasmic localization in early *C. elegans* embryos. *Cell*. [https://doi.org/10.1016/S0092-8674\(88\)80024-2](https://doi.org/10.1016/S0092-8674(88)80024-2)
- Kenyon C., 1988 The nematode *Caenorhabditis elegans*. *Science*. <https://doi.org/10.1126/science.3287621>
- Kimble J., and D. Hirsh, 1979 The postembryonic cell lineages of the hermaphrodite and male gonads in *Caenorhabditis elegans*. *Dev. Biol*. [https://doi.org/10.1016/0012-1606\(79\)90035-6](https://doi.org/10.1016/0012-1606(79)90035-6)

- Knight R. D., and S. M. Shimeld, 2001 Identification of conserved C2H2 zinc-finger gene families in the Bilateria. *Genome Biol.* <https://doi.org/10.1186/gb-2001-2-5-research0016>
- Kristjánisdóttir K., and J. Rudolph, 2004 Cdc25 phosphatases and cancer. *Chem. Biol.*
- Langeland J. A., J. M. Tomsa, W. R. Jackman, and C. B. Kimmel, 1998 An amphioxus snail gene: Expression in paraxial mesoderm and neural plate suggests a conserved role in patterning the chordate embryo. *Dev. Genes Evol.* <https://doi.org/10.1007/s004270050216>
- Lee C. H., W. H. Kuo, C. C. Lin, Y. J. Oyang, H. C. Huang, *et al.*, 2013 MicroRNA-regulated protein-protein interaction networks and their functions in breast cancer. *Int. J. Mol. Sci.* <https://doi.org/10.3390/ijms140611560>
- Liro M. J., D. G. Morton, and L. S. Rose, 2018 The kinases PIG-1 and PAR-1 act in redundant pathways to regulate asymmetric division in the EMS blastomere of *C. elegans*. *Dev. Biol.* 444: 9–19. <https://doi.org/10.1016/j.ydbio.2018.08.016>
- Lizcano J. M., O. Göransson, R. Toth, M. Deak, N. A. Morrice, *et al.*, 2004 LKB1 is a master kinase that activates 13 kinases of the AMPK subfamily, including MARK/PAR-1. *EMBO J.* 23: 833–43. <https://doi.org/10.1038/sj.emboj.7600110>
- Mailand N., A. V. Podtelejnikov, A. Groth, M. Mann, J. Bartek, *et al.*, 2002 Regulation of G2/M events by Cdc25A through phosphorylation-dependent modulation of its stability. *EMBO J.* <https://doi.org/10.1093/emboj/cdf567>
- Malumbres M., and M. Barbacid, 2003 RAS oncogenes: The first 30 years. *Nat. Rev. Cancer.*
- Manzanares M., A. Locascio, and M. A. Nieto, 2001 The increasing complexity of the Snail gene superfamily in metazoan evolution. *Trends Genet.* [https://doi.org/10.1016/S0168-9525\(01\)02232-6](https://doi.org/10.1016/S0168-9525(01)02232-6)
- Mataki H., N. Seki, K. Mizuno, N. Nohata, K. Kamikawaji, *et al.*, 2016 Dual-strand tumor-suppressor microRNA-145 (miR-145-5p and miR-145-3p) coordinately targeted MTDH in lung squamous cell carcinoma. *Oncotarget.* <https://doi.org/10.18632/oncotarget.12290>
- Mayer M., M. Depken, J. S. Bois, F. Jülicher, and S. W. Grill, 2010 Anisotropies in cortical tension reveal the physical basis of polarizing cortical flows. *Nature.* <https://doi.org/10.1038/nature09376>
- Meikrantz W., and R. Schlegel, 1995 Apoptosis and the cell cycle. *J. Cell. Biochem.* <https://doi.org/10.1002/jcb.240580205>
- Metzstein M. M., and H. R. Horvitz, 1999a The *C. elegans* cell death specification gene *ces-1* encodes a Snail family zinc finger protein. *Mol. Cell* 4: 309–319. [https://doi.org/10.1016/S1097-2765\(00\)80333-0](https://doi.org/10.1016/S1097-2765(00)80333-0)
- Metzstein M. M., and H. R. Horvitz, 1999b The *C. elegans* cell death specification gene *ces-1* encodes a Snail family zinc finger protein. *Mol. Cell.* [https://doi.org/10.1016/S1097-2765\(00\)80333-0](https://doi.org/10.1016/S1097-2765(00)80333-0)
- Mirey G., I. Chartrain, C. Froment, M. Quaranta, J. P. Bouché, *et al.*, 2005 CDC25B phosphorylated by

- pEg3 localizes to the centrosome and the spindle poles at mitosis. *Cell Cycle*.
<https://doi.org/10.4161/cc.4.6.1716>
- Mishra N., H. Wei, and B. Conradt, 2018 *Caenorhabditis elegans* ced-3 Caspase Is Required for Asymmetric Divisions That Generate Cells Programmed To Die. *Genetics*.
<https://doi.org/10.1534/genetics.118.301500>
- Mizuno K., H. Mataka, T. Arai, A. Okato, K. Kamikawaji, *et al.*, 2017 The microRNA expression signature of small cell lung cancer: Tumor suppressors of miR-27a-5p and miR-34b-3p and their targeted oncogenes. *J. Hum. Genet.* <https://doi.org/10.1038/jhg.2017.27>
- Morin X., and Y. Bellaïche, 2011 Mitotic Spindle Orientation in Asymmetric and Symmetric Cell Divisions during Animal Development. *Dev. Cell*.
- Motegi F., and A. Sugimoto, 2006 Sequential functioning of the ECT-2 RhoGEF, RHO-1 and CDC-42 establishes cell polarity in *Caenorhabditis elegans* embryos. *Nat. Cell Biol.*
<https://doi.org/10.1038/ncb1459>
- Motegi F., S. Zonies, Y. Hao, A. A. Cuenca, E. Griffin, *et al.*, 2011 Microtubules induce self-organization of polarized PAR domains in *Caenorhabditis elegans* zygotes. *Nat. Cell Biol.*
<https://doi.org/10.1038/ncb2354>
- Munro E., J. Nance, and J. R. Priess, 2004 Cortical flows powered by asymmetrical contraction transport PAR proteins to establish and maintain anterior-posterior polarity in the early *C. elegans* embryo. *Dev. Cell.* <https://doi.org/10.1016/j.devcel.2004.08.001>
- Nagata A., M. Igarashi, S. Jinno, K. Suto, and H. Okayama, 1991 An additional homolog of the fission yeast *cdc25+* gene occurs in humans and is highly expressed in some cancer cells. *New Biol.*
- Nakano I., A. A. Paucar, R. Bajpai, J. D. Dougherty, A. Zewail, *et al.*, 2005 Maternal embryonic leucine zipper kinase (MELK) regulates multipotent neural progenitor proliferation. *J. Cell Biol.* 170: 413–427. <https://doi.org/10.1083/jcb.200412115>
- Nibu Y., H. Zhang, and M. Levine, 1998 Interaction of short-range repressors with *Drosophila* CtBP in the embryo. *Science.* <https://doi.org/10.1126/science.280.5360.101>
- Nieto M. A., M. G. Sargent, D. G. Wilkinson, and J. Cooke, 1994 Control of cell behavior during vertebrate development by Slug, a zinc finger gene. *Science.*
<https://doi.org/10.1126/science.7513443>
- Nieto M. A., 2002 The snail superfamily of zinc-finger transcription factors. *Nat. Rev. Mol. Cell Biol.*
- Nieto M. A., R. Y. Y. J. Huang, R. A. A. Jackson, and J. P. P. Thiery, 2016 EMT: 2016. *Cell.*
- Nishi Y., E. Rogers, S. M. Robertson, and R. Lin, 2008 Polo kinases regulate *C. elegans* embryonic polarity via binding to DYRK2-primed MEX-5 and MEX-6. *Development.*
<https://doi.org/10.1242/dev.013425>
- Nusslein-Volhard C., E. Wieschaus, and H. Kluding, 1984 Mutations affecting the pattern of the larval

- cuticle in *Drosophila melanogaster*. Wilhelm Roux's Arch. Dev. Biol. <https://doi.org/10.1007/BF00848156>
- Nüsslein-volhard C., and E. Wieschaus, 1980 Mutations affecting segment number and polarity in *drosophila*. Nature. <https://doi.org/10.1038/287795a0>
- Offenburger S. L., D. Bensaddek, A. B. Murillo, A. I. Lamond, and A. Gartner, 2017 Comparative genetic, proteomic and phosphoproteomic analysis of *C. elegans* embryos with a focus on ham-1/STOX and pig-1/MELK in dopaminergic neuron development. Sci. Rep. <https://doi.org/10.1038/s41598-017-04375-4>
- Oldenbroek M., S. M. Robertson, T. Guven-Ozkan, S. Gore, Y. Nishi, *et al.*, 2012 Multiple RNA-binding proteins function combinatorially to control the soma-restricted expression pattern of the E3 ligase subunit ZIF-1. Dev. Biol. <https://doi.org/10.1016/j.ydbio.2012.01.002>
- Page Y. Le, I. Chartrain, C. Badouel, and J.-P. Tassan, 2011 A functional analysis of MELK in cell division reveals a transition in the mode of cytokinesis during *Xenopus* development. J. Cell Sci. <https://doi.org/10.1016/j.jlsc.2018.06.058>
- Peinado H., E. Ballestar, M. Esteller, and A. Cano, 2004 Snail Mediates E-Cadherin Repression by the Recruitment of the Sin3A/Histone Deacetylase 1 (HDAC1)/HDAC2 Complex. Mol. Cell. Biol. <https://doi.org/10.1128/MCB.24.1.306-319.2004>
- Peso L. Del, V. M. González, and G. Núñez, 1998 *Caenorhabditis elegans* EGL-1 disrupts the interaction of CED-9 with CED-4 and promotes CED-3 activation. J. Biol. Chem. <https://doi.org/10.1074/jbc.273.50.33495>
- Pinan-Lucarre B., C. V. Gabel, C. P. Reina, S. E. Hulme, S. S. Shevkopyas, *et al.*, 2012 The core apoptotic executioner proteins CED-3 and CED-4 promote initiation of neuronal regeneration in *caenorhabditis elegans*. PLoS Biol. <https://doi.org/10.1371/journal.pbio.1001331>
- Qi D., M. Bergman, H. Aihara, Y. Nibu, and M. Mannervik, 2008 *Drosophila* Ebi mediates Snail-dependent transcriptional repression through HDAC3-induced histone deacetylation. EMBO J. <https://doi.org/10.1038/emboj.2008.26>
- Reece-Hoyes J. S., B. Deplancke, M. I. Barrasa, J. Hatzold, R. B. Smit, *et al.*, 2009 The *C. elegans* Snail homolog CES-1 can activate gene expression in vivo and share targets with bHLH transcription factors. Nucleic Acids Res. <https://doi.org/10.1093/nar/gkp232>
- Reese K. J., M. A. Dunn, J. A. Waddle, and G. Seydoux, 2000 Asymmetric segregation of PIE-1 in *C. elegans* is mediated by two complementary mechanisms that act through separate PIE-1 protein domains. Mol. Cell. [https://doi.org/10.1016/S1097-2765\(00\)00043-5](https://doi.org/10.1016/S1097-2765(00)00043-5)
- Reya T., and H. Clevers, 2005 Wnt signalling in stem cells and cancer. Nature.
- Rijsewijk F., M. Schuermann, E. Wagenaar, P. Parren, D. Weigel, *et al.*, 1987 The *Drosophila* homology of the mouse mammary oncogene int-1 is identical to the segment polarity gene wingless. Cell. [https://doi.org/10.1016/0092-8674\(87\)90038-9](https://doi.org/10.1016/0092-8674(87)90038-9)

- Rose L., and P. Gonczy, 2014 Polarity establishment, asymmetric division and segregation of fate determinants in early *C. elegans* embryos. WormBook. <https://doi.org/10.1895/wormbook.1.30.2>
- Sadhu K., S. I. Reed, H. Richardson, and P. Russell, 1990 Human homolog of fission yeast *cdc25* mitotic inducer is predominantly expressed in G2. Proc. Natl. Acad. Sci. U. S. A. <https://doi.org/10.1073/pnas.87.13.5139>
- Saito R., Y. Tabata, A. Muto, K. Arai, and S. Watanabe, 2005 Melk-like kinase plays a role in hematopoiesis in the zebra fish. Mol Cell Biol. <https://doi.org/10.1128/MCB.25.15.6682-6693.2005>
- Schmitt E., R. Boutros, C. Froment, B. Monsarrat, B. Ducommun, *et al.*, 2006 CHK1 phosphorylates CDC25B during the cell cycle in the absence of DNA damage. J. Cell Sci. <https://doi.org/10.1242/jcs.03200>
- Schmutz C., J. Stevens, and A. Spang, 2007 Functions of the novel RhoGAP proteins RGA-3 and RGA-4 in the germ line and in the early embryo of *C. elegans*. Development 134: 3495–3505. <https://doi.org/10.1242/dev.000802>
- Schonegg S., 2006 CDC-42 and RHO-1 coordinate acto-myosin contractility and PAR protein localization during polarity establishment in *C. elegans* embryos. Development. <https://doi.org/10.1046/j.1469-0705.1993.03040240.x>
- Schonegg S., A. T. Constantinescu, C. Hoegge, and A. A. Hyman, 2007 The Rho GTPase-activating proteins RGA-3 and RGA-4 are required to set the initial size of PAR domains in *Caenorhabditis elegans* one-cell embryos. Proc. Natl. Acad. Sci. <https://doi.org/10.1073/pnas.0706941104>
- Schubert C. M., R. Lin, C. J. De Vries, R. H. A. Plasterk, and J. R. Priess, 2000 MEX-5 and MEX-6 function to establish soma/germline asymmetry in early *C. elegans* embryos. Mol. Cell. [https://doi.org/10.1016/S1097-2765\(00\)80246-4](https://doi.org/10.1016/S1097-2765(00)80246-4)
- Sefton M., S. Sánchez, and M. A. Nieto, 1998 Conserved and divergent roles for members of the Snail family of transcription factors in the chick and mouse embryo. Development.
- Shaham S., and H. R. Horvitz, 1996 Developing *Caenorhabditis elegans* neurons may contain both cell-death protective and killer activities. Genes Dev. <https://doi.org/10.1101/gad.10.5.578>
- Shaham S., 1998 Identification of multiple *Caenorhabditis elegans* caspases and their potential roles in proteolytic cascades. J. Biol. Chem. <https://doi.org/10.1074/jbc.273.52.35109>
- Shaham S., P. W. Reddien, B. Davies, and H. Robert Horvitz, 1999 Mutational analysis of the *Caenorhabditis elegans* cell-death gene *ced-3*. Genetics. <https://doi.org/10.1051/medsci/20031967725>
- Shaye D. D., and I. Greenwald, 2011 Ortholist: A compendium of *C. elegans* genes with human orthologs. PLoS One. <https://doi.org/10.1371/journal.pone.0020085>
- Shelton C. A., J. C. Carter, G. C. Ellis, and B. Bowerman, 1999 The nonmuscle myosin regulatory light chain gene *mlc-4* is required for cytokinesis, anterior-posterior polarity, and body morphology

- during *Caenorhabditis elegans* embryogenesis. *J. Cell Biol.* <https://doi.org/10.1083/jcb.146.2.439>
- Sherrard R., S. Luehr, H. Holzkamp, K. McJunkin, N. Memar, *et al.*, 2017 Mirnas cooperate in apoptosis regulation during *C. Elegans* development. *Genes Dev.* <https://doi.org/10.1101/gad.288555.116>
- Sonneville R., 2004 *zyg-11* and *cul-2* regulate progression through meiosis II and polarity establishment in *C. elegans*. *Development.* <https://doi.org/10.1242/dev.01244>
- Sugimoto A., R. R. Hozak, T. Nakashima, T. Nishimoto, and J. H. Rothman, 1995 *dad-1*, an endogenous programmed cell death suppressor in *Caenorhabditis elegans* and vertebrates. *EMBO J.*
- Sulston J. E., and H. R. Horvitz, 1977 Post-embryonic cell lineages of the nematode, *Caenorhabditis elegans*. *Dev Biol.* [https://doi.org/0012-1606\(77\)90158-0](https://doi.org/0012-1606(77)90158-0) [pii]
- Sulston J. E., E. Schierenberg, J. G. White, and J. N. Thomson, 1983 The embryonic cell lineage of the nematode *Caenorhabditis elegans*. *Dev. Biol.* 100: 64–119. [https://doi.org/10.1016/0012-1606\(83\)90201-4](https://doi.org/10.1016/0012-1606(83)90201-4)
- Sulston J., and J. Hodgkin, 1988 *Methods in the nematode C. elegans*. Cold Spring Harb. Lab. Press.
- Tabara H., R. J. Hill, C. C. Mello, J. R. Priess, and Y. Kohara, 1999 *pos-1* encodes a cytoplasmic zinc-finger protein essential for germline specification in *C. elegans*. *Development.* <https://doi.org/10.1167/iavs.07-1072.Complement-Associated>
- Takeshita H., and H. Sawa, 2005 Asymmetric cortical and nuclear localizations of WRM-1/ β -catenin during asymmetric cell division in *C. elegans*. *Genes Dev.* <https://doi.org/10.1101/gad.1322805>
- Tenlen J. R., J. N. Molk, N. London, B. D. Page, and J. R. Priess, 2008 MEX-5 asymmetry in one-cell *C. elegans* embryos requires PAR-4- and PAR-1-dependent phosphorylation. *Development.* <https://doi.org/10.1242/dev.027060>
- Teuliere J., and G. Garriga, Size Matters : How *C. elegans* Asymmetric Divisions Regulate Apoptosis. <https://doi.org/10.1007/978-3-319-53150-2>
- Teuliere J., I. Kovacevic, Z. Bao, and G. Garriga, 2018 The *Caenorhabditis elegans* gene *ham-1* regulates daughter cell size asymmetry primarily in divisions that produce a small anterior daughter cell. *PLoS One.* <https://doi.org/10.1371/journal.pone.0195855>
- Thellmann M., 2003 The Snail-like CES-1 protein of *C. elegans* can block the expression of the BH3-only cell-death activator gene *egl-1* by antagonizing the function of bHLH proteins. *Development.* <https://doi.org/10.1242/dev.00597>
- Thisse C., B. Thisse, and J. H. Postlethwait, 1995 Expression of *snail2*, a second member of the zebrafish snail family, in cephalic mesendoderm and presumptive neural crest of wild-type and *spadetail* mutant embryos. *Dev. Biol.* <https://doi.org/10.1006/dbio.1995.0007>
- Thorpe C. J., A. Schlesinger, J. Clayton Carter, and B. Bowerman, 1997 Wnt signaling polarizes an early *C. elegans* blastomere to distinguish endoderm from mesoderm. *Cell.* [https://doi.org/10.1016/S0092-8674\(00\)80530-9](https://doi.org/10.1016/S0092-8674(00)80530-9)

- Tsai M. C., and J. Ahringer, 2007 Microtubules are involved in anterior-posterior axis formation in *C. elegans* embryos. *J. Cell Biol.* <https://doi.org/10.1083/jcb.200708101>
- Tse Y. C., M. Werner, K. M. Longhini, J.-C. Labbe, B. Goldstein, *et al.*, 2012 RhoA activation during polarization and cytokinesis of the early *Caenorhabditis elegans* embryo is differentially dependent on NOP-1 and CYK-4. *Mol. Biol. Cell.* <https://doi.org/10.1091/mbc.E12-04-0268>
- Vulsteke V., M. Beullens, A. Boudrez, S. Keppens, A. Van Eynde, *et al.*, 2004 Inhibition of Spliceosome Assembly by the Cell Cycle-regulated Protein Kinase MELK and Involvement of Splicing Factor NIPP1. *J. Biol. Chem.* 279: 8642–8647. <https://doi.org/10.1074/jbc.M311466200>
- Weaver B. P., R. Zabinsky, Y. M. Weaver, E. S. Lee, D. Xue, *et al.*, 2014 CED-3 caspase acts with miRNAs to regulate non-apoptotic gene expression dynamics for robust development in *C. elegans*. *Elife.* <https://doi.org/10.7554/eLife.04265>
- Weaver B. P., Y. M. Weaver, S. Mitani, and M. Han, 2017 Coupled Caspase and N-End Rule Ligase Activities Allow Recognition and Degradation of Pluripotency Factor LIN-28 during Non-Apoptotic Development. *Dev. Cell.* <https://doi.org/10.1016/j.devcel.2017.05.013>
- Wei H., B. Yan, J. Gagneur, and B. Conradt, 2017 *Caenorhabditis elegans* CES-1 snail represses Pig-1 MELK expression to control asymmetric cell division. *Genetics* 206: 2069–2084. <https://doi.org/10.1534/genetics.117.202754>
- Wu J., S. Hu, Y. Chen, Z. Li, J. Zhang, *et al.*, 2017 BCIP: A gene-centered platform for identifying potential regulatory genes in breast cancer. *Sci. Rep.* <https://doi.org/10.1038/srep45235>
- Xue D., S. Shaham, and H. R. Horvitz, 1996 The *Caenorhabditis elegans* cell-death protein CED-3 is a cysteine protease with substrate specificities similar to those of the human CPP32 protease. *Genes Dev.* <https://doi.org/10.1101/gad.10.9.1073>
- Yan N., L. Gu, D. Kokel, J. Chai, W. Li, *et al.*, 2004 Structural, biochemical, and functional analyses of CED-9 recognition by the proapoptotic proteins EGL-1 and CED-4. *Mol. Cell.* <https://doi.org/10.1016/j.molcel.2004.08.022>
- Yan B., N. Memar, J. Gallinger, and B. Conradt, 2013 Coordination of Cell Proliferation and Cell Fate Determination by CES-1 Snail. *PLoS Genet.* 9. <https://doi.org/10.1371/journal.pgen.1003884>
- Yang X., H. Y. Chang, and D. Baltimore, 1998 Essential role of CED-4 oligomerization in CED-3 activation and apoptosis. *Science.* <https://doi.org/10.1126/science.281.5381.1355>
- Yee C., W. Yang, and S. Hekimi, 2014 The intrinsic apoptosis pathway mediates the pro-longevity response to mitochondrial ROS in *C. elegans*. *Cell.* <https://doi.org/10.1016/j.cell.2014.02.055>
- Yuan J., and H. R. Horvitz, 1990 The *Caenorhabditis elegans* genes *ced-3* and *ced-4* act cell autonomously to cause programmed cell death. *Dev. Biol.* [https://doi.org/10.1016/0012-1606\(90\)90174-H](https://doi.org/10.1016/0012-1606(90)90174-H)
- Yuan J., H. R. Horvitz, E. J. Lambie, H. Steller, and M. O. Hengartner, 1992 The *Caenorhabditis elegans* cell death gene *ced-4* encodes a novel protein and is expressed during the period of extensive

- programmed cell death. *Development*. [https://doi.org/10.1016/S0928-7655\(97\)00036-5](https://doi.org/10.1016/S0928-7655(97)00036-5)
- Yuan J., S. Shaham, S. Ledoux, H. M. Ellis, and H. R. Horvitz, 1993 The *C. elegans* cell death gene *ced-3* encodes a protein similar to mammalian interleukin-1 β -converting enzyme. *Cell*. [https://doi.org/10.1016/0092-8674\(93\)90485-9](https://doi.org/10.1016/0092-8674(93)90485-9)
- Zeitlinger J., R. P. Zinzen, A. Stark, M. Kellis, H. Zhang, *et al.*, 2007 Whole-genome ChIP-chip analysis of Dorsal, Twist, and Snail suggests integration of diverse patterning processes in the *Drosophila* embryo. *Genes Dev*. <https://doi.org/10.1101/gad.1509607>
- Zonies S., F. Motegi, Y. Hao, and G. Seydoux, 2010 Symmetry breaking and polarization of the *C. elegans* zygote by the polarity protein PAR-2. *Development*. <https://doi.org/10.1242/dev.045823>
- Zou H., W. J. Henzel, X. Liu, A. Lutschg, and X. Wang, 1997 Apaf-1, a human protein homologous to *C. elegans* CED-4, participates in cytochrome c-dependent activation of caspase-3. *Cell*. [https://doi.org/10.1016/S0092-8674\(00\)80501-2](https://doi.org/10.1016/S0092-8674(00)80501-2)

Acknowledgement

I would like to thank my supervisor Prof. Dr. Barbara Conradt, for offering me the opportunity to join her lab and for the excellent guidance and support throughout my whole doctoral study. I would also like to thank PD. Dr. Eric Lambie, who has always suggested me smart ideas when I faced difficult problems. Importantly, he taught me many great cloning techniques, which were important for proceeding my projects. I also want to thank our technicians, Nadja Lebedeva, Melanie Schwarz and Michaela Bauer, for their excellent technical support. Thanks to the three-month lab training with Sayantan Chakraborty and thanks to Fabian Köhler and Simon Häußler for offering me NGM medium plates.

Moreover, I would also like to thank Bo Yan and Julien Gagneur for analyzing the CES-1 ChIP-seq data. Specially thanks to Sriyash Mangal, Fabian Köhler, Simon Häußler, Ryan Sherrad, Jennifer Sacher and Nikhil Mishra for revising parts of my dissertation. Thanks to Saroj Regmi, Stephane Rolland and Nadin Memar for the technical suggestion at the time when I joined the lab.

Thanks to Fabian Köhler, Nadja Lebedeva and Ryan Sherrad, I had lots of great and memorable time with them in Germany. I also want to thank Jeffery Zielich and Simon Häußler for giving me an awesome birthday present, it will stay in my heart. Of course, I love my office colleagues, we had lots of great times when we were on our office retreats. Thanks to Laura Besora Casals, Fabian Köhler and Sriyash Mangal, we are the best office ever! In addition, thanks to all the other people in the lab for all their help and suggestions.

Last but not the least, heartily thanks to my family, especially thanks to my wife Fan Du. With their support in my life, I got the chance to be here and to pursue my dream.

Mailing Address:

LMU Biocenter, Department of Biology II, Prof. Barbara Conradt group

Großhaderner Str. 2, B02.030, 82152 Planegg-Martinsried, München, Germany

Publications:

1. H. Wei, B. Yan, J. Gagneur, and B. Conradt, 2017 *Caenorhabditis elegans ces-1* Snail represses *pig-1* MELK expression to control asymmetric cell division. *GENETICS* 206: 2069–2084.
2. Mishra N., H. Wei, and B. Conradt, 2018 *Caenorhabditis elegans ced-3* Caspase Is Required for Asymmetric Divisions That Generate Cells Programmed To Die. *GENETICS* 210: 3 983-998.
3. Qingliang Li* H. Wei* Lijing Liu Xiaoyuan Yang Xiansheng Zhang Qi Xie, 2017 Unfolded protein response activation compensates endoplasmic reticulum-associated degradation deficiency in *Arabidopsis*. *Journal of Integrative Plant Biology* 59: 7 506-52.
4. H. Wei, Barbara Conradt, *pig-1* MELK and *nmy-2* non-muscle myosin dependent non-random segregation of CES-1 Snail protein during NSM neuroblast asymmetric division. (Manuscript in preparation, supposed to submit soon)
5. H. Wei, Barbara Conradt, A split fluorescence-protein tool to directly observe and track active CED-3 Caspase in *C. elegans*. (Manuscript in preparation)
6. Wen Deng, Jack Bates, Hai Wei, Barbara Conradt and Heinrich Leonhardt, Reversible light or drug induced depletion of target proteins. *Nature Communications* (underreview)

Educational Background:**Ph.D., Cell and Developmental Biology**

10/2014-05/2019 (expected)

Ludwig Maximilian University of Munich (LMU)

Supervisor: Prof. Barbara Conradt

MSc., Molecular and Cell and Developmental Biology

Institute of Genetics and Developmental Biology (IGDB),

07/2012-07/2014

Chinese Academy of Sciences (CAS)

Supervisor: Prof. Qi Xie

&

Shandong Agricultural University (SDAU), China

09/2011-07/2014

State Key Laboratory of Crop Biology

Supervisor: Prof. Xiansheng Zhang

B.Sc., Agricultural (Chinese herbal medicine)

Shandong Agricultural University (SDAU)

09/2007-07/2011

Research Experience: (2007.09–present)**Ph.D. study in the Prof. Barbara Conradt lab (projects are listed as following)**

1. *C. elegans ces-1* Snail represses *pig-1* MELK expression to control asymmetric cell division (published)
2. *C. elegans ced-3* Caspase Is Required for Asymmetric Divisions That Generate Cells Programmed To Die (published)
3. MELK *pig-1* and non-muscle myosin *nmy-2* are required for asymmetric cell division and segregation of fate

determinants in neuroblast lineage (in preparation)

4. A tool to track and observe active Caspase CED-3 in vivo in *C. elegans* (in preparation)

5. *C. elegans ced-3* Caspase acts through *ect-2* to promote the establishment of cell polarity in the NSMnb (in preparation)

6. Reversible light or drug induced depletion of target proteins (In preparation, cooperation work with the Prof. Heinrich Leonhardt group)

MSc. Study in the prof. Qi Xie and Prof. Xiansheng Zhang lab (projects are listed as following)

1. Interaction between UPR (unfolded-protein response) and ERAD (endoplasmic- associated degradation) in plant response to stress (published)

2. UPR responses to ER stress depends on ER Ca²⁺ releasing (in preparation)

3. Using somatic protoplasts of *Arabidopsis thaliana* to regenerate stem cells

4. The role of plant hormones on the formation of cytoskeleton

B.Sc. Study in the Associated Prof. Lixiang Zhu lab

1. Functions of plant hormones on increasing yield and quality of *Platycodon grandiflorum* (published)

Techniques and Skills:

Molecular and Cell Biology

| | |
|--|---|
| Molecular cloning (Gibson, Gateway and classical method) | CRISP/Cas9 method |
| Genome engineering in <i>C. elegans</i> | RNAi screening (<i>C. elegans</i>) |
| Genomic DNA and mRNA purification | Reverse transcription to synthesis cDNA |
| Reverse PCR | RNA in situ hybridization |
| Quantitative Real-time PCR | Genetics |
| TAIL-PCR | Western Blot |
| Immunofluorescence | Yeast Two-Hybrid assay |
| E3 ligase activity test | Northern Blot |
| Cell Culture (plant) | Co-IP |
| Confocal microscopy | Optical microscopy |
| Various Fluorescence microscopies | |

Computer

Image editing (Image J, Photoshop, Affinity Designer, PowerPoint)

Statistical analysis (Prism, Excel, SPSS, SigmaPlot, R)

Sequence design and analysis (Vector NTI, SnapGene, DNAMAN)

Conferences and Abstracts:

1. 22nd International Worm Meeting, 2019

Abstract: "*pig-1* MELK-dependent non-random segregation of CES-1 Snail protein during NSM neuroblast division" (Oral Presentation in the Plenary session)

2. *C. elegans* Development, Cell Biology, and Gene Expression, EMBO 2018

Abstract: "Non-random segregation of CES-1 Snail protein during asymmetric neuroblast division through *pig-1* MELK-dependent CES-1 Snail gradient" (Poster Presentation)

3. THE ALLIED GENETICS CONFERENCE 2016 (TAGC)

4. International Meeting of the German Society for Cell Biology (DGZ) with support of the Austrian Association of Molecular Life Sciences and Biotechnology 2016

5. NATIONAL CONGRESS OF PLANT BIOLOGY 2012

6. NATIONAL CONGRESS OF PLANT GENOME 2012

Awards:

09/2007-07/2008, 09/2008-07/2009, 09/2009-07/2010, 09/2010-07/2011 Semesters:

Shandong Agricultural University (SDAU) Scholarship for excellent Bachelor students

12/2008: Honorable Award in Science and Technology Innovation Competition of SDAU

09/2010-06/2011: Scholarship of literary and sports of SDAU

06/2011: Award of excellent Bachelor thesis

04/2013: Shandong Agricultural University Scholarship for excellent Master students

07/2014: Award of excellent Master thesis

09/2014-09/2017: China Scholarship Council (CSC) Scholarship